

Integrated Biorefinery Strategies for Enhanced Production of Cellulose Nanocrystals and  
Fermentable Sugars from Wood

by

Dagem Zekaryas Haddis

A thesis submitted in partial fulfillment of the requirements for the degree of

Doctor of Philosophy

in

Bioresource and Food Engineering

Department of Agricultural, Food and Nutritional Science

University of Alberta

© Dagem Zekaryas Haddis, 2024

## Abstract

The industrial process to produce bioethanol from lignocellulosic biomass has focused on complete or nearly complete hydrolysis of cellulose to fermentable sugars. This entails utilizing different pretreatments and high amount of advanced cellulase cocktail to deconstruct the lignin and hemicellulose and depolymerize the recalcitrant crystalline region of cellulose to fermentable sugars. Thus, these enzymatic approaches are often associated with high costs due to the cost of cellulase cocktails. Therefore, to offset such economic challenges, biorefinery strategies need to be designed that provide high fermentable sugars recovery with additional high value-added products from lignocellulosic biomass. In this context, the crystalline region of cellulose serves as a precursor for producing a nanostructured material called cellulose nanocrystals (CNCs), while the amorphous chains can be hydrolyzed to sugars and subsequently fermented to ethanol. In this thesis a biorefinery strategy was designed to enhance the yield of CNCs and fermentable sugars through an integrated process beginning with either hydrothermal or steam explosion pretreatment followed by enzymatic hydrolysis and then acid hydrolysis.

The first study investigated the production of CNCs and fermentable sugars from wood pulp using a hybrid process that combined hydrothermal treatment, enzymatic hydrolysis, and acid hydrolysis. Hydrothermal treatment at 200°C improved cellulose crystallinity, forming CNC precursors through molecular reorientation. Subsequent enzymatic hydrolysis, employing a cellulase cocktail, released fermentable sugars from amorphous cellulose. Glucose and xylose yields plateaued at 24 h ( $32.8 \pm 0.3$  wt%) and ( $3.3 \pm 0.2$  wt%), respectively, during the 6-24 h enzymatic treatment. The hydrothermal and enzymatic treatment process significantly increased CNC yield by 2.1-fold and 1.4-fold compared to untreated wood pulp and hydrothermally treated

pulp alone, using acid hydrolyzed feedstock respectively. Consequently, the hybrid treatment improved overall CNC yield by 1.3-fold compared to untreated wood pulp, and it showed no significant difference compared to hydrothermally treated pulp alone. Furthermore, CNC yield started decreasing after 18 hours of enzyme treatment, likely due to the enzyme depolymerizing the crystalline region of the cellulose. Further analysis confirmed comparable CNC quality in the hybrid treatment through crystallinity, zeta potential, and thermal stability analysis.

The second study explored the impact of steam explosion pretreatment on the yield of CNCs. Conducting steam explosion prior to acid hydrolysis enhanced the crystallization of semi-crystalline/non-crystalline cellulose, generating additional CNC precursors from poplar wood as a feedstock. The crystallinity of steam-exploded poplar wood increased by 1.3-fold compared to untreated poplar wood, resulting in a 2.5-fold increase in the overall CNC yield. Importantly, the steam explosion pretreatment did not compromise CNC quality in terms of crystallinity and colloidal stability. However, the thermal stability of the CNCs improved due to an increase in crystal size caused by steam explosion. This study showcases a straightforward and scalable pretreatment approach that significantly enhances CNC yield during the acid hydrolysis step, thereby improving overall economic viability and commercial potential.

The third study extended the work from the second study by introducing an enzymatic hydrolysis step between steam explosion pretreatment and acid hydrolysis to produce CNCs and fermentable sugars from poplar wood. The objective was to achieve efficient saccharification of amorphous cellulose and enhancing CNC yield from acid hydrolysis reactions. The 24 h enzyme treatment showed increasing glucose yield over time for both untreated and steam-exploded poplar wood, with optimal improvement observed within 12 h for untreated wood ( $6.9 \pm 0.1$  wt %) and 18 h for steam-exploded poplar wood ( $29 \pm 1$  wt %). The xylose yield in untreated poplar wood did not

significantly increase with prolonged hydrolysis time, while in steam-exploded poplar wood, it increased until 18 h. Results indicated that steam explosion pretreatment and enzyme hydrolysis significantly enhanced the crystallinity of poplar wood, supporting the hypothesis increased accumulation of CNC precursors. This resulted in higher CNC yield for steam-exploded poplar wood ( $68.1 \pm 0.4$  wt % acid hydrolysis feedstock) compared to untreated poplar wood ( $23 \pm 2\%$  acid hydrolysis feedstock). Further characterization confirmed the combined steam explosion and enzymatic treatment of poplar wood resulted in CNCs of comparable quality, as evidenced by the stability of CNC suspensions, degree of crystallinity, and thermal stability analysis. The combined steam explosion and enzymatic treatment process proved effective in significantly enhancing CNC yield from poplar wood.

## Preface

This thesis constitutes the original work of Dagem Zekaryas Haddis. While a segment of the thesis has already been published, other sections are currently in the process of being prepared for publication.

The first study will be submitted to publication as Haddis, D. Z., Bernardo Araujo, Chae, M., Asomaning, J., & Bressler, D. C., titled " A comprehensive exploration of hybrid hydrothermal and enzymatic processes for enhanced the yield of cellulose nanocrystals and fermentable sugar as a by-product" In this publication, Material preparations, experiments, and analysis were performed by Dagem Zekaryas Haddis. The first draft of the manuscript was written by Dagem Zekaryas Haddis. Bernardo A. Souto collaborated by providing the introduction section. Supervision, project administration, conceptualization and funding acquisition were led by David C. Bressler. Dr. Justice Asomaning and Dr. Michael Chae contributed to discussions and editing manuscript writing. All authors read and approved the final manuscript.

The second study, authored by Haddis, D. Z., Chae, M., Asomaning, J., & Bressler, D. C., titled "Evaluation of steam explosion pretreatment on the cellulose nanocrystals (CNCs) yield from poplar wood," has been published in Carbohydrate Polymers (2024, 323, 121460, <https://doi.org/10.1016/j.carbpol.2023.121460>). In this publication, I, as the primary author, was responsible for designing, executing, and analyzing the experiments, as well as drafting the manuscript. Dr. Justice Asomaning and Dr. Michael Chae contributed to experiment design, discussions, and manuscript writing. Dr. David C. Bressler served as the supervisor, contributing to conceptualization, experiment design, discussions, and proofreading the manuscript.

The third study will be submitted to publications as Haddis, D. Z., Chae, M., Asomaning, J., & Bressler, D. C., titled " Steam explosion and enzymatic digestion as pretreatment for co-production of CNC and fermentable sugars" In this publication, Material preparations, experiments, and analysis were performed by Dagem Zekaryas Haddis. The first draft of the manuscript was written by Dagem Zekaryas Haddis. Supervision, project administration, conceptualization, funding acquisition, and editing the manuscript were led by David C. Bressler. Dr. Justice Asomaning and Dr. Michael Chae contributed to discussions and editing manuscript writing. All authors read and approved the final manuscript.

## **Acknowledgment**

The research presented in this thesis was carried out in the Biorefining Conversions and Fermentation Laboratory at the University of Alberta. The extensive four-and-a-half-year investigation at UofA represented a rewarding journey focused on exploring biorefinery strategies for producing cellulose nanocrystals and fermentable sugars.

First and foremost, I express my profound gratitude to the Almighty God for granting me the strength to navigate through challenges and overcome obstacles. His divine support has been a constant source of fortitude, enabling me to persevere and achieve my goals. In acknowledging the blessings of inner strength, I am grateful for the guidance and resilience provided by the Higher Power, shaping my journey and allowing me to face life's endeavors with courage and determination.

Above all, I extend my gratitude to Professor David C. Bressler, my Ph.D. supervisor, for his invaluable assistance, unwavering support, and patience over the past four and a half years. Dave consistently encouraged me to put forth any ideas while my study and was always accessible when I sought his guidance. Without his guidance and contributions, this thesis would not have taken its current form. Dave's continuous passion for science serves as both an inspiration and a commendable example. I hold him in the highest regard as an outstanding supervisor and offer my deepest thanks for his role not only as a mentor but also as a dear friend.

I extend my thanks to the members of the supervisory committee, Dr. Thava Vasanthan and Dr. Marleny Aranda Saldana, for their keen interest in my research. Their constructive comments, valuable suggestions, and insights during our committee meetings significantly contributed to the refinement of my work.

I am grateful to my former program managers, Dr. Michael Chae and Dr. Justice Asomaning, who introduced me to the world of science and illuminated the path of research. Their remarks and comments consistently provided me with inspiring insights for my study.

Appreciation is also extended to all the students, post-doctoral fellows and Jingui Lan in the Bressler lab team for their generous assistance and suggestions. Their encouragement and support during challenging periods were instrumental in keeping my spirits high. Special thanks to Dr. Dawit Beyene, my first friend at UofA, whose helping hand upon my arrival was truly appreciated. I consider myself fortunate to have forged strong friendships with all of them during my time at UofA.

I would like to extend my sincere gratitude for the invaluable collaboration experienced during my study program with the following organizations: Alberta Pacific (AI-Pac) Forest Industries Inc, Future Energy Systems (FES), FPIInnovation, Alberta Innovate, the Natural Sciences and Engineering Research Council of Canada (NSERC), Novozymes, and the various centers and facilities at the University of Alberta. I express my heartfelt thanks for the generous financial and material support that proved instrumental in bringing my project and PhD program to fruition. I extend my thanks to Dr. Jack Saddler for providing steam exploded poplar samples during my preilemanary experiment. The contributions from these entities have been pivotal, and I am truly appreciative of the opportunities and resources they provided.

My deepest thanks go to my true love, Kalkidan Bedassa, and my children. Kal (yene bicha), you are the most kind-hearted and patient person I have ever known. Your unwavering support, encouragement, and loving care provided me with the energy to carry out experiments and

complete my studies. I am grateful to God for blessing me with the best wife in the world and a profoundly happy life.

Lastly, I wish to express my gratitude to my Emma, Aba, Gashe and Etaba for their unwavering support through prayer. Their consistent prayers have been a source of strength, guiding me and providing a foundation of spiritual encouragement throughout my endeavors. Their heartfelt supplications have undoubtedly played a significant role in my journey, and I am profoundly thankful for the love and positive energy they have showered upon me. My parents' devotion and care, expressed through their prayers, have been a pillar of support, and I am truly blessed to have them by my side.

# Table of Contents

Abstract .....	ii
Preface.....	v
Acknowledgment .....	vii
1. Background.....	1
2. Literature Review.....	5
2.1. Lignocellulose .....	5
2.1.1. Lignin.....	5
2.1.2. Hemicellulose .....	6
2.1.3. Cellulose .....	7
2.2. Cellulose structure.....	8
2.2.1. Molecular structure of cellulose.....	9
2.2.2. Cellulose crystal structure and cellulose polymorphs.....	11
2.3. Challenges in lignocellulose hydrolysis.....	14
2.4. Production and properties of cellulose nanocrystals .....	15
2.4.1. Cellulosic source for cellulose nanocrystals .....	16
2.4.2. Pretreatment on cellulosic materials .....	17
2.4.3. Isolation of cellulose nanocrystals .....	18
2.5. Application of cellulose nanocrystals .....	22
2.6. Challenges on commercial cellulose nanocrystals production.....	23
3. Material and Methods .....	25
3.1. Chemicals.....	25
3.2. Sample collection .....	25
3.3. Hydrothermal and Cellulase treatment for Co-production of Cellulose nanocrystal and fermentable sugar from wood pulp .....	25
3.3.1. Hydrothermal treatment of wood pulp.....	26
3.3.2. Enzyme dosage curve for hydrothermally treated wood pulp .....	27
3.3.3. Enzyme hydrolysis as a function of time .....	27
3.3.4. Sugars and degradation products .....	28
3.3.5. Isolation of cellulose nanocrystal.....	28

3.4.	Evaluation of Steam Explosion pretreatment on the cellulose nanocrystal from Poplar wood	29
3.4.1.	Steam explosion pretreatment.....	30
3.4.2.	Delignification .....	31
3.4.3.	Isolation of cellulose nanocrystal.....	31
3.5.	Steam Explosion and Enzymatic digestion as Pretreatment for Co-production of Cellulose nanocrystal and Fermentable Sugar from Poplar Wood.....	32
3.5.1.	Enzyme dosage curve for poplar and steam exploded poplar wood.....	32
3.5.2.	Enzyme hydrolysis as a function of time .....	33
3.5.3.	Delignification .....	33
3.5.4.	Isolation of cellulose nanocrystals .....	33
3.6.	Characterization of Cellulose nanocrystals .....	33
3.6.1.	Degree of crystallinity.....	33
3.6.2.	Morphology and particle size.....	34
3.6.3.	Zeta potential .....	34
3.6.4.	Thermal stability of CNCs .....	34
4.	Results and Discussion .....	35
4.1.	Hydrothermal and Enzyme treatment for co-production of CNC and fermentable sugars from wood pulp.....	35
4.1.1.	Hydrothermal treatment of wood pulp.....	35
4.1.2.	Enzyme dosage curve for hydrothermally treated wood pulp .....	36
4.1.3.	Enzyme hydrolysis as a function of time .....	37
4.1.4.	Cellulose nanocrystal yield.....	38
4.1.5.	Morphological analysis of cellulose nanocrystals using transmission electron microscope .....	41
4.1.6.	Degree of crystallinity.....	43
4.1.7.	Zeta potential .....	45
4.1.8.	Thermal stability .....	46
4.2.	Evaluation of steam explosion pretreatment on the cellulose nanocrystal yield.....	49
4.2.1.	Delignification of steam exploded poplar.....	49
4.2.2.	Cellulose nanocrystal yield.....	49
4.2.3.	Fourier transform infrared spectroscopy (FTIR) .....	51

4.2.4.	Morphology analysis of CNCs using Transmission Electron Microscope.....	52
4.2.5.	Particle size and zeta potential.....	53
4.2.6.	Degree of crystallinity.....	54
4.2.7.	Thermogravimetric analysis.....	56
4.3.	Steam explosion and enzymatic digestion as pretreatment for co-production of CNC and fermentable sugars .....	57
4.3.1.	Enzyme dosage curve for poplar and steam exploded poplar wood.....	57
4.3.2.	Enzymatic hydrolysis as a function of time.....	58
4.3.3.	Degree of crystallinity of enzyme treated and delignified steam exploded poplar wood	59
4.3.4.	Cellulose nanocrystal yield.....	61
4.3.5.	Characteristics of cellulose nanocrystal from steam explosion and enzymatic treated wood.....	64
4.4.	Comparative analysis of cellulose nanocrystals and sugars yield across the three-biomass conversion pathway .....	67
5.	Conclusion and Future directions .....	70
5.1.	Conclusion.....	70
5.2.	Future directions.....	71
	Reference .....	73
	Appendix A: supplementary material on result discussion.....	85

## List of Tables

Table 4.1 Solid recovery and degradation products of hydrothermally treated pulp.....	36
Table 4.2 Sugar and undigested solid yields from enzymatic treatment of hydrothermally treated pulp for 6–24 h.....	38
Table 4.3 CNC yield from hydrothermal and enzymatic treated pulp.....	41
Table 4.4 Degree of crystallinity of hydrothermal and enzymatic treated wood pulp and CNCs.....	45
Table 4.5 The zeta potential of CNCs from hydrothermal and enzymatic treated pulp. ....	46
Table 4.6 The onset temperature of hydrothermal and enzymatic treated pulp and CNCs .....	48
Table 4.8 Cellulose nanocrystals yield isolated from steam exploded poplar wood .....	51
Table 4.9 Particle size and zeta potential of CNCs isolated from steam exploded poplar wood .	54
Table 4.10 Degree of crystallinity of untreated poplar, steam-exploded poplar, bleached poplar, bleached steam exploded poplar, cellulose nanocrystal from poplar and cellulose nanocrystal from steam exploded poplar.....	55
Table 4.11 Sugar and undigested solid yields from steam explosion and enzymatic treated poplar wood over a period of 6–24 h .....	59
Table 4.12 Degree of crystallinity of steam explosion and enzymatic treated poplar wood .....	60
Table 4.13 CNCs yield from steam explosion and enzymatic treated poplar wood.....	64
Table 4.14 Particle size of CNCs steam explosion and enzymatic treated poplar wood based on transmission electron microscopy (TEM) micrograph analysis .....	65
Table 4.15 Crystallinity, colloidal stability, and degradation temperature of CNCs from steam explosion and enzymatic treated poplar wood.....	66

## List of Figures

Figure 1.1 Hydrolysis to enhance the production of CNCs and the recovery of sugars from wood pulp and poplar wood.....	4
Figure 2.1 The molecular structure of cellulose polymer .....	10
Figure 2.2 Microstructure of cellulose microfibrils showing the highly ordered regions, Semi-crystalline, and less organized ones (amorphous) cellulose. ....	13
Figure 3.1 Integrated hydrothermal and enzymatic treatment with acid hydrolysis for production of cellulose nanocrystal and fermentable sugars. ....	26
Figure 3.2 Isolation of cellulose nanocrystal from steam exploded poplar wood .....	30
Figure 3.3 Steam explosion and enzymatic digestion as pretreatments for co-production of CNC and fermentable sugars .....	32
Figure 4.1 Glucose response curve for hydrothermally treated pulp as function of cellulase dosage.. ....	37
Figure 4.2 Mass balance for CNC isolated from hydrothermally and enzymatic treated pulp. All reported data represent analysis from triplicate samples. ....	39
Figure 4.3 Transmission electron microscopy (TEM) micrographs of CNC isolated from wood pulp (control) and hydrothermal and enzymatic-treated wood pulp.....	42
Figure 4.4 X-ray diffraction pattern of (a) wood pulp (control) and hydrothermal and enzymatic-treated pulp, (b) CNC isolated from wood pulp (control), and hydrothermal and enzymatic-treated wood pulp.....	44
Figure 4.5 Thermographs of (a) wood pulp and hydrothermal and enzymatic treated pulp, (b) CNCs isolated from wood pulp (control) and hydrothermal and enzymatic-treated pulp.....	47
Figure 4.6 Mass balance for CNC isolated from steam exploded poplar wood. . All reported data represent analysis from triplicate samples. ....	50
Figure 4.7 ATR-FTIR spectra: (a) Detail of the region 3700-2700 $\text{cm}^{-1}$ of the FT-IR. (b) Detail of the region 1800-600 $\text{cm}^{-1}$ of the FT-IR. ....	52
Figure 4.8 Transmission electron microscopy image of CNC isolated from (a) control and (b) steam exploded poplar. ....	53
Figure 4.9 Thermographs of untreated poplar, steam-exploded poplar, bleached poplar, bleached steam exploded poplar, cellulose nanocrystal from poplar and cellulose nanocrystal from steam exploded poplar.....	56
Figure 4.10 Glucose response curve as function of cellulase dosage (a) control and (b) steam exploded poplar wood.....	58
Figure 4.11 Mass balance for CNC isolated from steam explosion and enzyme treated poplar wood. All reported data represent analysis from triplicate samples. ....	61
Figure 4.12 Mass balance for CNC isolated from ground poplar (control). All reported data represent analysis from triplicate samples. ....	62

Figure 4.13 CNCs yield from an integrated process beginning with either hydrothermal or steam explosion pretreatment followed by enzymatic hydrolysis and then acid hydrolysis. .... 69

## List of Abbreviations

AGU	: anhydro glucose unit
ATR-FTIR	: Attenuated total reflection fourier transform infrared spectroscopy
CNCs	: cellulose nanocrystals
CrI	: crystallinity index
DP	: degree of polymerization
FPU	: filter paper unit
FTIR	: fourier transform infrared spectroscopy
G	: gram
Gt	: gauche–trans
H	: hour
HP/HT	: high pressure/high temperature
HPLC	: high performance liquid chromatography
kD	: kilodalton
L	: litter
M	: mol/L
Rpm	: revolution per minute
tg	: trans–gauche
TEM	: transmission electron microscopy
TGA	: thermogravimetric Analyzer
Wt %	: weight per unit weight percent
w/v	: weight per unit volume
$\omega$	: torsion angle

XRD : xray diffraction

## 1. Background

Producing bioethanol from lignocellulosic biomass faces significant challenges rooted in the complex composition of the biomass itself. The intricate structure comprising cellulose, hemicellulose, and lignin hinders efficient breakdown into fermentable sugars. Lignin, acting as a protective barrier, inhibits enzymatic access and necessitates energy-intensive separation processes (Malik et al., 2022). Overcoming this challenge requires effective pretreatment methods to make cellulose accessible for enzymatic hydrolysis (Du et al., 2017). These enzymatic approaches are often burdened by high expenses due to the substantial costs associated with the different pretreatment methods and the high cost of cellulase enzyme (Wang et al., 2021; Zhao & Liu, 2019; Zhu et al., 2011). To address these economic challenges, it is imperative to develop biorefinery strategies that not only maximize the recovery of fermentable sugars but also yield additional high-value products from lignocellulosic biomass.

Cellulose is a part of lignocellulose and an abundant natural polymer (Eyley & Thielemans, 2014), comprises highly packed crystalline regions and poorly ordered amorphous chains (Bano & Negi, 2017). The packed crystalline domains are a precursor for cellulose nanocrystals (CNCs), and the amorphous chains can hydrolyze sugars and further fermented to ethanol (Beyene et al., 2017; Wang et al., 2021). CNCs are nano-sized rod-like crystalline particles isolated from different sources of cellulose such as forestry (wood pulp, Beyene et al., 2017), agriculture (sugarcane bagasse, Camargo et al., 2016; Lam et al., 2017), and even bacterial cellulose (Anwar et al., 2015). It is produced from the highly ordered crystalline regions of cellulose by the delamination and fragmentation of the cellulose fibrils (Oun and Rhim 2016; Prasanna and Mitra 2020). The distinct physical and chemical properties of CNCs, such as high surface reactivity, excellent optical properties, biodegradability, and high mechanical strength, makes them a potential candidate for many industrial applications including the production of bioplastics (Kim et al., 2021), inks (Siqueira et al., 2017), and coatings

(Spagnuolo et al., 2022) , as well as being used in nanocomposites for the reinforcement of thermoplastics and thermosets (George & Sabapathi, 2015).

Different methods can be used to produce CNCs, including acid hydrolysis, enzyme hydrolysis, oxidation degradation, and the use of ionic liquids (Xie et al., 2018). Acid hydrolysis with sulfuric acid is the most common method to isolate CNC (Vanderfleet & Cranston, 2021). In this process, the acid is used to dissolve the disordered chains of cellulose under controlled conditions with the resultant release of the crystalline domain. One of the advantages of isolating CNCs using sulfuric acid is that the negatively charged sulfate groups attach on the surface of CNCs, which imparts high colloidal stability to the CNCs in an aqueous solution. However, this method generally produces low yield (Yu et al., 2013; Chen et al., 2015) and loss of sugars in monomeric and oligomeric forms in the acid waste liquor stream (Beyene et al., 2017).

Most studies reported in literature have focused on the acid hydrolysis parameters such as reaction temperature, time, and acid concentration to improve the CNCs yields (Chen et al., 2015; Sousa et al., 2019; Thakur et al., 2020). However, other factors like pretreatment before acid hydrolysis also affects the yield of CNCs. In our group, Beyene *et al.* (2017) reported increase of CNCs yield by 8-18% and 58-86% from 2 h to 10 h enzyme treated filter paper and wood pulp, respectively. Agarwal *et al.* (2018) observed an increase in CNCs yield due to hydrothermal treatment (hot liquid water treatment) and hypothesized that the hydrothermal treatment is responsible for the changing of the torsion angle ( $\omega$ ) of O<sub>6</sub>-C<sub>6</sub>-C<sub>5</sub>-O<sub>5</sub> from gauche-trans (gt,  $\omega=60^\circ$ ) to trans-gauche (tg,  $\omega=180^\circ$ ) orientation in glucose subunits, which favors more interplanar hydrogen bonding between chains and it forms a new CNC precursor that goes into acid hydrolysis and resulting high CNC yield. Beyene *et al.* (2020) observed a similar finding, reporting that hydrothermal treatment improved the CNC yield from wood pulp up to 4-folds as compared to the untreated wood pulp.

This research introduced two novel biorefinery approaches aimed at simultaneously boosting the production of cellulose nanocrystals (CNCs) and fermentable sugars through integrating the high temperature and high-pressure pretreatment with enzyme and acid hydrolysis process. These methods utilized hydrothermally treated wood pulp and steam-exploded poplar as the primary raw materials.

The uniqueness of this study lies in two key aspects. Firstly, it merged hydrothermal treatment with enzyme and acid hydrolysis to address challenges such as minimizing the loss of reusable sugars, reducing the acid requirement, and taking advantage of the crystallization effects resulting from both hydrothermal treatment and cellulase action. This, in turn, led to an increased abundance of CNC precursor material and subsequently elevated the CNCs yield.

Secondly, the research leveraged steam explosion pretreatment in combination with enzyme and acid hydrolysis to simultaneously enhance the production of CNCs and the recovery of sugars from poplar wood. The underlying hypothesis was that the steam explosion pretreatment, when paired with enzyme hydrolysis, effectively breaks down amorphous cellulose into sugars, consequently increasing the composition of CNC precursors available for acid hydrolysis. This strategic approach ultimately resulted in a higher CNC yield.

The objectives were:

- a) Explore the effect of hybrid hydrothermal and enzyme treatment on CNCs yield and fermentable Sugars from wood pulp:
  - Generate hydrothermally treated wood pulp.
  - Identify an efficient cellulase saccharification period that preferentially degrades non-crystalline cellulose and hemicellulose to fermentable sugars from hydrothermally treated pulp.

- Characterize hydrothermal and cellulase treated fiber.
  - Improve CNCs yield from acid hydrolysis of hydrothermally and enzyme treated pulp.
  - Characterize the CNCs isolated from hydrothermally and enzyme treated pulp.
- b) Evaluate the effect of steam explosion pretreatment on the characteristics and yield of CNC from poplar wood.
- c) Investigate the combined effect of steam explosion and enzyme treatment on CNC yield and fermentable sugar from poplar wood:
- Identify an effective cellulase saccharification period that preferentially degraded the amorphous domain and recover fermentable sugars.
  - Improve CNC yield from acid hydrolysis of steam explosion and enzyme treated feedstock that has high CNC precursor concentration.
  - Characterize the CNCs.

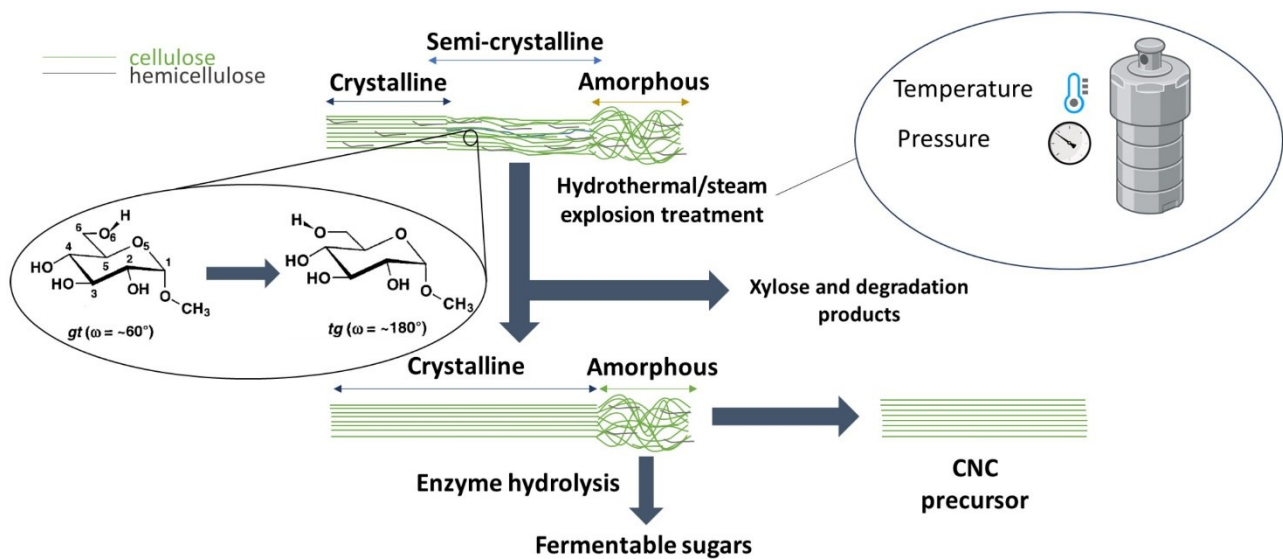


Figure 1.1 Hydrolysis to enhance the production of CNCs and the recovery of sugars from Northern bleached hardwood kraft (NBHK) wood pulp and poplar wood

## 2. Literature Review

### 2.1. Lignocellulose

Lignocellulosic biomass, a complex plant-derived material, possesses a hierarchical structure composed of cellulose, hemicellulose, and lignin. Cellulose, a linear polymer of glucose units, forms crystalline microfibrils, providing strength and rigidity to plant cell walls. Hemicellulose, on the other hand, is a branched polymer containing various sugar monomers and acts as a matrix material, linking cellulose microfibrils and providing flexibility to the overall structure. Lignin, a complex and irregularly structured polymer, surrounds and encrusts cellulose microfibrils, providing rigidity, impermeability, and protection against microbial degradation. The interplay of these three components forms a robust and resistant matrix, creating the challenging nature of lignocellulosic biomass for industrial processes (Isikgor & Becer, 2015; Malik et al., 2022).

Breaking down this intricate structure for bioethanol production involves overcoming the recalcitrance of lignocellulosic biomass. The cellulose microfibrils are shielded by the amorphous hemicellulose and lignin matrix, making it challenging for enzymes to access and hydrolyze cellulose into fermentable sugars. Consequently, effective pretreatment methods are employed to disrupt this matrix, separating the cellulose from hemicellulose and lignin, and rendering it more amenable to enzymatic hydrolysis. Understanding and modifying the complex structure of lignocellulosic biomass are essential steps in developing efficient and economically viable processes for bioethanol production.

#### 2.1.1. *Lignin*

Lignin, a complex polymer, plays a crucial role in the structural integrity of plant cell walls within lignocellulosic biomass. Comprising phenolic compounds such as coniferyl, sinapyl, and p-coumaryl alcohol, lignin forms a three-dimensional network that encases and cross-links with cellulose and hemicellulose (Behr et al., 2021). This intricate matrix provides rigidity, impermeability, and

protection against microbial degradation. The chemical structure of lignin involves various linkages, including ether and carbon-carbon bonds, resulting in a highly branched and heterogeneous macromolecule (Kathahira et al., 2018). The diversity in the composition and bonding arrangements of lignin contributes to its resistance to enzymatic degradation, making its separation from cellulose and hemicellulose a crucial step in lignocellulosic biomass processing for bioethanol production.

The unique composition of lignin and its resistance to degradation pose challenges in the utilization of lignocellulosic biomass for bioethanol production. During pretreatment processes, efforts are made to break down and remove lignin, allowing for enhanced access to cellulose for enzymatic hydrolysis. The structural complexity of lignin, however, makes its complete removal challenging, and strategies are continuously being developed to modify or utilize lignin byproducts in various industrial applications. Understanding the intricacies of lignin structure is paramount for optimizing bioethanol production processes and unlocking the full potential of lignocellulosic biomass as a sustainable feedstock.

### 2.1.2. *Hemicellulose*

Hemicellulose is a branched heteropolymer that constitutes a major component of the complex structure of lignocellulosic biomass. Unlike the cellulose, hemicellulose is an amorphous and more structurally diverse polymer. It consists of a variety of sugar monomers, including glucose, xylose, mannose, galactose, and others, forming a matrix that intertwines with cellulose microfibrils (Rao et al., 2023). The specific composition of hemicellulose varies among plant species, contributing to the diversity of lignocellulosic materials.

The backbone of hemicellulose is typically made up of short chains of sugar units linked by various glycosidic bonds (Huang et al., 2021). The branched nature of hemicellulose arises from side chains

composed of different sugar residues. The complexity and variability in hemicellulose structure make it more susceptible to degradation compared to the highly crystalline cellulose. During the bioethanol production process from lignocellulosic biomass, hemicellulose is often hydrolyzed into its constituent sugars through pretreatment and enzymatic processes, providing additional fermentable substrates alongside cellulose for ethanol production. Understanding the structure of hemicellulose is crucial for developing efficient strategies to break down lignocellulosic biomass into sugars for biofuel production.

### 2.1.3. *Cellulose*

In the last few decades, a considerable increase in research and development of nanocellulose with varying functional properties and morphology from renewable sources had been published (Mishra et al., 2012; Tsukamoto et al., 2013; Rambabu et al., 2016). As the most abundant component in most plants, cellulose is an almost inexhaustible polymeric raw material occurring in nature (Bano & Negi, 2017). It is the major structural component of the plant biomass and provides structural support and protection to the cells. Cellulose is continually produced by different species such as plant, bacteria, tunicates, fungi, and algae every day in the biosphere, providing a total annual production of around  $5 \times 10^{11}$  metric tons (El-Sakhawy et al., 2014; Mahfoudhi & Boufi, 2017). Cellulose also has the advantages of being renewable, biodegradable, and non-toxic to living organisms, including humans.

Cellulose, a substance with a rich historical association, has been utilized for various applications throughout the centuries (Marchessault & Sundararajan, 1983). Natural materials containing cellulose, like wood, have served diverse purposes for thousands of years. Notably, cellulose has been employed as a heat source for cooking and industrial processes, as well as in the construction of buildings, bridges, ships, and furniture. Furthermore, in its nearly pure form found in materials

like cotton and flax fibers, cellulose has been utilized for clothing and as a writing medium since ancient times (Marchessault & Sundararajan, 1983).

Cellulose currently is used as a feedstock in various industries and used to produce a wide variety of products and materials, ranging from packaging to biomedical fields (Asim et al., 2022; Seddiqi et al., 2021). Cellulose is used to produce textile fibers (Björquist et al., 2018), films, and a larger number of cellulose derivatives, such as cellulose ethers and esters (Laxmeshwar et al., 2012). For instance, carboxymethylcellulose is a cellulose derivative utilized in foodstuffs, cosmetics, detergents, paints, coatings, adhesives, and plastics (El-Sakhawy et al., 2014).

In addressing the growing demands for energy, chemicals, and materials in a sustainable manner, cellulose holds considerable significance due to its abundance and renewability. Consequently, extensive research endeavors have been directed towards developing efficient processing technologies for converting this biomass into various valuable bioproducts. As a result, cellulose emerges as a promising resource to produce energy, chemicals, and materials, offering the potential to reduce reliance on petroleum-based products. Simultaneously, it addresses the rising demand for environmentally friendly and biocompatible products while contributing to carbon neutrality.

## **2.2. Cellulose structure**

Despite extensive research on cellulose, its molecular structural features have not been definitively identified. The term "cellulose" was first introduced by the French chemist Anselme Payen in 1838 (Seymour et al., 1989), who, through his studies, revealed that treating various plant tissues with acid-ammonia followed by extraction in water, alcohol, and ether resulted in a consistent fibrous material. Payen determined the molecular formula to be  $C_6H_{10}O_5$  through elemental analysis and noted its isomerism with starch (Klemm et al., 2005).

Therefore, to fully comprehend the macroscopic properties of cellulose, a comprehensive understanding of its structural architecture is crucial, spanning from the atomic scale to the macro scale. This involves consideration of cellulose biosynthesis, its supramolecular structures, and hierarchical organization within the cell wall.

### 2.2.1. *Molecular structure of cellulose*

Cellulose polymer is a semi-crystalline long-chain linear homo-polysaccharide (Mariano et al., 2014). The molecular feature of cellulose arises from repeating  $\beta$ -D-glucopyranose (glucose) units that are covalently linked through acetal functions. This covalent bond known as  $\beta$ -(1,4)-glycosidic bond (Paukszta & Borysiak, 2013). The  $\beta$ -(1,4)-glycosidic bonds link each internal glucose unit with the neighbor unit at C1 and C4 positions. Each glucose molecule in cellulose is referred to as anhydroglucose unit (AGU). The AGUs are joined to one another in head-to-tail orientation and the C–O–C angle between two AGU rings is  $\sim 116^\circ$ . To keep the preferred bond angles of this acetal oxygen bridges formed by  $\beta$  1 $\rightarrow$ 4 links, the planes of subsequent glucoside residues are rotated with respect to each other by  $180^\circ$ , which means that the geometrically repeated element of the cellulose chain is made of two neighboring glucose residues known as cellobiose residues (Klemm et al., 2005). Therefore, cellulose can be deemed as an isotactic polymer of cellobiose. However, the chain length of cellulose is expressed in the number of constituents AGUs (degree of polymerization (DP)). DP is the number of glucose units in cellulose polymers (Rowell et al., 2012). It varies with different types of cellulose sources and the degradation treatments. Originally, DP ranges from several hundred to thousand. While after degradation reactions, the degree of polymerization could decrease to 300-1700 in cellulose. Some regenerated celluloses could even have a DP value of 250-500 (Klemm et al., 2005).

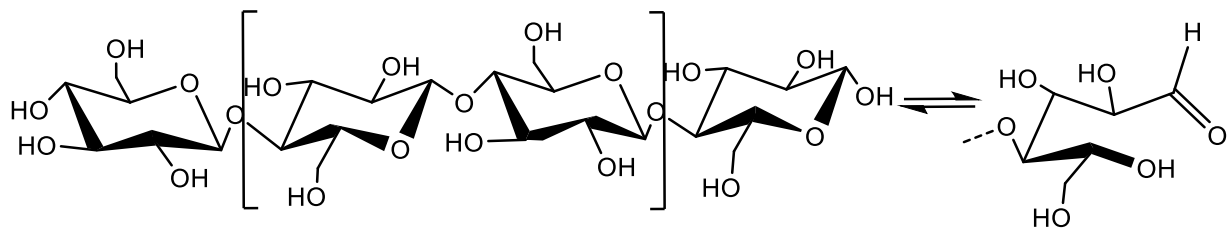


Figure 2.1 The molecular structure of cellulose polymer (Börjesson & Westman, 2015)

From Figure 2.1, each AGU ring consists of three hydroxyl groups. The hydroxyl group at the C6 position is a primary alcohol, while the hydroxyl groups at the C2 and C3 positions are secondary alcohols. These groups of hydroxyls are accessible sites for chemical reactions and the reactivity of these hydroxyl groups is usually controlled more by steric factors and molecular interactions (Börjesson & Westman, 2015). The cellulose molecule has a directional chemical asymmetry with respect to the termini of its chain axis. One end is a hemiacetal which is in equilibrium with the aldehyde structure (i.e., the reducing end); and the other end has a pendant hydroxyl group, the nominal non-reducing end (Habibi et al., 2010).

Due to the  $\beta$  configuration, molecular chains of cellulose are fully extended to form long, straight, chains, which is hexacalled shaped. The glycosidic bonds and the ring substituents are all positioned equatorially in the ring plane, while the hydrogen atoms are positioned axially in the vertical position. In this way all  $\beta$ -D-glucopyranose rings endorse a  ${}^4C_1$  chair conformation, which is the lowest free energy conformation of the molecule. Moreover, the hydroxyl groups jut out laterally along the extended chain and, consequently, these hydroxyl groups are readily available for hydrogen bonding, either intramolecular or intermolecular chains (Kovalenko, 2010; Rowell et al., 2012).

The presence of intramolecular and intermolecular hydrogen bonds is highly relevant to single-chain conformation of cellulose, since they hinder the free rotation of the rings along their linking glycoside bonds resulting in the stiffening of the cellulose chain and responsible to interchain cohesion, and thus, also to the aggregation state of cellulose from sheet-like to fibrillar aggregates, also known as

supramolecular structure, respectively. Moreover, these intramolecular hydrogen bonds between adjacent AGU rings stabilize the glycosidic linkage insomuch that the rigidity and the linear integrity of the polymer chain are enhanced (Festucci-Buselli et al., 2007).

Therefore, this very complex and strong hydrogen bonding network present in cellulose is extremely important for the characteristics of cellulose, such as reactivity, solubility, thermal stability, and mechanical properties. Besides The hydroxyl groups determine the crystalline structure and the physical properties of cellulose, since they can form different intermolecular hydrogen bonds or intramolecular hydrogen bonds, which could build a strong sheet structure in the linear polymer and provide strong stiffness for polymer chains (Gupta et al., 2019). This also might result in excellent thermal stability properties and make cellulose insoluble in water or most organic solvents.

### *2.2.2. Cellulose crystal structure and cellulose polymorphs*

Polymorphism is a fundamental characteristic of the solid state. It refers to the ability of a chemical compound's solid phase to exist in multiple crystal structures, even though the composition remains the same. These different crystal structures can exhibit distinct properties. The term "polymorphism" originates from the Greek words "poly," meaning "many," and "morph," meaning "form or shape." Therefore, polymorphism can be translated as "many forms." Each unique crystal structure of a compound is referred to as a polymorph or allomorph. Polymorphs have varying arrangements and conformations of molecules within the crystal lattice (Mahmud et al., 2019).

Polymorphism is quite common for crystals of organic compounds whose molecules contain groups capable of hydrogen bonding. The repeating unit of cellulose, or cellobiose, includes six hydroxyl groups and three oxygen atoms. Due to the presence of six hydrogen bond donors and nine hydrogen bond acceptors provides several possibilities for forming various hydrogen bond systems and the presence of different mutual arrangements of the glucopyranose rings and possibility of

conformational changes of the hydroxymethyl groups leads the cellulose chains to have different crystal packings such as cellulose I, II, III and IV and their varieties I $\alpha$ , I $\beta$ , III<sub>I</sub>, IV<sub>I</sub>, III<sub>II</sub> and IV<sub>II</sub> (Festucci-Buselli et al., 2007; Kovalenko, 2010). Most of these polymorphs result from chemical treatments of cellulose I. This cellulose I differ by unit cell parameters and polarity of the constituting chains, as well as the hydrogen bond patterns established between them (Lavoine et al., 2012; Srivastava et al., 2020).

The many hydroxyl groups readily available for hydrogen bonding associated to “extended” chain structure of cellulose macromolecule causes the chains, or part of them, to become sufficiently aligned parallel to each other forming a compact packing that gives rise to three-dimensional highly ordered structures (crystal like) of long-range, viz. order extending to distances of hundreds or thousands of times the molecular size of the repeating unit. However, seeing that the chains are usually longer than these crystalline regions, they are thought to pass through several different crystalline regions which have less ordered areas in between them. These less-ordered regions are also frequently referred to as amorphous or non-crystalline regions. Unlike the crystalline region, the cellulose chains in the amorphous region are arranged irregularly and loosely, so the distance between molecules is larger. The amorphous state is thus characterized by an absence of long-range ordering and greater orientation disorder of cellulose chains.

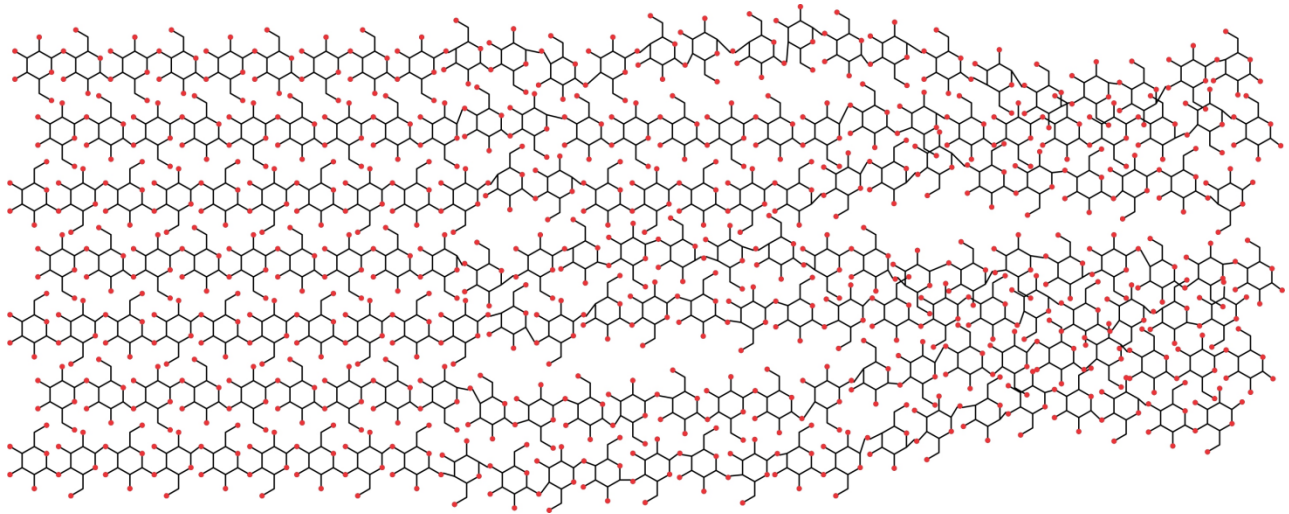


Figure 2.2 Microstructure of cellulose microfibrils showing the highly ordered regions, Semi-crystalline, and less organized ones (amorphous) cellulose.

The hydrogen bonds between hydroxyl groups could form the microfibrils, which are the arrangement of the fibrillar bundles leading to the higher amount of crystalline regions than the amorphous regions (Hon, 1994). Furthermore, the sources of cellulose could also determine the fractions of crystalline and amorphous regions. For instance, the crystalline region content is much higher in the cellulose obtained from cotton. On the other hand, there are much higher amount of amorphous regions for regenerated cellulose.

The crystalline region is the important factor for the crystallinity of cellulose. The degree of crystallinity varies from 60-80% depending on various sources of cellulose. Cellulose I has two allomorphs, which are allomorphs I $\alpha$  and I $\beta$ . Cellulose I $\alpha$  is mainly stored in lower plants, while I $\beta$  is dominant in higher plant cellulose (Atalla & VanderHart, 1984). Both lattices present the hydrogen bonds between polysaccharide chains inside the layer, even though the hydrogen bond patterns are different. In addition, one research shows that crystallinity of I $\alpha$  is higher than in cellulose I $\beta$ .

The amorphous regions in cellulose have relatively lower density than crystalline regions, since the cellulose chains are oriented randomly with irregular arrangement (Li et al., 2009). The higher amorphous fraction results in the higher accessibility to accept the attack by the other molecules such

as acid. In general, nanocrystalline cellulose could be produced after chemical treatments that have the capable of removing most of amorphous regions and leaving the crystalline regions intact in the cellulose materials.

### **2.3. Challenges in lignocellulose hydrolysis**

Lignocellulose hydrolysis for ethanol production encounters formidable challenges, particularly in the realms of pretreatment and enzyme cost, intricately linked to the complex structure of lignocellulose. The structural composition of lignocellulose, comprised of cellulose, hemicellulose, and lignin, forms a robust matrix that impedes efficient hydrolysis. The intricate association of these components necessitates effective pretreatment strategies to break down the recalcitrant structure, with the aim of facilitating enzymatic access to cellulose. However, identifying economically viable pretreatment methods that selectively target lignin while preserving cellulose and hemicellulose integrity remains a significant hurdle. Moreover, the harsh conditions often required during pretreatment may yield inhibitory by-products, complicating subsequent fermentation processes and highlighting the need for precision in optimizing pretreatment parameters (Bura et al., 2009).

Enzymatic hydrolysis represents the heart of the cellulose-to-ethanol conversion, where cellulase enzymes play a central role in breaking down cellulose into glucose. Cellulase hydrolysis of lignocellulosic biomass involves a complex synergistic interplay of enzymes to break down the intricate structure of cellulose, hemicellulose, and lignin. The process begins with endo- $\beta$ -1,4-glucanases, which cleave internal  $\beta$ -1,4-glycosidic bonds within the cellulose chains, generating shorter oligomers. These shorter chains are then targeted by exo- $\beta$ -1,4-glucanases (cellobiohydrolases), which act from the chain ends, releasing cellobiose units. Simultaneously,  $\beta$ -glucosidases hydrolyze cellobiose into glucose (Hall et al., 2010). Hemicellulose degradation involves various enzymes, such as xylanases and mannanases, which break down hemicellulose into

monomeric sugars (Houfani et al., 2020). The synergistic effect arises as these enzymes work collaboratively, with the endo- and exo-acting enzymes complementing each other in cellulose breakdown. Lignin, acting as a barrier, is also partially disrupted during this process, aiding access to cellulose and hemicellulose. The concerted action of cellulases in lignocellulose hydrolysis enhances the efficiency of biomass conversion, allowing for the release of fermentable sugars that can be subsequently utilized in biofuel production.

One major challenge lies in the cost and efficiency of these enzymes (Liu et al., 2019). Cellulases are expensive, and optimizing their performance to achieve high sugar yields within an economically viable framework remains a persistent challenge. Additionally, cellulose's inherent resistance to enzymatic breakdown due to its crystalline structure necessitates continuous research to develop or enhance enzymes that can efficiently tackle this complexity. The synergy between pretreatment and enzymatic hydrolysis is critical, and advancements in both areas are essential for overcoming the challenges associated with cellulose hydrolysis and realizing a cost-effective and sustainable ethanol production process (Geddes et al., 2011).

#### **2.4. Production and properties of cellulose nanocrystals**

Producing CNCs involves extracting and refining cellulose from diverse sources like forestry (wood pulp, (Beyene et al., 2017), agriculture (sugarcane bagasse, Camargo et al., 2016; Lam et al., 2017), and even bacterial cellulose (Anwar et al., 2015). Acid hydrolysis and enzymatic hydrolysis stand out as the predominant techniques in CNC production (Nagarajan et al., 2021). Acid hydrolysis entails subjecting cellulose fibers to treatment with potent acids, typically sulfuric acid, selectively removing cellulose's amorphous regions and leaving behind highly crystalline nanocrystals. Despite its efficacy, the acid hydrolysis method raises environmental concerns due to the use of strong acids, necessitating meticulous by-product and waste management (Vanderfleet & Cranston, 2021).

Mechanical methods involve physically breaking down cellulose fibers into nanocrystals, utilizing techniques like grinding and homogenization to achieve size reduction. While simpler, these mechanical processes may yield broader size distributions and reduced control over final properties compared to chemical methods (Mohd Amin et al., 2015; Rana et al., 2021). Enzymatic hydrolysis, a milder and eco-friendly alternative to acid hydrolysis, employs cellulase enzymes to break cellulose down into nanocrystals. The specificity of enzymes in cleaving cellulose chains offers a more controlled and selective approach to nanocrystal production (Rana et al., 2021; Raza & Abu-Jdayil, 2022; Xie et al., 2018). Hybrid strategies balance precision and scalability, integrating chemical, enzymatic, and mechanical processes. These methods enhance CNC production efficiency, enabling a more tailored nanocrystal synthesis. The choice of the production method hinges on the specific requirements of the intended application. Ongoing exploration and optimization of these methods aim to improve cellulose nanocrystal production's efficiency, sustainability, and scalability, contributing to the expanding field of nanomaterials with diverse applications across industries.

#### 2.4.1. *Cellulosic source for cellulose nanocrystals*

Sustainable materials from renewable resources have attracted immense research interest during the last two decades owing to their potential for producing several high value products with environmentally friendly advantages. CNCs have been extracted from a broad range of cellulose sources, e.g., from higher plants, like poplar (Agarwal et al., 2018; Zhao et al., 2019), and algae, sea animals, such as tunicates, and bacteria, and in principle it could be extracted from almost any cellulosic material (Druzhinina et al., 2017; George & Sabapathi, 2015). In practice, for most studies, researchers have shown preferences to commercial microcrystalline cellulose (MCC), filter paper, bleached wood pulp or related products, owing to their purity and availability in laboratories.

The properties and morphological features of the CNCs such as crystallinity, aspect ratio, specific surface area, crystal structure, shape, and size, depending on the source of the original cellulose, which is linked to the biosynthesis of cellulose microfibrils, and the isolation process of the CNCs including any pretreatment or deconstruction processes. Therefore, specific pretreatments and extraction procedures have been developed depending on the source of cellulose (Brinchi et al., 2013).

#### 2.4.2. *Pretreatment on cellulosic materials*

Cellulose microfibrils consists of crystalline domains interspersed with disordered amorphous regions. The preparation of cellulose nanocrystals involves a chemical hydrolysis process to dissolve amorphous chains and release crystalline domains from cellulose fibers (Hon-meng et al., 2015). But before acid hydrolysis, cellulose fibers need to be treated and purified in order to obtain the desired crystallinity (Sundari & Ramesh, 2012). Therefore, some mechanical and chemical pretreatments are necessary for cellulose purification.

Size reduction of the lignocellulosic biomass is the prior step using mechanical treatment with high shear and energy transfer to form uniform size and improve the swelling capacity in water (Zimmermann et al., 2010). Then the ground fibers are dewaxed in a soxhlet apparatus to remove the dirt or waxing substances and make fibers easy to split. The dewaxed cellulose fiber, since it is embedded by hemicellulose and lignin, requires chemical treatment for purification. These materials are necessary to be removed to obtain pure cellulosic fibers prior to extraction of CNCs (Zhao et al., 2019).

The alkaline and bleaching treatment is good for removing hemicellulose, lignin, pectin, and wax in the fibers. It increases the accessibility of cellulose to enzyme/acid hydrolysis (Adney et al., 2009). Bleaching treatment is always followed by alkali treatment to remove lignin residue in the fibers.

Various chemical agents are also used based on different cellulose sources during bleaching processes (Hon-meng et al., 2015; Hubbell & Ragauskas, 2010). This process could further remove the lignin and hemicellulose, thus isolating more pure cellulose fibers to achieve the higher crystallinity of CNCs. And some research also found the CNCs obtained from fibers after bleaching procedure have more stable thermal stability than that from no bleaching treatment (Shin et al., 2012).

#### 2.4.3. *Isolation of cellulose nanocrystals*

Cellulose microfibrils consist of packed crystalline domains interspersed with disordered amorphous regions and these packed crystalline regions are a precursor for CNCs. CNCs have high crystallinity with a diameter of less than 100 nm and length less than 500 nm (Xie et al., 2018), the preparation of CNCs involves the dissolution of amorphous chains and release crystalline domains from cellulose fibers. CNCs are usually isolated from cellulose pulp through acid hydrolysis or enzymatic hydrolysis. The acid hydrolysis processes need to go through very harsh reaction conditions which usually require concentrated acid, while the enzymatic hydrolysis process requires a long time (Beyene et al., 2017; Felix Santana et al., 2019).

The first successful CNC was prepared by Nickerson and Habrle in 1947 through hydrolyzing cellulose with hydrochloric acid and sulfuric acid (Xie et al., 2018). In 1951, Rånby prepared the stable CNCs colloidal suspensions through sulfuric acid hydrolysis of wood fiber (Rånby, 1951). After that, a lot of research has been done by different researchers. The dominant principle of CNCs preparation is to dissolve amorphous regions in cellulose chains and release the crystalline regions. Acid hydrolysis is the most popular and conventional approach to isolate nanocrystalline cellulose. However, some novel methods have been developed recently for improving CNCs properties and changing the defects arising from using a large amount of acid, such as enzymatic hydrolysis, ionic liquid, organic acid hydrolysis, and subcritical hydrolysis.

## **Acid hydrolysis**

### *I. Mineral Acid Hydrolysis.*

mineral acid hydrolysis is the most popular method for the isolation of CNCs. CNCs have been extracted from a broad range of cellulose sources by mineral acid hydrolysis, such as wood pulp, poplar, rice straw, and cucumber peels (Agarwal et al., 2018; Beyene et al., 2017; Moradbak et al., 2018; Prasanna & Mitra, 2020; Trilokesh & Uppuluri, 2019; Zhao et al., 2019). The mechanism is that the hydrogen ions from acid can easily attack the amorphous regions of cellulose to break the 1,4- $\beta$ -glycoside bonds, resulting in the hydrolysis of amorphous regions, while the crystalline region of cellulose could be kept in the process which is attributed to the inherent compact structure that prevented the permeation of the acid. Therefore, the relatively complete crystalline structure of CNCs can be obtained by the hydrolysis of mineral acid.

The main used mineral acids are sulfuric acid (Bano & Negi, 2017; Bondeson et al., 2006; P. Lu & Hsieh, 2010), hydrochloric acid (Yu et al., 2013), and phosphoric acid (Camarero Espinosa et al., 2013; Tang et al., 2015). Isolation of CNCs using sulfuric acid is the most used method and can produce a negative surface charge on the particles which leads to more stable suspension. In general, the hydrolysis process using sulfuric acid needs the sulfuric acid concentration to be 60–65%, reaction temperature to be 40–50°C, and reaction time to be 30–120min. However, the yield of CNCs is less than 20wt.% due to the excessive degradation. Agarwal *et al.* (2015) found that the yield of CNCs could be significantly improved by decreasing the concentration of sulfuric acid. For example, the yield of CNCs could reach 78% when 58 wt.% sulfuric acid was used. CNCs from sulfuric acid hydrolysis have poor thermal stability due to the sulfate group which is a significant barrier for thermal process in composites. The thermal stability of CNCs can be improved through neutralization with NaOH. The morphology of CNCs can also be modified by controlling the reaction conditions.

Hydrochloric acid was also commonly used for the preparation of CNCs. The common acid concentration, reaction temperature, and reaction time are 2.5 N–6.0N, reflux temperature, and 2–4 h, respectively (Araki et al., 1998). The CNCs prepared by hydrochloric acid are easily flocculation in water as it lacks charge on the surface of CNCs. But the thermal stability of CNCs by HCl is higher than that by H<sub>2</sub>SO<sub>4</sub>. Yu *et al.*, used hydrochloric acid to treat raw cellulose materials under hydrothermal conditions. The crystallinity of the resultant CNCs was 88.6% with high yield of 93.7% (Yu et al., 2013). The maximum degradation temperature was 363.9 °C which was determined by TGA analysis.

## *II. Organic Acid Hydrolysis*

Recently, organic acid (like formic acid, oxalic acid, malic acid) potentially used for the preparation of CNCs since organic acid is mild, recyclable, and environment-friendly and low corrosiveness (Fu et al., 2020; Li et al., 2015; Xu et al., 2017). However, to improve hydrolysis efficiency, higher temperature and longer reaction time are necessary because of the weak acidity of organic acid. Li and coworkers reported a two-step strategy to produce CNCs from bleached chemical pulp under mild conditions (Li et al., 2015). In the first stage, formic acid was used to hydrolyze the amorphous region of cellulose and release CNCs. In the second stage, the generated CNCs were further oxidized by TEMPO to increase the surface charge. The results showed that the CNCs modified by TEMPO have much higher crystalline and much more surface charge.

### ***Enzyme hydrolysis***

The concentrated acid used in the acid hydrolysis procedures is hazardous, toxic, and corrosive; hence highly corrosion-resistant reactor and extreme precaution in material handling are needed in the process. This makes acid treatment an expensive route. Furthermore, the concentrated acid should be recovered after treatment to make the method economically and environmentally feasible. However, the loss of reusable sugars from hydrolysis of amorphous cellulose in the acid waste stream, and

reaction of the acid with sugars in the waste stream reduces acid recovery efficiency and increase the cost (Beyene et al., 2017). Due to the above facts, as compared with acid hydrolysis method, enzymatic fabricating of CNCs is a less expensive alternative preparation technique that removes or reduce the need for harsh chemicals and necessitates much less energy for mechanical fibrillation and heating. Furthermore, enzymes that selectively degrade the amorphous domains of cellulose fibers, and do not considerably digest the crystalline areas, result in CNCs that preserve a hydroxyl group surface chemistry which allows for easier chemical manipulation, and thus an expanded commercial potential(Filson et al., 2009).

Enzymatic routes for the synthesis of CNCs have been found to offer the potential for acceptable yields, advanced selectivity, and milder operating conditions in comparison to the chemical processes. Exploring a variety of CNCs production methods using enzymes, cellulose samples from loblolly pine wood underwent progressive delignification and enzymatic hydrolysis, revealing that the removal of lignin creates pores and enhances internal surfaces for improved enzyme access to cellulose (Agarwal et al., 2013). Similarly, fresh Douglas-Fir wood chips were mechanically pretreated, enzymatically hydrolyzed using CTec2 and HTec2 enzymes, and subjected to neutral sulfite delignification. This process resulted in the co-production of CNCs, sugars, lignosulfonates, and upgraded cellulose, highlighting the importance of emphasizing control over processing conditions for a balanced distribution of products (Du et al., 2017). Additionally, cotton linters, enzymatically treated with cellulase followed by acid hydrolysis, demonstrated a 9% increase in CNC yield compared to untreated fibers (Beltramino et al., 2016). Sugarcane bagasse, after steam explosion, alkaline delignification, and alkaline peroxide bleaching, underwent enzymatic hydrolysis using Cellic CTec2, yielding superior CNCs compared to those from acid or enzymatic hydrolysis alone (Pereira & Arantes, 2020). Furthermore, filter paper and wood pulp were subjected to enzymatic hydrolysis with cellulase cocktail enzyme solution (NS 51129), then acid hydrolyzed.

These studies demonstrated the dual benefits of ethanol production and high-quality CNC co-production (Beyene et al., 2017; J. Wang et al., 2021). These findings suggest that combining enzymatic hydrolysis with other pretreatment steps can improve the separation of by-products, enhance the CNCs yield, and even improve their quality.

However, this technique is also still hindered by economical (i.e., high cost of cellulase enzyme) and technical (rate limiting step of cellulose degradation with a long processing period) constraints. The slow rate of enzymatic hydrolysis has been found to be affected by numerous factors that also comprise structural features resulting from pretreatment and enzyme mechanism (Dai et al., 2018; Du et al., 2017).

## **2.5. Application of cellulose nanocrystals**

CNCs represent state-of-the-art nanomaterials derived from cellulose. They are distinguished by their renewable nature, biodegradability, and exceptional mechanical and optical properties (Grishkewich et al., 2017). In recent years, CNCs have attracted considerable attention due to these attributes, and the production process can be tailored to precisely control the size, aspect ratio, and surface chemistry of the nanocrystals, allowing for customization based on specific applications (Vanderfleet & Cranston, 2021). One of the most promising applications of CNCs lies in developing biocompatible materials for medical and pharmaceutical purposes. CNCs, owing to their biodegradability and low toxicity, are under exploration for use in drug delivery systems, wound healing, and tissue engineering. These nanocrystals can be functionalized to enhance compatibility with biological systems, providing a versatile platform for medical advancements (Lam et al., 2017; Malik et al., 2022).

The outstanding mechanical properties of CNCs, including high tensile strength and stiffness, make them ideal candidates for reinforcing polymer nanocomposites. Incorporating CNCs into materials

such as plastics and composites enhances their mechanical performance without a significant increase in weight, extending this application to various industries, from automotive to aerospace, where lightweight and robust materials are in high demand (Calvino et al., 2020). Cellulose nanocrystals have shown promise in enhancing paper and packaging materials' strength and barrier properties. By incorporating CNCs into paper products, manufacturers can improve paper strength, reduce weight, and increase resistance to moisture, ultimately leading to more sustainable and durable packaging solutions (Andrade et al., 2022; Xiang et al., 2022). In the food industry, CNCs are being explored as additives to enhance packaging materials' mechanical and barrier properties. The nanocrystals can help extend the shelf life of perishable goods by improving the packaging's resistance to gases and moisture. Additionally, CNCs can be employed as thickeners or stabilizers in food formulations due to their biocompatibility (Mu et al., 2019; Zhang et al., 2023).

## **2.6. Challenges on commercial cellulose nanocrystals production**

The commercial production of CNCs faces several challenges that hinder its widespread adoption in various industries. Primarily related to environmental impact, energy consumption, and scalability. The reliance on strong acids, such as sulfuric acid, raises environmental concerns due to waste disposal and the overall ecological footprint of the process (Beyene et al., 2017). Energy-intensive conditions, including elevated temperatures and prolonged reaction times, contribute to high production costs and hinder the sustainability of CNC manufacturing. Optimizing these methods to ensure consistent CNC quality, yield, and cost-effectiveness remains a key challenge for commercial viability (Raza & Abu-Jdayil, 2022).

Another obstacle in commercial CNC production is Scalability. While laboratory-scale methods can produce CNCs with high quality and purity, transferring these processes to large-scale industrial settings is complex. Maintaining consistent quality and yield becomes challenging when scaling up

production. Several manufacturing facilities have been constructed or are under development, aiming to increase CNC production to multiple tons annually. Notably, in January 2012, CellForce inaugurated a plant dedicated to cellulose nanocrystal production, targeting a daily output of 1 ton. Despite these efforts, a substantial challenge lies in the development of practical applications for cellulose nanocrystal-based materials, even though considerable information on potential uses has been identified and demonstrated in laboratory settings (Lin, 2014) .

### **3. Material and Methods**

#### **3.1. Chemicals**

Acetic acid ( $\text{CH}_3\text{COOH}$  >99%), calcium carbonate ( $\text{CaCO}_3$  >99%), and sulfuric acid ( $\text{H}_2\text{SO}_4$ , 72% and 95 – 98%) were acquired from Sigma-Aldrich (Oakville, ON, Canada). Sodium hydroxide ( $\text{NaOH}$ , 96%) and sodium chlorite ( $\text{NaClO}_2$  80%) were purchased from Fisher Scientific Company (Toronto, ON, Canada). Sodium chlorite and acetic acid were used to remove lignin from poplar and steam-exploded poplar wood. Sulfuric acid was used for acid hydrolysis process to generate CNCs and sodium hydroxide was also used to neutralize the process after the CNCs production.

#### **3.2. Sample collection**

The poplar wood and Northern bleached hardwood kraft (NBHK) wood pulp ( $79 \pm 1$  % cellulose,  $21.2 \pm 0.6$  hemicellulose, and  $4.1 \pm 0.1$  % lignin (Beyene et al., 2017)) were procured from Alberta Pacific Forest Industries Inc. (Al-Pac Inc, Edmonton, AB, Canada) and the poplar wood was transported to FPInnovation (Quebec, QC, Canada) for steam explosion pretreatment. Poplar wood and wood pulp were used to produce CNCs and fermentable sugars. Cellulase enzymes (NS 51129), consisting of endoglucanase, cellobiohydrolase, and  $\beta$ -glucosidase enzymes, were generously supplied by Novozymes® A/S (Bagsvaerd, Denmark). The untreated poplar wood was milled using Retsch ZM 200 Ultra Centrifugal Mill (Newton, PA, USA) while running at 8000 rpm and passing through a 0.15 mm screen and used as a control for CNC isolation for the second and third objective.

#### **3.3. Hydrothermal and Cellulase treatment for Co-production of Cellulose nanocrystal and fermentable sugar from wood pulp**

The objective of this research was to enhance the yield of CNC derived from Northern bleached hardwood kraft (NBHK) wood pulp by employing a hybrid process. This process integrates hydrothermal treatment with enzymatic hydrolysis and acid hydrolysis. The underlying hypothesis

was that hydrothermal treatment and annealing after the treatment induced the crystallization of semi-crystalline/amorphous cellulose chains, generating additional CNC precursors. Subsequently, enzymatic hydrolysis breaks down and liberates the amorphous component into sugars. This sequential methodology was anticipated to augment CNC yield during the ensuing acid hydrolysis phase.

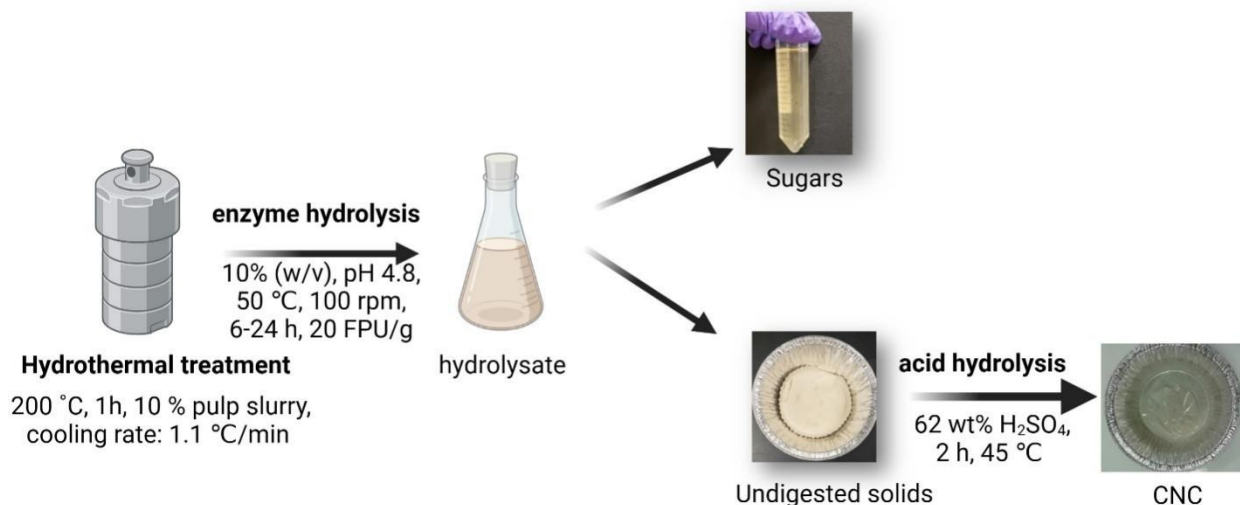


Figure 3.1 Integrated hydrothermal and enzymatic treatment with acid hydrolysis for production of cellulose nanocrystal and fermentable sugars.

### 3.3.1. Hydrothermal treatment of wood pulp

Hydrothermal treatment of the wood pulp suspension (10 % solid consistency) was carried out in batch mode for 1 hour at 200 °C with stirring of 100 rpm using Parr® High Pressure/High Temperature reactor (Parr Series 4580 5.5 L HP/HT reactor and Parr 4848 controller, Parr Instrument Company, Moline, IL, USA). The reactor vessel and the lines in the system were purged with nitrogen three times. The starting pressure and hold time were 0.1 MPa (atmospheric pressure) and 1.5 h, respectively. The reaction was cooled using a chiller at a cooling rate of 1.1 °C/min.

After pretreatment, liquid and solid fractions were separated under vacuum filtration. The solid fraction was washed with deionized water to remove residual liquid, filtered again, and then dried in the oven at 105 °C, and solid recovery was calculated based on Equation 3.1. The liquid fraction was stored in the refrigerator until further analysis.

$$\text{Solid recovery (wt \%)} = \frac{W_2}{W_1} * 100\% \quad (3.1)$$

Where  $W_1$  is the mass of the sample (g) before hydrothermal treatment, and  $W_2$  is the mass of the sample after hydrothermal treatment (g).

### 3.3.2. *Enzyme dosage curve for hydrothermally treated wood pulp*

The determination of the optimal cellulase dosage was accomplished by creating a cellulase dosage response curve through the hydrolysis of hydrothermally treated wood pulp, utilizing a solid consistency of 10% w/v and a cellulase loading range of 5-30 FPU/g. The hydrolysis process was conducted in a shake flask, buffered with a 0.05 M sodium citrate solution, at a temperature of 50 °C and a pH of 4.8. The flask was incubated for 24 hours at a speed of 100 revolutions per minute.

### 3.3.3. *Enzyme hydrolysis as a function of time*

Enzymatic hydrolysis of hydrothermally treated pulp was conducted at a solid concentration of 10% (w/v) in 50 mM sodium acetate buffer (pH 4.8) at 50 °C with 100 rpm agitation using cellulase enzyme (20 FPU/g). The extent of enzymatic hydrolysis as a function of time was investigated.

After enzyme hydrolysis, the hydrolysates were separated under vacuum filtration. The undigested solid was washed with deionized water and filtered again, and then dried in the oven at 105 °C, and undigested solid was calculated based on Equation 3.2.

$$\text{Undigested solid (wt \%)} = \frac{W_4}{W_3} * 100\% \quad (3.2)$$

Where  $W_3$  is the mass of hydrothermally treated pulp (g) used for enzyme hydrolysis, and  $W_4$  is the mass of the sample after enzyme hydrolysis (g).

#### 3.3.4. *Sugars and degradation products*

Glucose and xylose sugar yields in the liquid fractions resulting from hydrothermal and enzyme treatments were assessed using a high-performance liquid chromatography (HPLC) system (Agilent 1200, Santa Clara, California, USA) equipped with a refractive index detector (RID, Agilent 1100 series, Agilent Technologies, Santa Clara, California, USA). The samples (20  $\mu$ L injection volume) were separated on an HPX-87P column (Bio-Rad Aminex, Hercules, California, USA) using water as the mobile phase, flowing at 0.5 mL/min at 80 °C for 40 minutes. For the liquid fraction from hydrothermal treatment, degradation products were separated on an HPX-87H column (Bio-Rad Aminex, Hercules, California, USA). The column was eluted with 5 mM H<sub>2</sub>SO<sub>4</sub> at a flow rate of 0.5 mL/min at 60 °C for 90 minutes. Refractive index and ultraviolet detectors were employed to analyze organic acids (acetic and formic acids) and sugar degradation products (hydroxymethyl furfural at 284 nm and furfural at 275 nm), respectively. Calibration curves were generated by simultaneously running standards of sugars and degradation products at varying concentrations on HPLC.

#### 3.3.5. *Isolation of cellulose nanocrystal*

CNCs were extracted according to the method (Beyene et al. (2017) with some modifications. Briefly, 5 g of hydrothermal and enzyme treated pulps were hydrolyzed with 62 wt % H<sub>2</sub>SO<sub>4</sub> (8 % w/v, solid to acid ratio) for 2 h at 45 °C and 200 rpm in a water bath. The reactions were halted by diluting with 10-fold (v/v) cold deionized water. The CNC suspensions were centrifuged (Avanti J-26 XP, JLA 8.1000 fixed angle rotor) at 6,400  $\times$  g for 10 min to get the precipitates, and the acid solutions were

decanted. The CNCs precipitate was re-suspended in deionized water, and the pH was adjusted to 7 using NaOH (10 %, w/v). The resuspended CNCs were centrifuged at  $3,700 \times g$  for 10 min to remove salts in a liquid phase formed by neutralization. The CNCs precipitate was resuspending in deionized water followed by centrifugation until the supernatant became turbid. Further, the supernatant was dialyzed with deionized water for three to five days using a regenerated cellulose membrane tube with 12–14 kD molecular weight cut off (Spectrum™ Spectra/Por™, Rancho Dominguez, CA, USA). The CNCs obtained after acid hydrolysis and dialysis, were freeze dried (Labconco ‘Freeze 12’ Freeze dryer). The yield was calculated using the equation developed by (Beyene et al., 2017) as shown in Equation 3.3 and 3.4.

$$CNC \text{ yield (wt \%)} = \frac{W_6 * F}{W_5} * 100\% \quad (3.3)$$

$$Overall \text{ CNC yield (wt \%)} = \frac{CNC \text{ yield} * \text{solid recovery} * \text{undigested solid}}{100\%} \quad (3.4)$$

Where Equation 3.3: CNC yield (wt % fixed mass (5 g) used during acid hydrolysis reaction), Equation 3.4: Overall CNC yield (wt % the starting material). Where  $W_5$  is the mass of the sample (g) before acid hydrolysis,  $W_6$  is the mass of oven-dried CNC (g),  $F$  is the ratio of the colloid's total weight to that of the aliquot.

### **3.4. Evaluation of Steam Explosion pretreatment on the cellulose nanocrystal from Poplar wood**

This study aims to increase CNC yield isolated from poplar wood through integrating steam explosion pretreatment with acid hydrolysis. We hypothesized that the high temperature and pressure during steam explosion pretreatment and cooling (annealing) after the treatment facilitate the crystallization

of semi-crystalline/ non-crystalline cellulose by reorienting the cellulose molecule to form new CNC precursors, which will increase the CNC yield during acid hydrolysis.

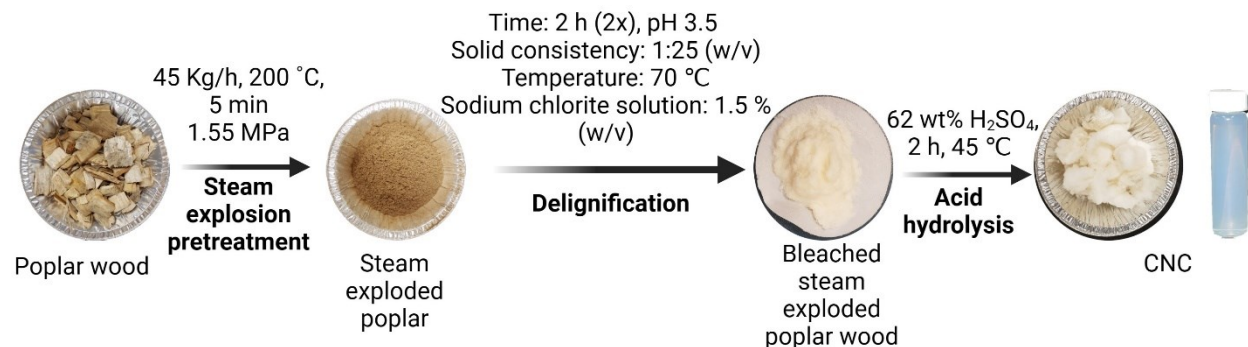


Figure 3.2 Isolation of cellulose nanocrystal from steam exploded poplar wood

#### 3.4.1. *Steam explosion pretreatment*

The steam explosion pretreatment was performed at FPInnovation (Quebec, QC, Canada) using a continuous Andritz 22-inc pressurized refining system. Before steam explosion pretreatment, the poplar wood chips were soaked in 3 wt% sulfur dioxides in a vacuumed plastic bag. Impregnation of the poplar samples with  $\text{SO}_2$  prior to pretreatment was used to reduce the formation of sugar degradation products such as furfurals. The bag was turned upside-down to ensure proper contact between the gas and the wood chips and left at room temperature overnight. The soaked poplar wood chips (45 kg/hr through put) were forced fed through the plug screw feeder to the digester, then digested at 200 °C and 15.5 bar for 5 min. After the steam explosion, the steam-exploded poplar chips went through the refinery disc to separate into individual fibers. The rotation speed of the refining disc was set at 2000 rpm, and the plate gap was adjusted to 0.15 mm. Finally, the steam exploded poplar was flash dried at 105 °C.

### 3.4.2. Delignification

Steam-exploded poplar wood and untreated poplar wood (10 g each) were bleached with 1.5 % w/v sodium chlorite solution (pH 3.5) for 2 h at 70 °C. The solid-to-liquid ratio was 1:25 (w/v). The bleaching procedure was done twice, and the solid recovered was conventionally washed with deionized water until the pH was neutral and oven dried at 105 °C. The solid recovered was determined using Equation 3.1.

### 3.4.3. Isolation of cellulose nanocrystal

CNC from the steam exploded poplar wood was isolated using 62 wt % H<sub>2</sub>SO<sub>4</sub> (8% solid consistency) subsequently neutralized with 10 % NaOH, dialysis in water and centrifugation to produce colloiddally stable CNCs suspension based on the protocol discussed in section 3.3.4. The CNC yield was calculated based on Equation 3.3. The overall CNC yield and over-size rejects were calculated using the equation developed by (Beyene et al. (2017) as shown in Equation 3.5 and 3.6.

$$\text{Overall CNC yield (wt \%)} = \frac{\text{CNC yield} * \text{solid recovery}}{100\%} \quad (3.5)$$

$$\text{Over size reject (wt \%)} = \frac{W_8}{W_7} * 100\% \quad (3.6)$$

Equation 3.5: Overall CNC yield (wt % original feedstock), and Equation 3.6: Over-size rejects (wt % acid hydrolyzed feedstock) and  $W_7$  is the mass of the sample (g) before acid hydrolysis,  $W_8$  is the mass of unhydrolyzed pellet after acid hydrolysis.

### 3.5. Steam Explosion and Enzymatic digestion as Pretreatment for Co-production of Cellulose nanocrystal and Fermentable Sugar from Poplar Wood

The study explored the efficient production of CNCs and fermentable sugars from poplar wood through a comprehensive process integrating steam explosion pretreatment, enzymatic hydrolysis, and acid hydrolysis. The primary goals were to induce crystallization in semi-crystalline/amorphous cellulose, achieve effective saccharification of amorphous cellulose, and enhance CNC recovery during acid hydrolysis. Steam explosion treatment was employed to promote the crystallization of semi-crystalline cellulose, while enzymatic hydrolysis selectively targets amorphous cellulose, enriching the feedstock with CNC precursors.

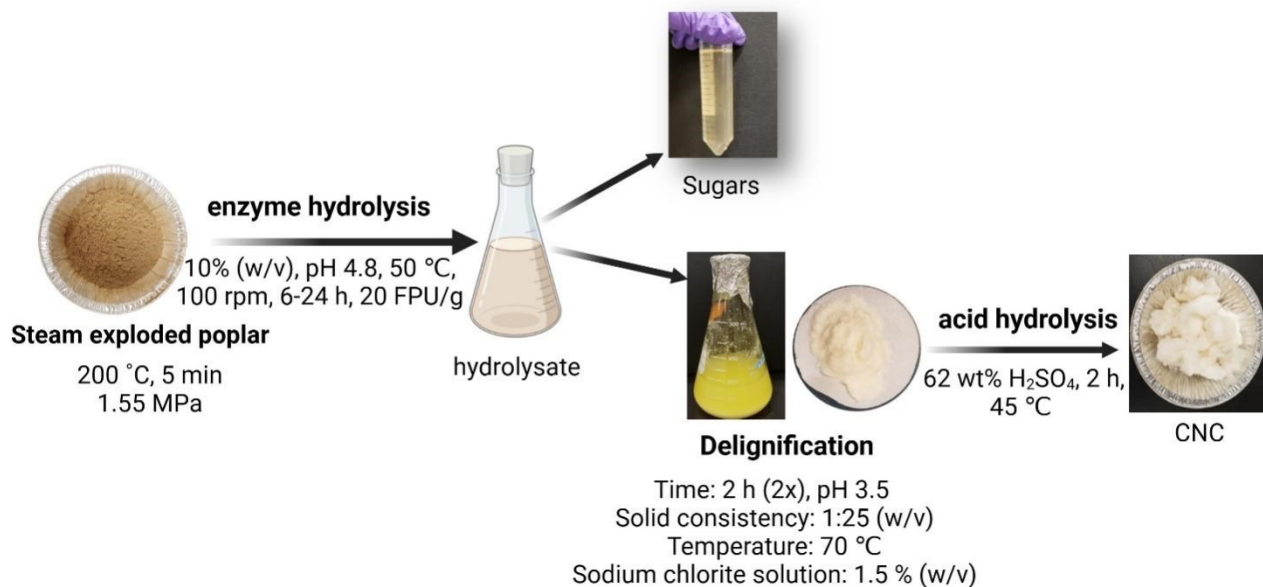


Figure 3.3 Steam explosion and enzymatic digestion as pretreatments for co-production of CNC and fermentable sugars

#### 3.5.1. Enzyme dosage curve for poplar and steam exploded poplar wood

The determination of the optimal cellulase dosage was accomplished by the method discussed in section 3.3.2.1 and creating a cellulase dosage response curve through the hydrolysis of ground poplar and steam-exploded poplar.

### 3.5.2. *Enzyme hydrolysis as a function of time*

Grounded poplar and steam exploded poplar (10 % w/v solid consistency) were hydrolyzed according to the method discussed in section 3.3.2.2, with 20 FPU/g cellulase loading over a period of 6 – 24 h, buffer 0.05 M sodium citrate solution at pH 4.8 in a shake flask. The flask was incubated at 50 °C with 100 rpm shaking.

### 3.5.3. *Delignification*

Enzyme-treated steam-exploded poplar wood and untreated poplar wood (10 g each) were subjected to bleaching using a 1.5% w/v sodium chlorite solution (pH 3.5) for a duration of 2 hours at a temperature of 70 °C. The solid-to-liquid ratio was 1:25 (w/v). The bleaching process was conducted twice, and the resultant solid was subjected to conventional washing using deionized water until a neutral pH was achieved.

### 3.5.4. *Isolation of cellulose nanocrystals*

CNCs were isolated using the procedure outlined in section 3.3.4. Where 62 wt % H<sub>2</sub>SO<sub>4</sub> (8% solid consistency) was used to hydrolyze the bleached samples and subsequently neutralized with 10 % NaOH, dialysis in water and centrifugation to produce colloiddally stable CNCs. The CNC yield was calculated based on Equation 3.3. The overall CNC yield was calculated using the Equation 3.4.

## **3.6. Characterization of Cellulose nanocrystals**

### 3.6.1. *Degree of crystallinity*

The crystallinity of all samples and CNCs were determined according to the method (Beyene et al., 2018) using XRD Rigaku Ultima IV diffractometer (Rigaku Corporation, Tokyo, Japan), at the nanoFAB fabrication and characterization center (University of Alberta). JADE software (Jade Software Corporation Limited, Christchurch, Australia) was used to access the intensity values from the spectra. The crystallinity index (CrI) was determined based on the peak height method (Longaresi et al., 2019; Segal et al., 1959).

$$\text{CrI (\%)} = \frac{I_{total} - I_{am}}{I_{total}} * 100 \% \quad (3.7)$$

Where  $I_{am}$  is the intensity count at the minimum peak between the 110 and 200 planes (around Bragg's angle  $2\theta = 18^\circ$ ), and  $I_{total}$  is the intensity count at the maximum height of the peak at 200 planes (Bragg's angle  $2\theta = 22^\circ - 24^\circ$ ).

### 3.6.2. *Morphology and particle size*

The size and structures of CNCs were characterized using transmission electron microscope (Philips/FEI Morgagni 268, Hillsboro, OR, USA) according to the method developed by (Beyene et al., 2018). The length and width of CNC rods were analyzed by measuring 100 CNC particles using Image J software.

### 3.6.3. *Zeta potential*

The average hydrodynamic diameter and zeta potential of the CNCs were determined by dynamic light scattering using a Nano-ZS Malvern Zetasizer (Malvern analytical Ltd., Almelo, Netherlands). 0.1 % (w/v) of the CNCs were suspended in deionized water at 25 °C and placed in an ultrasonic bath for 5 min.

### 3.6.4. *Thermal stability of CNCs*

The thermal stability of all samples and CNCs were analyzed using Perkin Elmer Thermogravimetric Analyzer (TGA 8000, Shelton, USA). 5-10 mg samples were heated with a temperature increasing rate of 10 °C/min from 30 °C to 500 °C under nitrogen atmosphere (60 mL/min).

## 4. Results and Discussion

### 4.1. Hydrothermal and Enzyme treatment for co-production of CNC and fermentable sugars from wood pulp

#### 4.1.1. *Hydrothermal treatment of wood pulp*

Wood pulp with 10 % solid consistency was hydrothermally treated in batch mode for 1 h, resulting in a pressure increase in the reactor vessel from 0.1–1.6 MPa as the temperature reached 200 °C. The hydrothermal treatment caused a significant loss of hemicellulose at 200 °C. Beyene et al. (2020) reported up to 15 wt% reduction in hemicellulose content after subjecting wood pulp to hydrothermal treatment at 200°C for 1 hour. This was likely due to the release of organic acids from xylose degradation, which promotes autohydrolysis reactions. As Table 4.1 shows, despite considerable hemicellulose degradation, there was a low recovery of xylose sugar at 200 °C in the liquid hydrolysate of hydrothermally treated pulp, indicating that the hydrothermal treatment caused further degradation of xylose to furfural and other degradation products. Various byproducts such as furfural, 5-hydroxymethylfurfural, acetic acid, formic acid, levulinic acid have been reported from hemicellulose degradation through hydrothermal processing (Xiao et al., 2017). In a present study in addition to glucose and xylose, furfural, acetic acid, formic acid, and unidentified peak was observed. Furfural, primarily derived from pentose sugars like xylose and arabinose, forms via dehydration, while formic acid can result from intermediate products during furfural transformation.

Moreover, this process led to a notable rise in cellulose crystallinity. As shown in Table 4.4, the increase in crystallinity could be attributed to the concentration of crystalline chains due to significant hemicellulose and amorphous cellulose degradation. Another hypothesis suggests that hydrothermal treatment can also facilitate the crystallization of para-crystalline/amorphous cellulose, forming new crystals by changing the torsion angle ( $\omega$ ) of O6–C6–C5–O5 from gauche–trans (gt,  $\omega=60^\circ$ ) to trans–gauche (tg,  $\omega=180^\circ$ ) orientation in glucose subunits, which favors more interplanar hydrogen bonding

between chains (Agarwal *et al.* 2017). Similarly, Beyene *et al.* (2020) reported an increase in the degree of crystallinity of wood pulp due to the hydrothermal treatment.

Table 4.1 Solid recovery and degradation products of hydrothermally treated pulp (10 % solid consistency, 200 °C, 1 h, and cooling rate: 1.1 °C/min)

Solid recovery (wt % starting material)	Sugars and Degradation products (wt% original feedstock)					
	Glucose	Xylose	Acetic acid	Formic acid	Furfural	unaccounted
79.3 ± 0.6	1.2 ± 0.1	2.2 ± 0.2	0.08 ± 0.004	0.3 ± 0.008	3.6 ± 0.1	13.3 ± 0.1

#### 4.1.2. Enzyme dosage curve for hydrothermally treated wood pulp

As shown in Figure 4.1, glucose yield curves were examined over a 24 h hydrolysis of hydrothermally treated pulp at various cellulase loadings. The point at which glucose yield leveled off was identified as the effective cellulase loading. Despite the lack of a significant increase in glucose yield between enzyme loadings of 15 FPU/g and 20 FPU/g, a noticeable distinction was evident at 15 FPU/g compared to loadings beyond 20 FPU/g during the hydrolysis of hydrothermally treated pulp. However, there was no significant difference observed between 20 FPU/g and loadings beyond 20 FPU/g. This suggests that all enzyme-accessible binding sites were saturated at or beyond 20 FPU/g. Thus, addition of enzymes beyond this point was deemed redundant for cellulose hydrolysis and would only add unnecessary costs to the process. As a result, 20 FPU/g cellulase loading was chosen for subsequent enzyme treatment investigations on the feedstocks.

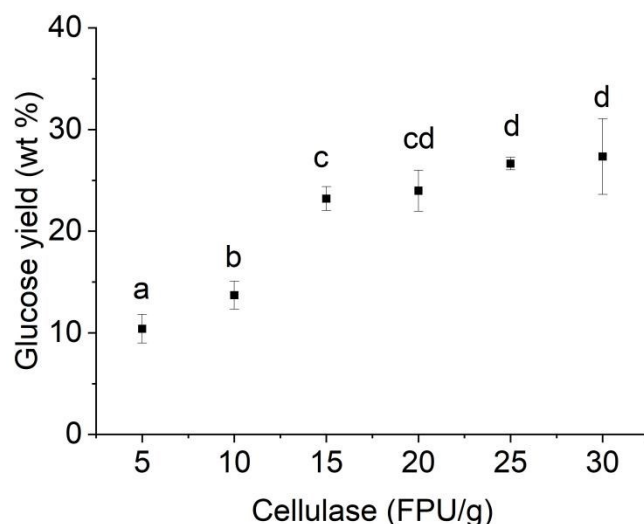


Figure 4.1 Glucose response curve for hydrothermally treated pulp as function of cellulase dosage. Condition (10% w/v, 50 °C, a pH 4.8, 24 h and 100 rpm). <sup>A,a</sup> Points that are denoted by non-identical letters are significantly different.

#### 4.1.3. Enzyme hydrolysis as a function of time

Efficiently hydrolyzing the readily available amorphous cellulose in hydrothermally treated pulp leaving the resistant crystalline content is crucial to increasing the yield of CNCs and recovering fermentable sugars. Hydrothermally treated wood pulp was hydrolyzed with the cellulase cocktail for 6-24 h. The fermentable sugars liberated during enzyme hydrolysis were calculated based on the feedstock used during enzyme hydrolysis and the starting material. As Table 4.2 shows, the conversion yield of the sugars from hydrothermally treated pulp increased with increasing time, showing a significant increase in the yield of both sugars (glucose and xylose) during the 6-24 h treatments. It is apparent that as the contact time between the enzyme and substrate increases, the concentration of the enzyme-substrate complex increases, which leads to an increase in the yield of sugars until a limiting rate is reached. Thus, the increase in the sugar yield indicated no rate limiting factor for enzyme hydrolysis except for xylose. No significant increase was shown after 18 h, and the yield from hydrothermally treated pulp was low and did not exceed 3.3 % (based on the starting material). This was due to a fraction of the hemicellulose being hydrolyzed to xylose and degradation products during hydrothermal treatment.

Nevertheless, it's important to highlight that the glucose and xylose yield levels from hydrothermally treated wood pulp in our study were significantly lower than the findings in a previous investigation conducted by Beyene *et al.* (2017) with the same cellulase cocktail. Beyene *et al.* (2017) reported that wood pulp hydrolysis resulted in glucose release (ranging from  $21.0 \pm 0.6$  to  $44.2 \pm 1.4$  wt% substrate conversion) and xylose ( $6.1 \pm 0.2$  to  $12.1 \pm 0.3$  wt% substrate conversion) through cellulose and xylan degradation for 2–10 h treatment (Beyene *et al.*, 2017). This indicated that the hydrothermal treatment enhances the crystallization of semi-crystalline/ non-crystalline cellulose, forming crystalline cellulose that exhibits resistance to enzyme hydrolysis.

Table 4.2 Sugar and undigested solid yields from enzymatic treatment of hydrothermally treated pulp for 6–24 h

Enzymatic treatment (h)	Yield (wt% enzyme hydrolysis feedstock)			Overall yield (wt% starting material)	
	Glucose	Xylose	Undigested solid	Glucose	Xylose
0	$0.0 \pm 0.0$	$0.0 \pm 0.0$	$99.7 \pm 0.1^a$	$0.0 \pm 0.0$	$0.0 \pm 0.0$
6	$21.6 \pm 0.4^d$	$2.2 \pm 0.1^C$	$76.4 \pm 0.2^b$	$17.1 \pm 0.2^d$	$1.7 \pm 0.1^C$
12	$29 \pm 1^c$	$2.9 \pm 0.3^{BC}$	$66 \pm 2^c$	$23 \pm 1^c$	$2.3 \pm 0.2^B$
18	$36 \pm 1^b$	$3.6 \pm 0.3^{AB}$	$60 \pm 2^c$	$28.5 \pm 0.8^b$	$2.8 \pm 0.2^{AB}$
24	$41.4 \pm 0.8^a$	$4.2 \pm 0.3^A$	$54 \pm 3^d$	$32.8 \pm 0.3^a$	$3.3 \pm 0.2^A$

Enzymatic hydrolysis of hydrothermally treated pulp (solid concentration of 10% (w/v), 50 mM sodium acetate buffer (pH 4.8), 50 °C, 100 rpm, cellulase (NS 51129): 20 FPU/g. <sup>A,a</sup> Means denoted by non-identical letters are significantly different ( $p < 0.05$ ); comparisons done throughout the treatment time for each class.

#### 4.1.4. Cellulose nanocrystal yield

After the enzymatic treatment, the solid residues (undigested solid) were then subjected to standard acid hydrolysis to produce CNCs. The CNC yield was calculated based on weight of CNC recovered per weight of a feedstock used during acid hydrolysis and per weight of starting material. The CNC yield based on the feedstock used during acid hydrolysis shows the effect of hydrothermal and

enzymatic treatment on the acid hydrolysis process and the overall CNC yield based on the starting material indicated the CNC precursor dissolution during the enzyme or acid hydrolysis. The flow chart in Figure 4.2 shows the detailed mass balance for CNC isolation from hydrothermally and enzymatic treated pulp.

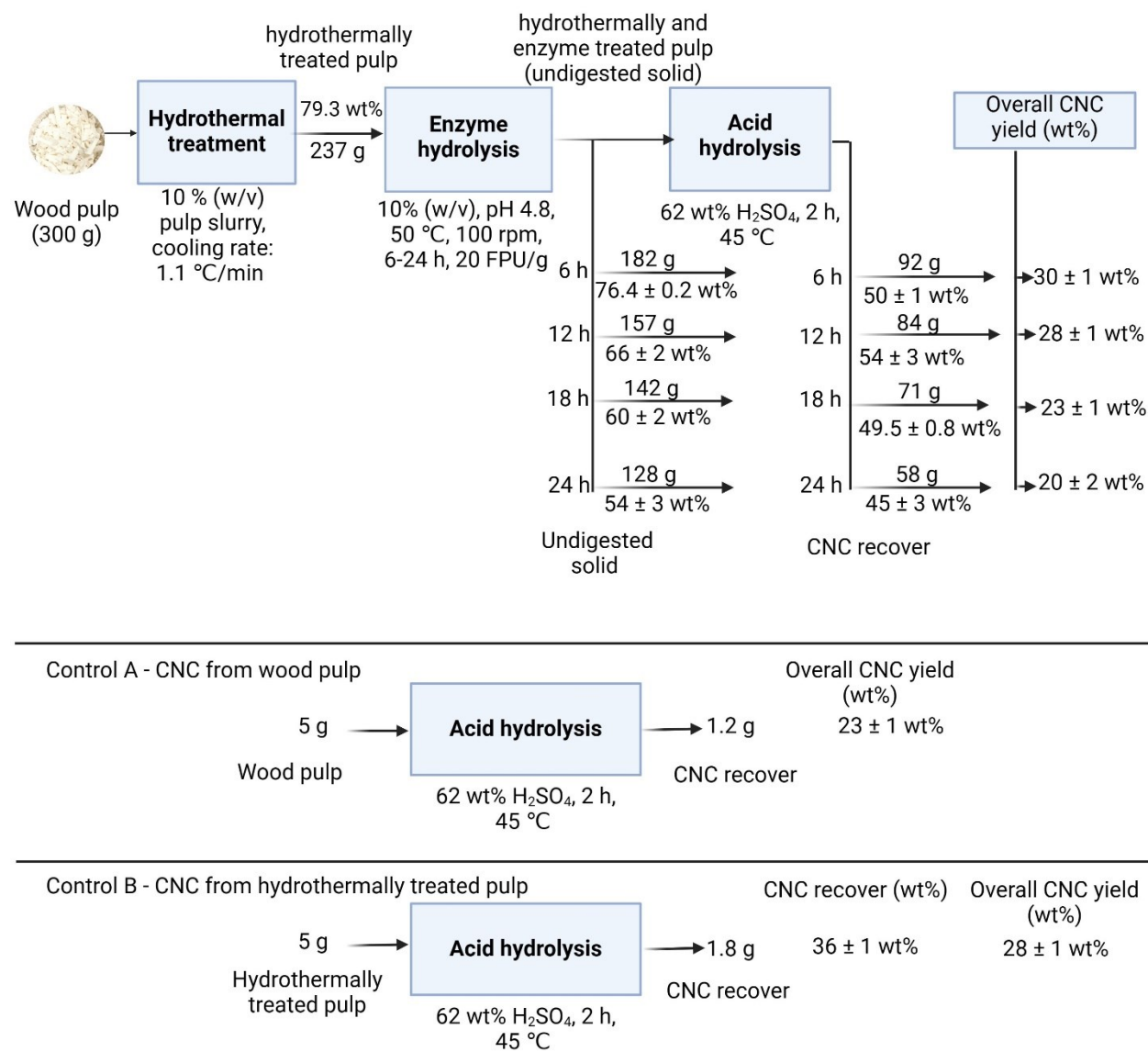


Figure 4.2 Mass balance for CNC isolated from hydrothermally and enzymatic treated pulp. All reported data represent analysis from triplicate samples.

The yield of CNCs (based on acid hydrolysis feedstock), as shown in Table 4.3, indicated that the hydrothermal and enzymatic treatment significantly increased the CNCs yield as compared to the control without enzyme treatment (only from wood pulp) and hydrothermally treated pulp (0 h). The increased CNC yield based on acid hydrolysis feedstock suggested a significant accumulation of CNC precursor in the hybrid treated pulp due to the removal of amorphous cellulose and hemicellulose at the initial stage of the enzyme hydrolysis. The increase in the crystallinity index supports the hypothesis. However, the CNC yield was not increased as the hydrolysis time of the enzyme increased. This indicated that the enzyme treatment after 6 h did not exhibit exclusive selectivity for amorphous cellulose but instead simultaneously degraded both amorphous and crystalline cellulose.

Furthermore, a significant increase in the overall CNC yield was observed for hydrothermally and enzymatic treated pulp for 0, 6, and 12 h compared to untreated wood pulp. However, this increase started to decline after 18 h (Table 4.3), reaching a point where there was no significant difference compared to the control. This suggests that the enzyme hydrolyzed the amorphous cellulose in the hydrothermally treated pulp during the initial phase of enzyme hydrolysis and concentrated the CNC precursor for acid hydrolysis. Thus, the 18 h period may have been a critical juncture when CNC precursors became equally susceptible to disintegration and/or dissolution through enzyme/acid hydrolysis. Previous research on enzymatic hydrolysis of wood pulp using a cellulase cocktail solution, followed by acid hydrolysis, has reported a preferential cleavage of amorphous cellulose by the enzyme, enhancing CNC yield and generating fermentable sugars as a by-product (Beyene *et al.*, 2017; Yupanqui-Mendoza *et al.*, 2023). In a related study by Beltramino *et al.* (2016) the effect of enzymatic treatment on the total CNC yield from cotton linter was investigated, and a significant increase in CNC yield was reported. According to the researchers, the cellulase cocktail selectively

degraded the amorphous cellulose and enhanced the accessibility of CNC precursors to acid (62 wt % H<sub>2</sub>SO<sub>4</sub> for 45 minutes).

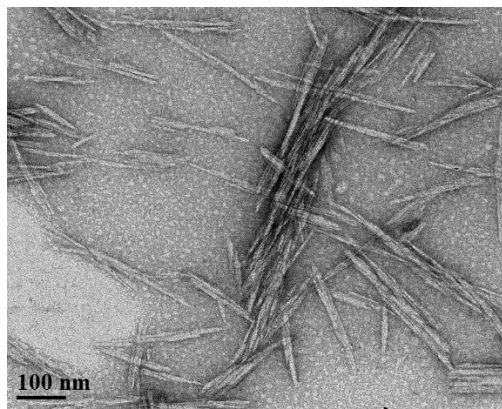
Table 4.3 CNC yield from hydrothermal and enzymatic treated pulp

<b>Enzymatic treatment (h)</b>	<b>CNC yield (wt% acid hydrolyzed feedstock)</b>	<b>CNC yield (wt% starting material)</b>
Control A	23 ± 1 <sup>d</sup>	23 ± 1 <sup>BC</sup>
Control B	36 ± 1 <sup>c</sup>	28 ± 1 <sup>A</sup>
6	50 ± 1 <sup>ab</sup>	30 ± 1 <sup>A</sup>
12	54 ± 3 <sup>a</sup>	28 ± 1 <sup>A</sup>
18	49.5 ± 0.8 <sup>ab</sup>	23 ± 1 <sup>B</sup>
24	45 ± 3 <sup>b</sup>	20 ± 2 <sup>C</sup>

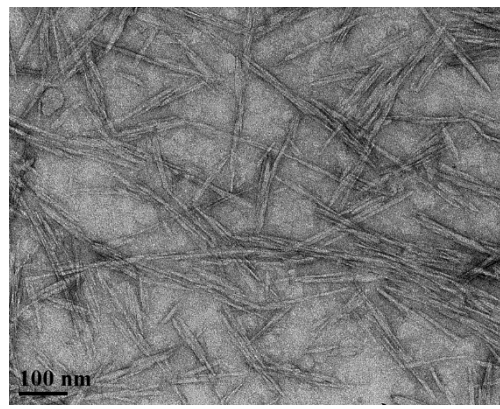
CNC isolation from hydrothermal and enzyme treated pulp (62 wt % H<sub>2</sub>SO<sub>4</sub> (8 % w/v, solid to acid ratio), 2 h, 45 °C and 200 rpm). <sup>A,a</sup> Means denoted by non-identical letters are significantly different (p < 0.05); comparisons done throughout the treatment time for each class. Control A was from wood pulp, Control B was from hydrothermally treated pulp (without enzyme).

#### 4.1.5. Morphological analysis of cellulose nanocrystals using transmission electron microscope

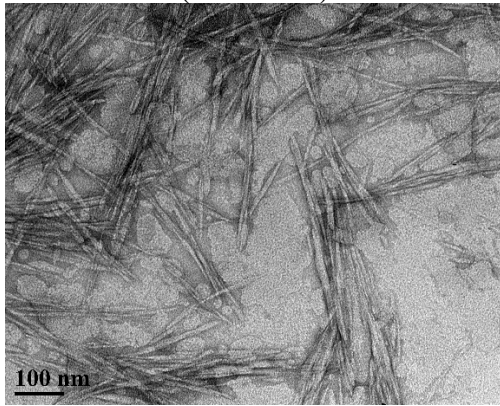
CNC particles isolated from the untreated and hydrothermal and enzymatic treated pulp exhibited nanoscale size in length and width (Figure 4.2). The particles from both feedstocks had elongated needle-like shapes. Although, the CNCs isolated from all samples showed rod-like morphologies, determining the size of the CNCs from transmission electron microscopy poses several challenges including potentially biased stemming from factors such as identifying edges, sample selection and aggregation (Chen et al., 2021).



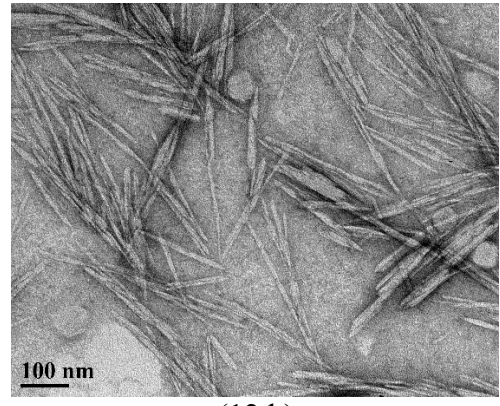
(Control A)



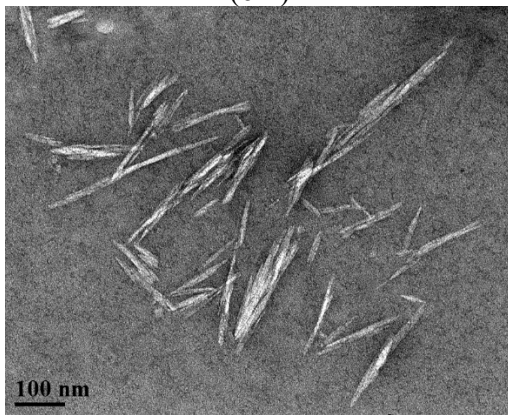
(Control B)



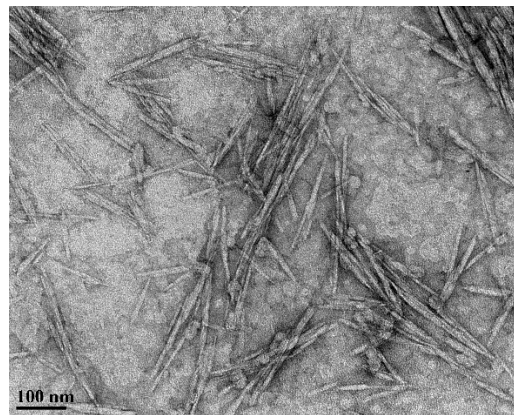
(6 h)



(12 h)



(18 h)



(24 h)

Figure 4.3 Transmission electron microscopy (TEM) micrographs of CNC isolated from wood pulp (control) and hydrothermal and enzymatic-treated wood pulp. Condition (hydrothermal treatment: 10 % solid consistency, 200 °C, 1 h, and cooling rate: 1.1 °C/min; enzymatic treatment: 10% (w/v), pH 4.8, 50 °C, 100 rpm, 6-24 h, cellulase (NS 51129): 20 FPU/g). Control A was from wood pulp, Control B was from hydrothermally treated pulp (without enzyme).

#### 4.1.6. Degree of crystallinity

The crystallinity index (CrI) was determined through X-ray diffraction, as illustrated in Figure 4.3. The peaks observed in all samples were located approximately at  $2\theta$  angles of  $15^\circ$ ,  $22^\circ$ , and  $34^\circ$ . These angles correspond to the (110 and 1-10), (200), and (004) planes, respectively, indicative of cellulose I (Zhao *et al.*, 2019). Table 4.4 shows that the degree of crystallinity of hybrid-treated pulp increased significantly compared to untreated wood pulp. The increase in crystallinity may be attributed to the concentration of crystalline chains due to the degradation of amorphous cellulose and hemicellulose (Yupanqui-Mendoza *et al.*, 2023). The degradation of hemicellulose and, to some extent, cellulose, as discussed in polysaccharide compositional analysis (Table 4.1), supports this hypothesis. Beyene *et al.* (2020) observed a rise in the crystallinity of wood pulp from  $76.7 \pm 0.8\%$  to  $83.8 \pm 2.4\%$  following hydrothermal treatment. They hypothesized that the hydrothermal treatment could facilitate the reorientation of para-crystalline celluloses, forming new compact crystals.

However, with an increase in enzyme hydrolysis time, no significant difference was observed in the degree of crystallinity. This suggested that either the accumulation of crystalline cellulose was not significant to detect using XRD or there was concurrent hydrolysis of non-crystalline and crystalline cellulose. A similar result was observed by Beyene *et al.* (2020), who suggested that the enzymes hydrolyze the crystalline domains on the exposed surfaces as amorphous cellulose embedded within the core of crystalline chains are inaccessible to hydrolysis. As a result, the simultaneous degradation of crystalline and amorphous cellulose has led to a constant crystallinity index for enzyme treatment (Beyene *et al.*, 2017).

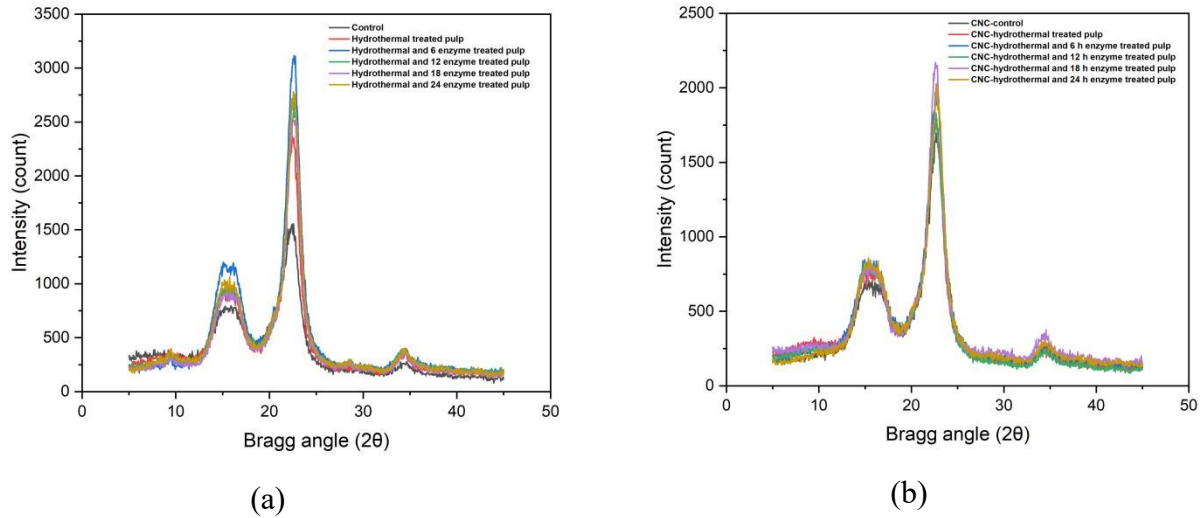


Figure 4.4 X-ray diffraction pattern of (a) wood pulp (control) and hydrothermal and enzymatic-treated pulp, (b) CNC isolated from wood pulp (control), and hydrothermal and enzymatic-treated wood pulp. Condition (hydrothermal treatment: 10 % solid consistency, 200 °C, 1 h, and cooling rate: 1.1 °C/min; enzymatic treatment: 10% (w/v), pH 4.8, 50 °C, 100 rpm, 6-24 h, cellulase (NS 51129): 20 FPU/g)

Additionally, as Table 4.4 indicated, the hybrid treatment had no impact on the crystallinity of CNCs. This implies that the degree of crystallinity of CNC is intricately influenced by the acid hydrolysis conditions employed during their synthesis rather than by pretreatment steps. The choice of acid concentration, reaction temperature, and duration play pivotal roles in determining the resulting degree of crystallinity (Lu *et al.*, 2022). Higher acid concentrations or prolonged reaction times often increase crystallinity as more amorphous regions are removed (Kusmono *et al.*, 2020). Thus, careful optimization is crucial to prevent excessive hydrolysis that could compromise the integrity of the cellulose nanocrystals.

Table 4.4 Degree of crystallinity of hydrothermal and enzymatic treated wood pulp and CNCs.

Degree of crystallinity (%)		
Enzymatic treatment (h)	Hydrothermal and enzymatic treated pulp	CNC
Control A	73.5 ± 0.6 <sup>B</sup>	80.4 ± 0.6 <sup>ab</sup>
Control B	84.8 ± 0.4 <sup>A</sup>	81.7 ± 0.3 <sup>ab</sup>
6	86.6 ± 0.8 <sup>A</sup>	81.8 ± 0.4 <sup>ab</sup>
12	86.3 ± 0.7 <sup>A</sup>	80.4 ± 0.3 <sup>b</sup>
18	85.8 ± 0.5 <sup>A</sup>	83 ± 1 <sup>a</sup>
24	86.3 ± 0.4 <sup>A</sup>	82 ± 1 <sup>ab</sup>

<sup>A,a</sup> Means denoted by non-identical letters are significantly different ( $p < 0.05$ ); comparisons done throughout the treatment time for each class. Condition (hydrothermal treatment: 10 % solid consistency, 200 °C, 1 h, and cooling rate: 1.1 °C/min; enzymatic treatment: 10% (w/v), pH 4.8, 50 °C, 100 rpm, 6-24 h, cellulase (NS 51129): 20 FPU/g). Control A was from wood pulp, Control B was from hydrothermally treated pulp (without enzyme).

#### 4.1.7. Zeta potential

The zeta potential indicates the surface charge of CNCs suspended in a liquid medium. Maintaining a stable colloid is essential to prevent self-aggregation, a key factor for the reinforcement filler to enhance the strength of the composite material. During the process of producing nanocrystals from hydrolysis with sulfuric acid, sulfonation reactions of the hydroxyls occur forming sulfate esters that are negatively charged. However, the hydrothermal and enzyme treatment prior to acid hydrolysis caused changes in the distribution of hydroxyl groups on the surface of CNC, potentially influencing the esterification of the sulfate group and thereby impacting the surface's charge density (Beltramino et al., 2015). In this experiment the effect of hydrothermal and enzymatic treatment was analyzed using zeta potential. Typically, when the zeta potential values fall below -30 mV, it suggests a strong negative electrostatic force from the sulfate group, resulting in a high degree of CNC dispersion (Mohaiyiddin *et al.*, 2016; Naduparambath *et al.*, 2018; Sai Prasanna and Mitra 2020). The results in

Table 4.5 indicate that hydrothermal and enzyme treatments did not impact the colloidal stability of CNCs. The CNCs demonstrated good stability, as zeta potential values lower than -30 mV were shown. The sulfate groups introduced during acid hydrolysis were identified as the main factor affecting colloidal stability. Interestingly, enzyme hydrolysis, consistent with Beyene *et al.* (2017), did not influence the zeta potential of the CNCs.

Table 4.5 The zeta potential of CNCs from hydrothermal and enzymatic treated pulp.

<b>Enzymatic treatment (h)</b>	<b>Zeta potential (mV)</b>
Control A	-40.5 ± 0.9 <sup>A</sup>
Control B	-40.4 ± 0.9 <sup>A</sup>
6	-39.4 ± 0.3 <sup>A</sup>
12	-39.9 ± 0.9 <sup>A</sup>
18	-39.7 ± 0.1 <sup>A</sup>
24	-40.1 ± 0.5 <sup>A</sup>

<sup>A</sup> Means denoted by non-identical letters are significantly different ( $p < 0.05$ ). Condition (hydrothermal treatment: 10 % solid consistency, 200 °C, 1 h, and cooling rate: 1.1 °C/min; enzymatic treatment: 10% (w/v), pH 4.8, 50 °C, 100 rpm, 6-24 h, cellulase (NS 51129): 20 FPU/g). Control A was from wood pulp, Control B was from hydrothermally treated pulp (without enzyme)

#### 4.1.8. Thermal stability

CNC's thermal stability significantly impacts their potential applications, particularly in fields that involve exposure to elevated temperatures. Performing thermogravimetric analysis, Figure 4.4 presents the thermographs of untreated wood pulp, hydrothermally treated wood pulp, hybrid-treated pulp, and CNCs to understand the effect of hydrothermal and enzymatic treatment on the thermal stability of CNCs. The thermographs displayed three main weight loss stages in all samples. The weight loss profiles suggest a multistep decomposition process. The initial weight loss at around 100°C corresponds to removing physically adsorbed water. The subsequent weight loss indicates a

complex degradation mechanism, possibly involving depolymerization and subsequent pyrolysis of the cellulose molecules (Lam *et al.*, 2017; Longaresi *et al.*, 2019).

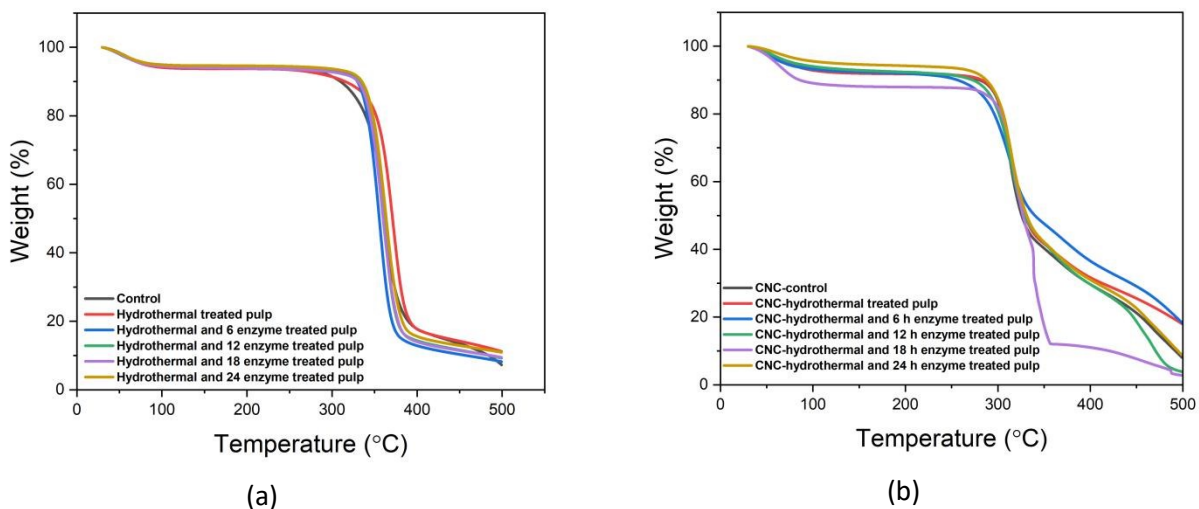


Figure 4.5 Thermographs of (a) wood pulp and hydrothermal and enzymatic treated pulp, (b) CNCs isolated from wood pulp (control) and hydrothermal and enzymatic-treated pulp. Condition (hydrothermal treatment: 10 % solid consistency, 200 °C, 1 h, and cooling rate: 1.1 °C/min; enzymatic treatment: 10% (w/v), pH 4.8, 50 °C, 100 rpm, 6-24 h, cellulase (NS 51129): 20 FPU/g). thermogravimetric analysis: 5-10 mg, temperature increasing rate of 10 °C/min from 30 °C to 500 °C under nitrogen atmosphere (60 mL/min).

Hydrothermal treatment has significantly improved the thermal stability of wood pulp. As shown in Table 4.6, the onset temperature significantly increased following the hydrothermal treatment. The ordered structure of crystalline cellulose imparts greater thermal stability due to the increased resistance to thermal decomposition. However, a further increase in the enzyme hydrolysis time did not show a significant difference in the thermal stability of the hybrid-treated pulp. This supports the hypothesis discussed in section 4.1.6, which the enzyme simultaneously hydrolyzes the crystalline and the amorphous cellulose.

Additionally, the thermal stability of CNCs did not show a significant difference, indicating that neither hydrothermal treatment nor enzyme treatment resulted in alterations in the produced CNCs.

Instead, the acid hydrolysis conditions intricately influence CNC's thermal stability (Lu *et al.*, 2022). Higher acid concentrations and prolonged reaction times often increase crystallinity, positively impacting CNC's thermal stability (Kargarzadeh *et al.*, 2012). The choice of acid and its concentration influence the extent of hydrolysis and, subsequently, the size and thermal stability of the resulting nanocrystals. Moreover, variations in reaction temperature and solid-to-liquid ratio can impact CNC size and crystallinity, both critical factors in determining thermal stability. Post-hydrolysis processes, such as washing, purification, and surface modification, also affect CNC thermal stability (Lima *et al.*, 2020; Arserim-Uçar *et al.*, 2021). Overall, precise control of acid hydrolysis conditions is essential for tailoring the thermal stability of CNC, which is crucial for applications in fields such as polymer composites, biomedical materials, and flame-retardant products.

Table 4.6 The onset temperature of hydrothermal and enzymatic treated pulp and CNCs

Onset temperature (°C)		
Enzymatic treatment (h)	Hydrothermal and enzymatic treated pulp	CNC
Control A	318.4 ± 0.2 <sup>B</sup>	284 ± 1 <sup>a</sup>
Control B	329 ± 2 <sup>A</sup>	282 ± 2 <sup>a</sup>
6	328 ± 4 <sup>A</sup>	273 ± 5 <sup>a</sup>
12	335 ± 2 <sup>A</sup>	279 ± 4 <sup>a</sup>
18	330 ± 2 <sup>A</sup>	285 ± 7 <sup>a</sup>
24	331.5 ± 0.6 <sup>A</sup>	282 ± 2 <sup>a</sup>

<sup>A,a</sup> Means denoted by non-identical letters are significantly different ( $p < 0.05$ ); comparisons done throughout the treatment time for each class. Condition (hydrothermal treatment: 10 % solid consistency, 200 °C, 1 h, and cooling rate: 1.1 °C/min; enzymatic treatment: 10% (w/v), pH 4.8, 50 °C, 100 rpm, 6-24 h, cellulase (NS 51129): 20 FPU/g). thermogravimetric analysis: 5-10 mg, temperature increasing rate of 10 °C/min from 30 °C to 500 °C under nitrogen atmosphere (60 mL/min). Control A was from wood pulp, Control B was from hydrothermally treated pulp (without enzyme).

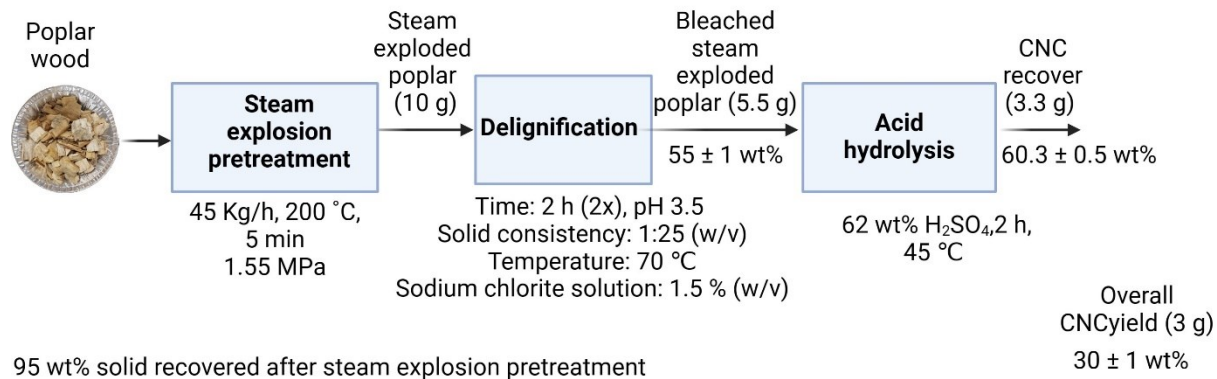
## **4.2. Evaluation of steam explosion pretreatment on the cellulose nanocrystal yield**

### *4.2.1. Delignification of steam exploded poplar*

Poplar wood was subjected to a steam explosion pretreatment and bleached with sodium chlorite to accumulate CNCs precursors with high degrees of crystallinity. The result for solid recovery after delignification showed that  $80.9 \pm 0.4$  wt% and  $55 \pm 1$  wt% bleached poplar wood and bleached steam exploded poplar wood recovered. The statistics revealed that a significant amount of lignin was removed from steam-exploded poplar wood as compared to untreated poplar wood. Steam explosion pretreatment cleaves  $\beta$ -O-4 and  $\beta$ -5 aryl ether bonds of the higher molecular lignin and generates low molecular weight lignin (Wang et al., 2020). Thus, after steam explosion pretreatment lower molecular lignin melts and condenses on the surface of the cellulose microfibrils and increases its accessibility and enhances the bleaching process. According to the findings, bleached steam-exploded poplar contained 96% (w/w) pure cellulose, compared to 55% (w/w) for bleached poplar wood.

### *4.2.2. Cellulose nanocrystal yield*

CNCs were isolated by subjecting bleached poplar and bleached steam-exploded poplar wood to acid hydrolysis using 8 % w/v, solid to acid ratio. The CNC yield was calculated using acid hydrolyzed feedstock (CNC yield per weight of a feedstock used during acid hydrolysis) and original feedstock (CNC yield per weight of original feedstock). The flow chart in Figure 4.6 shows the detailed mass balance for CNC isolation from steam exploded poplar wood.



Control - CNC isolated from ground poplar wood

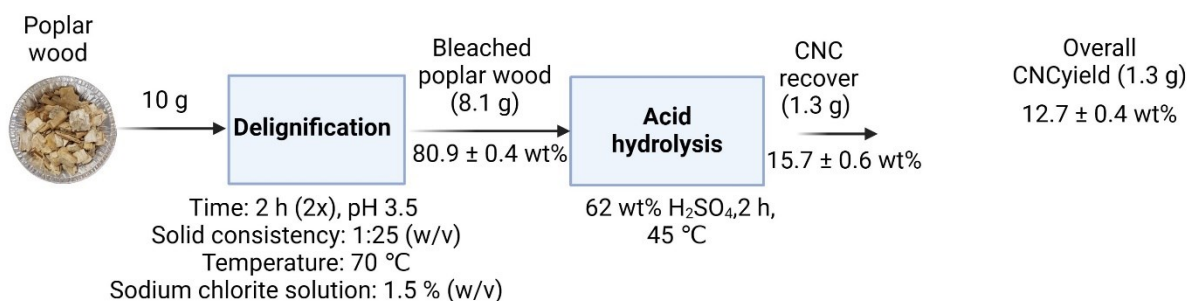


Figure 4.6 Mass balance for CNC isolated from steam exploded poplar wood. . All reported data represent analysis from triplicate samples.

The yield of CNCs as shown in Table 4.8 indicated that the steam explosion pretreatment significantly increased the CNCs yield by 3.8-fold based on the feedstock used during acid hydrolysis and 2.5-fold based on the original feedstock as compared to the control. The increased CNCs yield based on acid hydrolysis feedstock suggested a significant accumulation of CNC precursor in the steam exploded poplar wood due to the removal of hemicellulose and lignin by steam explosion pretreatment and delignification. The increase in the crystallinity index (discussed in Section 3.6) and the chemical composition analysis (discussed in Section 3.1) supports the hypothesis.

Table 4.7 Cellulose nanocrystals yield isolated from steam exploded poplar wood

CNC yield (wt % Acid hydrolysis feedstock)		Overall CNC yield (wt % original feedstock)		Over-size rejects (wt % original feedstock)	
Control	Steam exploded poplar	Control	Steam exploded poplar	Control	Steam exploded poplar
15.7 ± 0.6 <sup>B</sup>	60.3 ± 0.5 <sup>A</sup>	12.7 ± 0.4 <sup>b</sup>	30 ± 1 <sup>a</sup>	15 ± 1 <sup>a</sup>	2.7 ± 0.1 <sup>b</sup>

<sup>A,a</sup> Means denoted by non-identical letters are significantly different ( $p < 0.05$ ). Condition (62 wt % H<sub>2</sub>SO<sub>4</sub> (8 % w/v, solid to acid ratio), 2 h, 45 °C and 200 rpm)

Furthermore, the oversize reject (Table 4.8) for steam-exploded poplar wood was lowered by 5.5-fold than untreated poplar wood. The high overall CNC yield and lower oversize reject for steam exploded poplar wood suggested that there was a new CNC precursor accumulation due to the steam explosion pretreatment and overnight cooling (annealing) after the treatment.

#### 4.2.3. Fourier transform infrared spectroscopy (FTIR)

Fourier transform infrared spectroscopy (FTIR) was used to analyze the change in chemical functional groups for untreated poplar, steam exploded and delignified poplar wood, and CNCs isolated from untreated poplar wood and steam exploded poplar wood. The peak shown in Figure 7 at 3325 cm<sup>-1</sup> wavenumber in all samples was attributed to O–H stretching vibration in cellulose (Lu et al. 2022; Yang et al. 2010; Prado and Spinacé 2019; Prasanna and Mitra 2020). The peaks 2900 cm<sup>-1</sup> and 1035 cm<sup>-1</sup> found in all samples were assigned to C–H and C–O stretching vibrations on cellulose, respectively (Zhao et al. 2019). The peak 1735 cm<sup>-1</sup> contributed to C=O stretching vibrations that existed in the acetyl group and ester group from lignin or hemicellulose. This peak was only observed on untreated poplar and bleached poplar wood. However, the peak intensity decreased in bleached poplar wood as the hemicellulose and lignin content decreased. A weak absorption around 1235 cm<sup>-1</sup> belonging to the C–O–C linkage of the ether and phenol group in lignin

disappeared in bleached poplar wood, bleached steam-exploded poplar wood, and CNCs and it indicated that the lignin was removed during the CNC preparation processes.

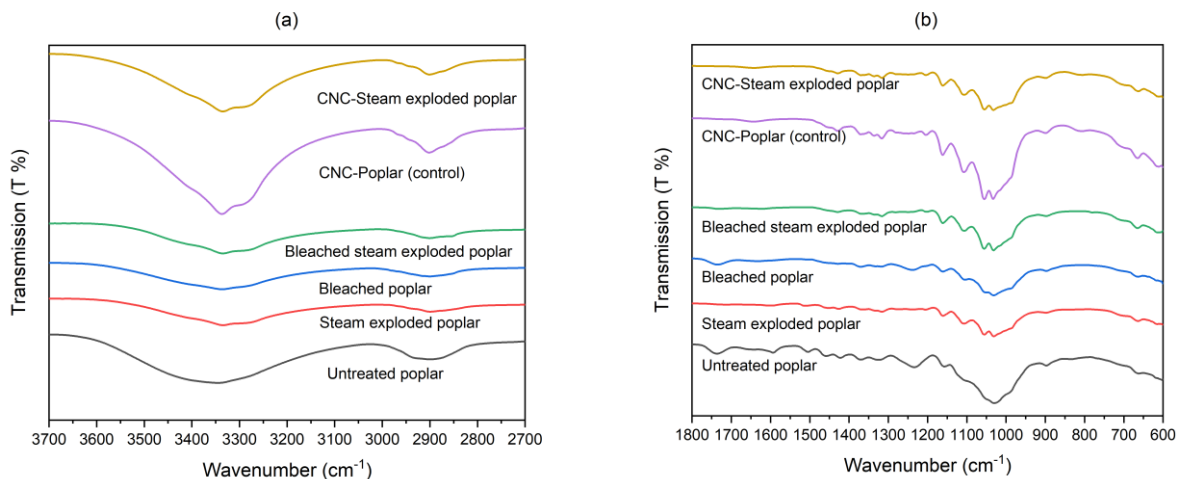


Figure 4.7 ATR-FTIR spectra: (a) Detail of the region 3700-2700  $\text{cm}^{-1}$  of the FT-IR. (b) Detail of the region 1800-600  $\text{cm}^{-1}$  of the FT-IR.

#### 4.2.4. Morphology analysis of CNCs using Transmission Electron Microscope

The effect of steam explosion pretreatment on the morphological structure and crystal size of CNCs were analyzed using Transmission Electron Microscope. Figure 4.6 shows a successful production of CNCs particles with rod-like morphologies for the control and steam-exploded poplar. The statistical analysis revealed that there was no significant difference in the mean length of CNC between the control ( $116 \pm 45$  nm) and the steam-exploded poplar ( $124 \pm 49$  nm). Similarly, steam explosion pretreatment had no effect in the nanocrystal widths (control  $9 \pm 3$  nm and the steam-exploded poplar  $9 \pm 2$  nm). These results suggested that the longer reaction time and the higher acid concentration reduce the crystal length of the CNCs (Naduparambath et al., 2018; Chen et al., 2015).

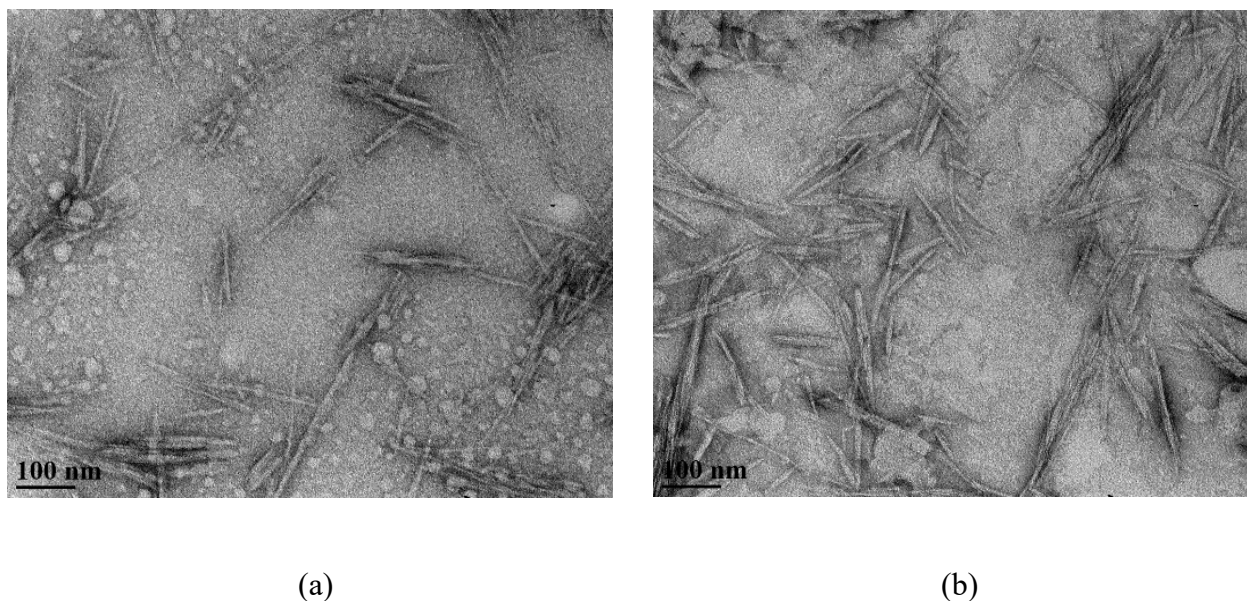


Figure 4.8 Transmission electron microscopy image of CNC isolated from (a) control and (b) steam exploded poplar. Condition: Steam explosion pretreatment (200 °C, 1.55 Mpa, 5 min), acid hydrolysis (62 wt%, H<sub>2</sub>SO<sub>4</sub>, 2 h, 45 °C).

#### 4.2.5. Particle size and zeta potential

In addition to the crystal size analysis using transmission electron microscope, the average hydrodynamic diameter and zeta potential of the CNCs were determined using dynamic light scattering. Table 4.9 shows the average hydrodynamic diameter (nm) and zeta potential (mV) of CNC-control and CNC-steam exploded poplar. The result confirmed that the steam explosion pretreatment did not influence the particle size of CNCs and therefore, argues against the co-crystallization upon hydrothermal treatment (Agarwal et al., 2018; Agarwal et al., 2023). However, the average hydrodynamic diameter result found for the CNCs from the control and steam-exploded poplar were high as compared to the crystal size found using transmission electron microscope. This is because dynamic light scattering measurement does not measure the size directly for non-spherical particles. It measures the equivalent hydrodynamic diameter, which is the diameter of a sphere that diffuses at the same rate.

The zeta potential reflects the stability of CNC suspension in aqueous medium. Higher zeta potential values of a suspension are related to a more stable suspension (Ferreira et al., 2018). Typically, when the zeta potential values fall below -30 mV, it suggests the strong negative electrostatic force from the sulfate group, resulting in a high degree of CNCs dispersion (Mohaiyiddin et al., 2016; Naduparambath et al., 2018; Prasanna & Mitra, 2020). The result indicated in Table 4.9 that the CNC-control and CNC-steam exploded poplar had a good stability as the value obtained was lower than -30 mV. This was due to the sulfate group attached to CNCs during acid hydrolysis. However, steam explosion pretreatment had no significant effect on the zeta potential of CNCs.

Table 4.8 Particle size and zeta potential of CNCs isolated from steam exploded poplar wood

<b>Samples</b>	<b>Average hydrodynamic diameter (nm)</b>	<b>Zeta potential (mV)</b>	<b>Intensity abundance (%)</b>
CNC-control	250 ± 20 <sup>a</sup>	-43.5 ± 0.9 <sup>A</sup>	98 ± 2
CNC-steam exploded poplar	220 ± 20 <sup>a</sup>	-43 ± 1 <sup>A</sup>	98 ± 1

<sup>A,a</sup> Means denoted by non-identical letters are significantly different ( $p < 0.05$ ). Condition: Steam explosion pretreatment (200 °C, 1.55 Mpa, 5 min), acid hydrolysis (62 wt%, H<sub>2</sub>SO<sub>4</sub>, 2 h, 45 °C).

#### 4.2.6. Degree of crystallinity

The degree of crystallinity (CrI) was measured using x-ray diffraction. As shown in Table 4.10, the degree of crystallinity of poplar wood increased by 1.3-fold due to the steam explosion treatment. The removal of hemicellulose has been reported to have improved cellulose crystallinity (Agarwal et al., 2013; Kapoor et al., 2015). Additionally, the high temperature and pressure during steam explosion pretreatment is responsible for transforming the CH<sub>2</sub>OH group of cellulose from gauche-trans conformation to the trans-gauche conformation. Consequently, this structural change promotes crystallization of cellulose and increases the crystallinity (Agarwal et al., 2018; Beyene et al., 2020).

Moreover, bleaching with sodium chlorite dissolves the lignin and improved the degree of crystallinity of bleached poplar and bleached steam exploded poplar (Agarwal et al., 2013; Jiang and Hsieh 2015). The degree of crystallinity of bleached poplar and steam-exploded poplar increased by 1.2-fold and 1.1-fold as compared to untreated poplar and steam-exploded poplar wood, respectively. Furthermore, the result showed that the degree of crystallinity of bleached steam exploded poplar was  $80.5 \pm 0.7 \%$  and this was significantly higher than that of bleached poplar ( $65 \pm 1\%$ ) and suggested that the steam explosion pretreatment enhance the removal of lignin and hemicellulose to obtain higher amount of cellulose that is more crystalline. However, as shown in Table 12, the steam explosion pretreatment did not influence the crystallinity of CNCs. These suggested that the degree of crystallinity of the CNCs depends on the hydrolysis conditions especially on reaction time. The longer hydrolysis time accelerates the cleavage of the glycosidic bonds in crystalline cellulose and decreased crystallinity (Kusmono et al., 2020).

Table 4.9 Degree of crystallinity of untreated poplar, steam-exploded poplar, bleached poplar, bleached steam exploded poplar, cellulose nanocrystal from poplar and cellulose nanocrystal from steam exploded poplar

<b>Degree of crystallinity (%)</b>		
<b>Material</b>	<b>Untreated (control)</b>	<b>Steam-exploded</b>
Poplar wood	$53 \pm 2^b$	$70 \pm 1^a$
Bleached	$65 \pm 1^b$	$80.5 \pm 0.7^a$
CNC	$77.3 \pm 0.8^a$	$78 \pm 1^a$

<sup>a</sup> Means denoted by non-identical letters are significantly different ( $p < 0.05$ ). Condition: Steam explosion pretreatment (200 °C, 1.55 Mpa, 5 min), delignification (Time: 2 h (2x), pH 3.5, solid consistency: 1:25 (w/v), 70 °C, sodium chlorite solution: 1.5 % (w/v)), acid hydrolysis (62 wt%, H<sub>2</sub>SO<sub>4</sub>, 2 h, 45 °C).

#### 4.2.7. Thermogravimetric analysis

Figure 4.7 shows the thermographs of untreated poplar, steam exploded poplar, bleached poplar, bleached steam-exploded poplar, CNC-control, and CNC-Steam-exploded poplar. The result indicated that the weight loss of all samples with respect to temperature took place in multiple steps. The weight loss was mainly due to the decomposition of the cellulose molecules. However, the evaporation of water, the oxidation, and the breakdown of char residue into lower molecular weight gaseous products also contribute to weight loss during thermal analysis (Zhao et al., 2019; Sukyai et al., 2018; Kalita et al. 2015; Longaresi et al., 2019).

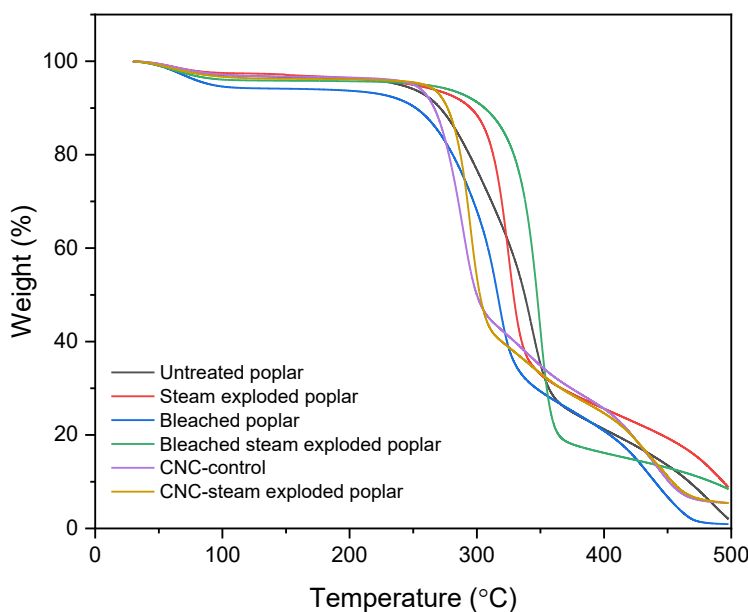


Figure 4.9 Thermographs of untreated poplar, steam-exploded poplar, bleached poplar, bleached steam exploded poplar, cellulose nanocrystal from poplar and cellulose nanocrystal from steam exploded poplar. Condition: Steam explosion pretreatment (200 °C, 1.55 Mpa, 5 min), delignification (Time: 2 h (2x), pH 3.5, solid consistency: 1:25 (w/v), 70 °C, sodium chlorite solution: 1.5 % (w/v)), acid hydrolysis (62 wt%, H<sub>2</sub>SO<sub>4</sub>, 2 h, 45 °C). Thermogravimetric analysis: 5-10 mg, temperature increasing rate of 10 °C/min from 30 °C to 500 °C under nitrogen atmosphere (60 mL/min).

Moreover, the thermal stability of steam-exploded poplar has been significantly improved by steam explosion pretreatment. The onset temperature for untreated poplar wood was  $260 \pm 1$  °C. Following steam explosion pretreatment, the onset temperature substantially increased to  $290 \pm 4$  °C. This was due to the reduction in hemicellulose content and increase of the crystallinity of steam-exploded poplar (Wan et al., 2010). Consequently, CNC-steam-exploded poplar had higher thermal stability than the CNC-control. The onset temperature for CNC-steam-exploded poplar and CNC-control was  $260 \pm 2$  °C and  $250 \pm 2$  °C, respectively. However, the presence of the sulfate groups on the CNCs made the CNCs have lower thermal stability than the untreated poplar and steam-exploded poplar. This is due to the sulfate groups on the CNCs acting as a catalyst during the thermal degradation process and resulting in a negative influence on the thermal stability of CNCs (Prado & Spinacé, 2019).

### **4.3. Steam explosion and enzymatic digestion as pretreatment for co-production of CNC and fermentable sugars**

#### *4.3.1. Enzyme dosage curve for poplar and steam exploded poplar wood*

Glucose yield curves from 24 h hydrolysis of untreated poplar and steam exploded poplar wood as a function of cellulase loadings were evaluated (Figure 11). The enzyme dosage at the point when glucose yield levelled off was identified as an effective cellulase loading. There was no significant increase in glucose yield from hydrolysis of both feedstock at enzyme dosages above 20 FPU/g. It was evident that higher glucose yield was observed for steam exploded poplar wood relative to untreated poplar wood. The steam explosion pretreatment, leading to the breakdown of hemicellulose and a reduction in cellulose polymerization. The resulting structural changes make the wood more susceptible to enzymatic degradation, facilitating higher sugar yields during hydrolysis.

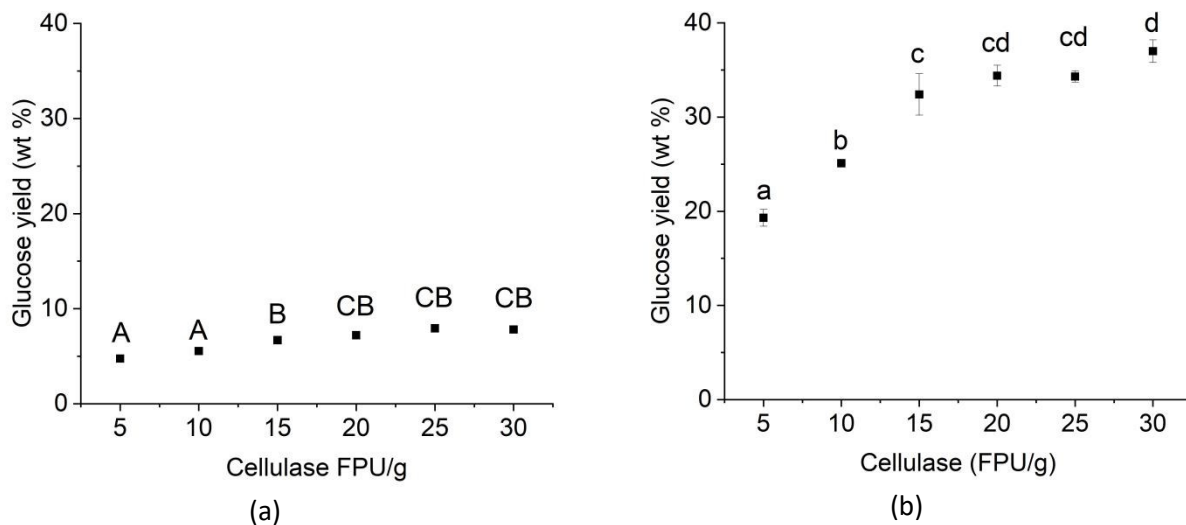


Figure 4.10 Glucose response curve as function of cellulase dosage (a) control and (b) steam exploded poplar wood. Condition (10% w/v, 50 °C, a pH 4.8, 24 h and 100 rpm). <sup>A,a</sup> Points that are denoted by non-identical letters are significantly different.

#### 4.3.2. *Enzymatic hydrolysis as a function of time*

The untreated poplar wood and steam exploded poplar wood were hydrolyzed with the cellulase cocktail for 6–24 h. The fermentable sugars liberated during enzyme hydrolysis were calculated based on the original feedstock. The residual solids that remain undigested were assessed. Table 4.11 illustrates the conversion yield of sugars from the control and steam exploded poplar wood. Glucose from the control and steam-exploded poplar wood increased with prolonged enzyme hydrolysis time. Nevertheless, there was a notable threshold effect on enzyme hydrolysis time, with an optimal enhancement in glucose yield observed up to 12 h for the control and 18 h for the steam-exploded poplar wood. In contrast, the conversion yield of xylose for the control did not exhibit a significant increase with prolonged hydrolysis time. However, in the case of steam-exploded poplar wood, the xylose yield increased with hydrolysis time until reaching 18 h.

The increased sugar yield observed in the steam-exploded poplar wood compared to the control can be attributed to the effects of steam explosion pretreatment. Steam explosion is a thermo-mechanical

process that involves exposing biomass to high-pressure steam followed by a rapid decompression, causing the materials to swell, and then rapidly decompressing them. These extreme conditions induce structural modifications in the biomass, addressing key barriers to efficient enzymatic breakdown. Firstly, the process disrupts the lignocellulosic matrix, breaking down complex structures of hemicellulose and lignin. This disruption enhances the accessibility of cellulose to enzymes, facilitating a more effective conversion into glucose during subsequent hydrolysis.

Table 4.10 Sugar and undigested solid yields from steam explosion and enzymatic treated poplar wood over a period of 6–24 h

Enzymatic treatment (h)	Control (yield wt %)			Steam exploded poplar (yield wt %)		
	Glucose	xylose	Undigested solid	Glucose	xylose	Undigested solid
0	0.06 ± 0.01 <sup>z</sup>	0.0 ± 0.0 <sup>X</sup>	99.1 ± 0.4 <sup>W</sup>	0.3 ± 0.0 <sup>D</sup>	2.1 ± 0.1 <sup>d</sup>	96.3 ± 0.9 <sup>d</sup>
6	5.9 ± 0.1 <sup>Y</sup>	1.84 ± 0.02 <sup>W</sup>	91.6 ± 0.2 <sup>X</sup>	14.2 ± 0.3 <sup>C</sup>	4.7 ± 0.1 <sup>c</sup>	79.1 ± 0.4 <sup>A</sup>
12	6.9 ± 0.1 <sup>W</sup>	1.9 ± 0.2 <sup>W</sup>	89.8 ± 0.2 <sup>Y</sup>	22 ± 1 <sup>B</sup>	5.2 ± 0.1 <sup>b</sup>	70.4 ± 0.6 <sup>B</sup>
18	7.5 ± 0.2 <sup>WX</sup>	1.85 ± 0.03 <sup>W</sup>	88.9 ± 0.5 <sup>Y</sup>	29 ± 1 <sup>A</sup>	5.6 ± 0.2 <sup>ab</sup>	63 ± 1 <sup>C</sup>
24	8.2 ± 0.4 <sup>W</sup>	2.2 ± 0.2 <sup>W</sup>	88.9 ± 0.9 <sup>Y</sup>	29.9 ± 0.7 <sup>A</sup>	5.7 ± 0.1 <sup>a</sup>	63.1 ± 0.4 <sup>C</sup>

<sup>A,X, x,a</sup> Means denoted by non-identical letters are significantly different ( $p < 0.05$ ). pulp (solid concentration of 10% (w/v), 50 mM sodium acetate buffer (pH 4.8), 50 °C, 100 rpm, cellulase (NS 51129): 20 FPU/g

#### 4.3.3. Degree of crystallinity of enzyme treated and delignified steam exploded poplar wood

The degree of crystallinity of poplar wood at various reaction conditions (steam explosion pretreatment, enzyme hydrolysis and delignification) was assessed from XRD spectra analyses based on the peak height method. Table 4.12 presents the degree of crystallinity of untreated poplar, steam exploded poplar, enzyme treated and delignified (poplar and steam exploded poplar wood) for a period of 6-24 h. The steam explosion pretreatment significantly improved the degree of crystallinity of poplar wood. The removal of hemicellulose due to steam explosion pretreatment has been reported to have improved cellulose crystallinity (Agarwal et al., 2013; Kapoor et al., 2015). Additionally, the

high temperature and pressure during steam explosion pretreatment is responsible for structural change. Consequently, this structural change promotes crystallization of cellulose and increases the crystallinity (Agarwal et al., 2018; Beyene et al., 2020).

Moreover, bleaching with sodium chlorite dissolves the lignin and improved the degree of crystallinity of the raw poplar, steam exploded poplar and enzymatic treated poplar and steam exploded poplar over a period of 6-24 h (Agarwal et al., 2013; Jiang and Hsieh 2015). In addition, the result showed that the degree of crystallinity of bleached steam exploded poplar was significantly higher than that of bleached poplar and suggested that the steam explosion pretreatment enhance the removal of lignin and hemicellulose to obtain higher amount of cellulose that is more crystalline. However, after 6 h of enzymatic treatment, there was no significant different in degree of crystallinity of both unbleached and bleached poplar and steam exploded poplar wood observed.

Table 4.11 Degree of crystallinity of steam explosion and enzymatic treated poplar wood

Degree of crystallinity (%)				
Enzyme treatment (h)	Enzyme treated samples		Delignified samples	
	Control	Steam exploded poplar	Control	Steam exploded poplar
0	53 ± 2 <sup>B</sup>	70 ± 1 <sup>ab</sup>	65 ± 1 <sup>A</sup>	80 ± 1 <sup>b</sup>
6	62 ± 3 <sup>A</sup>	71 ± 1 <sup>a</sup>	67.1 ± 0.9 <sup>A</sup>	84.1 ± 0.4 <sup>a</sup>
12	63 ± 2 <sup>A</sup>	69.1 ± 0.5 <sup>ab</sup>	67 ± 2 <sup>A</sup>	84 ± 1 <sup>a</sup>
18	61.8 ± 0.6 <sup>A</sup>	65 ± 3 <sup>b</sup>	66.2 ± 0.9 <sup>A</sup>	83.8 ± 0.7 <sup>a</sup>
24	63.4 ± 0.6 <sup>A</sup>	66.9 ± 0.8 <sup>ab</sup>	66 ± 1 <sup>A</sup>	84 ± 1 <sup>a</sup>

<sup>A,a</sup> Means denoted by non-identical letters are significantly different ( $p < 0.05$ ). Condition: Steam explosion pretreatment (200 °C, 1.55 Mpa, 5 min), delignification (Time: 2 h (2x), pH 3.5, solid consistency: 1:25 (w/v), 70 °C, sodium chlorite solution: 1.5 % (w/v)), acid hydrolysis (62 wt%, H<sub>2</sub>SO<sub>4</sub>, 2 h, 45 °C). Enzyme treatment: solid concentration of 10% (w/v), 50 mM sodium acetate buffer (pH 4.8), 50 °C, 100 rpm, cellulase (NS 51129): 20 FPU/g

#### 4.3.4. Cellulose nanocrystal yield

Following the enzymatic treatment of the steam exploded poplar and control, the remaining undigested solids underwent a delignification process to eliminate lignin. Subsequently, they were subjected to acid hydrolysis to generate CNCs. The CNC yield was determined using the formula outlined in section 3.5.4. The flow chart in Figure 4.2 shows the detailed mass balance for CNC isolation from steam explosion and enzymatic treated poplar wood.

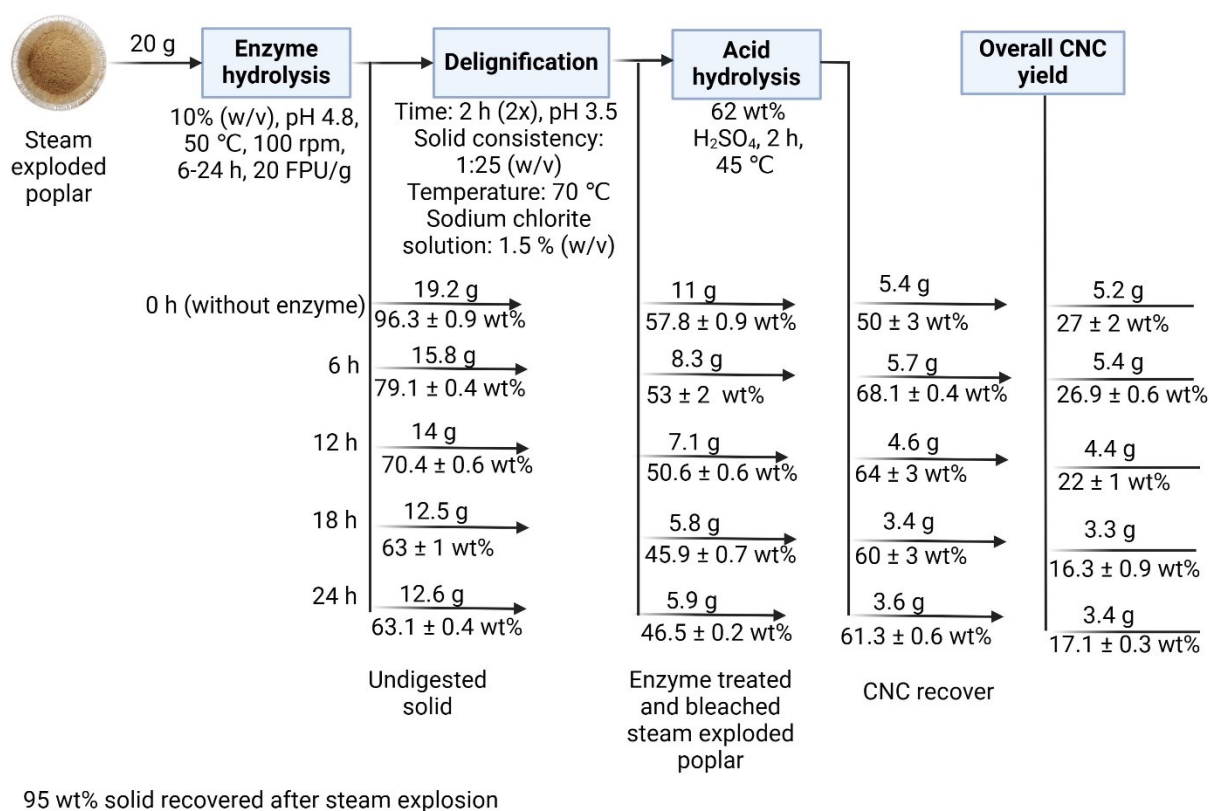


Figure 4.11 Mass balance for CNC isolated from steam explosion and enzyme treated poplar wood. All reported data represent analysis from triplicate samples.

Control - CNC isolated from poplar wood

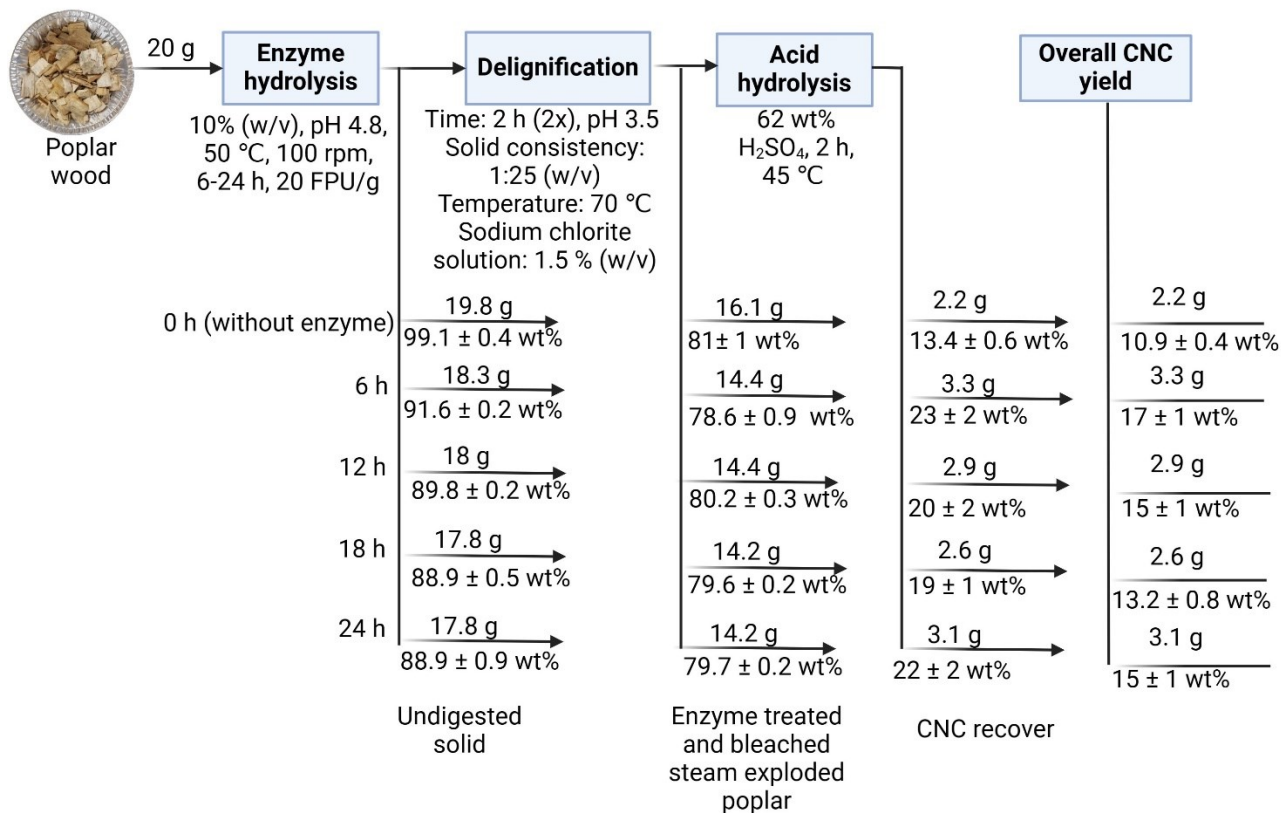


Figure 4.12 Mass balance for CNC isolated from ground poplar (control). All reported data represent analysis from triplicate samples.

Enzyme treatment increased the yield of CNCs (wt % acid hydrolysis feedstock) for the control and steam exploded poplar wood compared with the 0 h (without enzyme treatment) feedstock (Table 4.13). It can be suggested that there was significant accumulation of recalcitrant CNC precursor in the residual solids due to the rapid degradation of non-crystalline cellulose and hemicellulose by enzyme treatment during the study period. However, despite such strong implications of significant CNC precursors accumulation because of the enzyme hydrolysis, extending the enzyme hydrolysis time did not improve the CNC yield for the control and even start decreasing after 18 h for the steam exploded poplar wood. It is likely that CNC precursors exposed to enzyme attack are simultaneously disintegrated by hydrolytic cellulases (Beltramino et al., 2016; Beyene et al., 2017; Yupanqui-

Mendoza et al., 2023). The constant crystallinity index values as a function of time (Table 16) also support these findings. This implies that the enzyme treatment did not show exclusive preference to non-crystalline cellulose due to inaccessibility.

The overall CNC yield data provides insights into the breakdown or dissolution of CNC precursors through enzymatic and/or acid hydrolysis in comparison to the untreated feedstock. As shown in Table 4.13, the overall CNC yield from the control notably rose compared to the initial state at 0 hours (without enzyme treatment). This suggests that amorphous celluloses underwent degradation to form sugar, concentrating the CNC precursors during the enzyme treatment. However, extending the enzyme hydrolysis period did not lead to a further increase in overall CNC yield. One contributing factor is that the presence of hemicellulose and lignin in untreated poplar wood acts as an impediment, hindering yield enhancement.

For steam-exploded poplar wood, there was no significant difference in overall yield of CNC between 6 hours and 0 hours (without enzyme treatment). It is suggested that a relatively more preferential degradation of the more abundant non-crystalline cellulose substrate occurred during the 6 h enzyme treatment. However, after a 12-hour period, CNC precursors became substantially more accessible to disintegration or dissolution through enzymes and/or acid hydrolysis, resulting in a subsequent decrease in the overall CNC yield. Beyene *et al.* (2017) investigated the impact of cellulase treatment on filter paper and wood pulp CNC yield. They observed that filter paper, with a significant more CNC precursors than wood pulp, experienced cellulase dissolution and leading to a 17% reduction in CNC yield compared to the undigested substrate during the early stages of cellulase hydrolysis (2 hours).

In comparing the two feedstocks, the CNC yield from steam-exploded poplar wood was notably higher than that from the control, regardless of cellulase treatment. This enhancement is likely attributed to the formation of new CNC precursors through steam explosion pretreatment. The

combined effect of steam explosion and enzyme treatment not only improves the CNC yield but also proportionally reduces the input needed for subsequent acid hydrolysis processes. Consequently, the volumes of water and H<sub>2</sub>SO<sub>4</sub> required for acid hydrolysis are correspondingly reduced. This improvement in CNC yield from the reactor also decreases the NaOH requirements and enhances the efficiency of downstream purification operations, resulting in time and energy savings.

Table 4.12 CNCs yield from steam explosion and enzymatic treated poplar wood

Enzymatic treatment (h)	CNC yield (wt % acid hydrolysis feedstock)		CNC yield (wt % original feedstock)	
	Control	Steam exploded poplar	Control	Steam exploded polar
0	13.4 ± 0.6 <sup>Y</sup>	50 ± 3 <sup>C</sup>	10.9 ± 0.4 <sup>Y</sup>	27 ± 2 <sup>a</sup>
6	23 ± 2 <sup>X</sup>	68.1 ± 0.4 <sup>A</sup>	17 ± 1 <sup>x</sup>	26.9 ± 0.6 <sup>a</sup>
12	20 ± 2 <sup>X</sup>	64 ± 3 <sup>AB</sup>	15 ± 1 <sup>x</sup>	22 ± 1 <sup>b</sup>
18	19 ± 1 <sup>X</sup>	60 ± 3 <sup>B</sup>	13.2 ± 0.8 <sup>xy</sup>	16.3 ± 0.9 <sup>c</sup>
24	22 ± 2 <sup>X</sup>	61.3 ± 0.6 <sup>B</sup>	15 ± 1 <sup>x</sup>	17.1 ± 0.3 <sup>c</sup>

<sup>A,X, x,a</sup> Means denoted by non-identical letters are significantly different ( $p < 0.05$ ). Condition (62 wt % H<sub>2</sub>SO<sub>4</sub> (8 % w/v, solid to acid ratio), 2 h, 45 °C and 200 rpm)

#### 4.3.5. Characteristics of cellulose nanocrystal from steam explosion and enzymatic treated wood

The impact of steam explosion pretreatment and subsequent enzyme treatment on the morphological structure and crystal size of CNCs were assessed, utilizing Transmission Electron Microscopy (TEM). Despite the anticipated synergistic effects of steam explosion and enzyme hydrolysis in enhancing size reduction and inducing structural changes in CNCs, the statistical analysis presented in Table 4.14 indicated no significant difference in the mean length and width of CNCs between the control group and the steam-exploded poplar. These findings imply that the size of cellulose nanocrystals is predominantly influenced by hydrolysis conditions.

Table 4.13 Particle size of CNCs steam explosion and enzymatic treated poplar wood based on transmission electron microscopy (TEM) micrograph analysis

Particle size of CNCs (nm)				
Enzyme treatment (h)	Control		Steam exploded poplar	
	Length	Width	Length	Width
0	120 ± 50 <sup>A</sup>	9 ± 3 <sup>a</sup>	120 ± 50 <sup>X</sup>	9 ± 2 <sup>x</sup>
6	110 ± 50 <sup>A</sup>	9 ± 3 <sup>a</sup>	150 ± 60 <sup>X</sup>	8 ± 3 <sup>x</sup>
12	120 ± 50 <sup>A</sup>	9 ± 3 <sup>a</sup>	110 ± 40 <sup>X</sup>	10 ± 3 <sup>x</sup>
18	130 ± 50 <sup>A</sup>	10 ± 3 <sup>a</sup>	130 ± 40 <sup>X</sup>	9 ± 3 <sup>xy</sup>
24	160 ± 60 <sup>A</sup>	12 ± 4 <sup>a</sup>	130 ± 50 <sup>X</sup>	10 ± 4 <sup>x</sup>

<sup>A,X, x,a</sup> Means denoted by non-identical letters are significantly different ( $p < 0.05$ ). Condition: Steam explosion pretreatment (200 °C, 1.55 Mpa, 5 min), delignification (Time: 2 h (2x), pH 3.5, solid consistency: 1:25 (w/v), 70 °C, sodium chlorite solution: 1.5 % (w/v)), acid hydrolysis (62 wt%, H<sub>2</sub>SO<sub>4</sub>, 2 h, 45 °C). Enzyme treatment: solid concentration of 10% (w/v), 50 mM sodium acetate buffer (pH 4.8), 50 °C, 100 rpm, cellulase (NS 51129): 20 FPU/g

Additionally, as Table 4.15 indicated crystallinity, zeta potential and thermal stability of CNCs. The crystallinity indices of the CNC's did not show any significant difference due to the synergetic effect of steam explosion and enzyme treatment as a function of time in both feedstocks. This implies that despite some evident crystalline cellulose degradation during enzyme hydrolysis, steam explosion and enzyme treatment does not change the quality of the CNC precursor crystals and the degree of crystallinity of CNC is intricately influenced by the acid hydrolysis conditions employed during their synthesis rather than by pretreatment steps.

The zeta potential indicated the stability of the CNC suspension in an aqueous medium. Generally, when the zeta potential values drop below -30 mV, it signifies the presence of a strong negative electrostatic force originating from the sulfate group, which contributes to a significant dispersion of CNCs (Mohaiyiddin et al., 2016; Naduparambath et al., 2018; Prasanna & Mitra, 2020). The results in Table 4.15 indicate that the enzyme treatments for the control did not impact the colloidal stability of CNCs. However, the zeta potential of CNCs isolated from steam exploded poplar wood showed a

significant difference at for 18 h and 24 h. This could be the enzymes altered the hydroxyl groups distribution on the CNC surface, which could affect the esterification of the sulfate group and hence the charge density on the surface.

The onset temperature observed in Thermogravimetric Analysis (TGA) of CNCs is a critical parameter that provides insights into the thermal stability of these nanomaterials. The TGA onset temperature represents the temperature at which the CNCs begin to undergo thermal decomposition. A higher onset temperature generally indicates greater thermal stability and resistance to degradation. As Table 4.15 presents, it was evident that there was no substantial difference due to enzyme treatment and/or as a function of time for CNC isolated from steam exploded poplar wood. However, for the control, there was no clear trend observed. For both feedstocks with the onset temperature of degradation falling between 250–270 °C.

Table 4.14 Crystallinity, colloidal stability, and degradation temperature of CNCs from steam explosion and enzymatic treated poplar wood

Enzyme treatment (h)	Degree of crystallinity of CNCs (%)		Zeta potential of CNCs (mV)		Onset temperature of CNCs (°C)	
	control	Steam exploded poplar	control	Steam exploded poplar	control	Steam exploded poplar
0	78 ± 2 <sup>b</sup>	78 ± 1 <sup>B</sup>	-43.9 ± 0.5 <sup>a</sup>	-44 ± 1 <sup>xy</sup>	253 ± 2 <sup>d</sup>	265 ± 2 <sup>A</sup>
6	80.5 ± 0.4 <sup>ab</sup>	82 ± 1 <sup>A</sup>	-44 ± 1 <sup>a</sup>	-48 ± 1 <sup>x</sup>	268 ± 1 <sup>bc</sup>	269 ± 1 <sup>A</sup>
12	79.7 ± 0.5 <sup>ab</sup>	82 ± 1 <sup>A</sup>	-42.8 ± 0.9 <sup>a</sup>	-48.3 ± 0.6 <sup>x</sup>	265 ± 0.3 <sup>c</sup>	269 ± 2 <sup>A</sup>
18	81.1 ± 0.7 <sup>a</sup>	82 ± 1 <sup>A</sup>	-41 ± 1 <sup>a</sup>	-42 ± 2 <sup>y</sup>	274 ± 2 <sup>a</sup>	271 ± 2 <sup>A</sup>
24	79.5 ± 0.2 <sup>ab</sup>	82.2 ± 0.4 <sup>A</sup>	-41 ± 1 <sup>a</sup>	-39 ± 2 <sup>y</sup>	270 ± 0.2 <sup>b</sup>	270 ± 2 <sup>A</sup>

<sup>A,a</sup> Means denoted by non-identical letters are significantly different ( $p < 0.05$ ). Condition: Steam explosion pretreatment (200 °C, 1.55 Mpa, 5 min), delignification (Time: 2 h (2x), pH 3.5, solid consistency: 1:25 (w/v), 70 °C, sodium chlorite solution: 1.5 % (w/v)), acid hydrolysis (62 wt%, H<sub>2</sub>SO<sub>4</sub>, 2 h, 45 °C). Enzyme treatment: solid concentration of 10% (w/v), 50 mM sodium acetate buffer (pH 4.8), 50 °C, 100 rpm, cellulase (NS 51129): 20 FPU/g

#### **4.4. Comparative analysis of cellulose nanocrystals and sugars yield across the three-biomass conversion pathway**

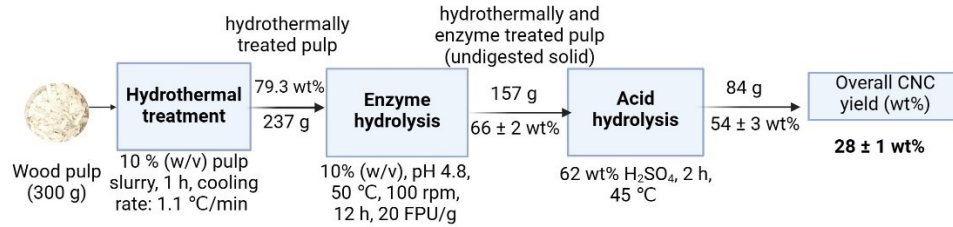
The lignocellulose biorefinery concept offers a promising approach for sustainable production of renewable chemicals, fuels, and materials by integrating various biomass conversion processes in a single facility. This approach maximizes the use of biomass resources and generates a diverse range of valuable products through physical, chemical, biological, and thermochemical methods. The selection of an appropriate pretreatment technology is crucial within this framework as it enables the production of biochemicals, enhances the yield of CNCs, and improves the accessibility of enzymes during saccharification. Steam explosion pretreatment is widely employed, involving pressurized steam treatment followed by depressurization to hydrolyze hemicellulose and increase cellulose accessibility, with minimal environmental impact and low energy consumption. In contrast, hydrothermal treatment utilizes water alone as the reaction medium, leading to alterations in cellulose structures and partial solubilization of hemicellulose (Sarker et al., 2021).

This study aimed to enhance the production of cellulose nanocrystals (CNCs) and fermentable sugars by integrating various processes within a biorefinery framework. Three approaches were explored: (a) hydrothermal treatment combined with enzymatic treatment and acid hydrolysis, (b) steam explosion pretreatment followed by acid hydrolysis, and (c) steam explosion followed by enzymatic treatment and acid hydrolysis. Results revealed that both steam explosion and hydrothermal treatment facilitated the formation of additional CNC precursors, leading to increased CNC yield. However, steam explosion required a shorter reaction time compared to hydrothermal treatment due to its rapid heating and sudden decompression process. This characteristic makes steam explosion more suitable for continuous processing in industrial scale biorefineries.

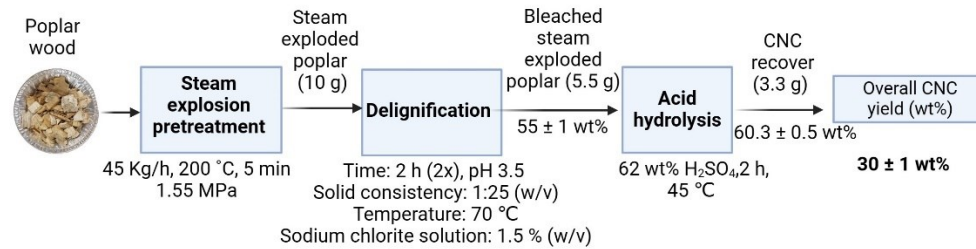
Figure 4.13 depicted the CNC yield under optimal conditions achieved through this integrated approach. CNC yields were measured as  $28 \pm 1$  wt%,  $30 \pm 1$  wt%, and  $22 \pm 1$  wt% for hydrothermal and 12 h enzymatically treated pulp, steam-exploded poplar wood, and steam explosion combined with 12 h enzymatically treated poplar wood, respectively. CNC yield from hydrothermal treatment and 12 h enzymatically treated pulp, as well as steam-exploded poplar wood, higher than that of steam explosion combined with 12 h enzymatically treated poplar wood.

Notably, CNC isolated via steam explosion followed by acid hydrolysis did not yield fermentable sugars from the hydrolysis of non-crystalline cellulose. Conversely, CNC isolated from hydrothermal and enzymatically treated pulp, as well as steam explosion and enzymatically treated poplar wood resulted in the recovery of  $23 \pm 1$  wt% and  $29 \pm 1$  wt% glucose and  $2.3 \pm 0.2$  wt% and  $5.6 \pm 0.2$  wt% xylose, respectively. Co-production of sugars alongside enhanced acid hydrolysis efficiency could significantly improve the economic viability of the CNC industry. However, the observed reduction in CNC yield, particularly in the steam explosion and enzymatic process, may pose challenges from an economic standpoint, warranting further feasibility studies.

### 1. Integrated hydrothermal and enzymatic treatment with acid hydrolysis for production of CNC



### 2. Isolation of cellulose nanocrystal from steam exploded poplar wood



### 3. Steam explosion and enzymatic digestion as pretreatments for co-production of CNC

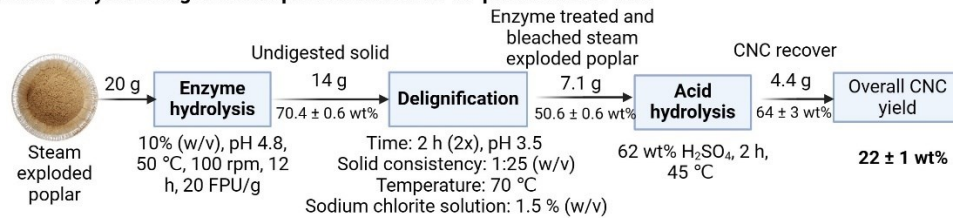


Figure 4.13 CNCs yield from an integrated process beginning with either hydrothermal or steam explosion pretreatment followed by enzymatic hydrolysis and then acid hydrolysis.

## **5. Conclusion and Future directions**

### **5.1. Conclusion**

In conclusion, the research presented in this thesis demonstrates the technical feasibility and efficacy of integrated biorefinery strategies to produce CNCs and fermentable sugars from lignocellulosic biomass. The first study showcased a hydrothermal and enzymatic treatment and acid hydrolysis, resulting in a substantial increase in CNC yield from wood pulp. The optimized conditions led to a CNC yield of 54 %, significantly higher than untreated and hydrothermally treated pulp alone. This integrated approach not only enhanced CNC production but also generated valuable fermentable sugars as by-products, addressing economic challenges associated with enzymatic hydrolysis.

The second study focused on the impact of steam explosion pretreatment on CNC yield, revealing a simple and scalable method to improve overall economics and commercial viability. Steam explosion pretreatment before acid hydrolysis increased the crystallinity of semi-crystalline/non-crystalline cellulose, leading to a 2.5-fold increase in CNC yield from poplar wood. Importantly, the quality of the CNCs remained unaffected, and their thermal stability improved. This study highlights the potential of steam explosion as a strategic pretreatment step to enhance CNC production efficiency.

The third study expanded on the integrated approach by combining steam explosion pretreatment, enzymatic hydrolysis, and acid hydrolysis for poplar wood. The results demonstrated that this multi-step process effectively facilitated the crystallization of semi-crystalline cellulose and improved saccharification of amorphous cellulose. The CNC yield from steam-exploded poplar wood reached 68.1%, showcasing a significant improvement over untreated poplar wood. The study also emphasized the stability and quality of CNCs produced through this integrated process, further supporting its potential for sustainable and diverse industrial applications.

In summary, these studies collectively contribute valuable insights into designing efficient biorefinery strategies for lignocellulosic biomass, focusing on both high CNC yield and additional high-value products such as fermentable sugars. The integration of various treatments and hydrolysis steps not only enhances economic feasibility but also aligns with the broader goal of sustainable and environmentally conscious bioethanol production. These findings provide a foundation for further research and development in the field of lignocellulosic biomass utilization, offering innovative pathways towards a more sustainable and integrated bio-based economy.

## **5.2. Future directions**

Moving forward, the findings from this research suggest several recommendations and avenues for future exploration in the realm of lignocellulosic biomass utilization and biorefinery strategies. Firstly, further optimization and scaling-up of the integrated processes should be pursued to enhance their industrial applicability. This includes fine-tuning the conditions of hydrothermal treatment, enzymatic hydrolysis, and acid hydrolysis for different feedstocks and exploring the feasibility of continuous processing systems. Additionally, assessing the economic viability of these integrated approaches on a larger scale is crucial to establish their competitiveness against traditional bioethanol production methods.

Secondly, the exploration of alternative feedstocks for CNC production should be expanded. While wood pulp and poplar wood were investigated in this thesis, different lignocellulosic sources, such as agricultural residues and dedicated energy crops, could offer unique properties and challenges. Understanding the variability in biomass composition and structure among different feedstocks will be key to developing versatile and adaptable biorefinery processes. Moreover, considering the potential impact of regional and seasonal variations on feedstock characteristics is vital for designing robust and flexible biorefinery systems.

Lastly, the integration of circular economy principles in the biorefinery framework should be explored. This involves exploring ways to utilize by-products and residues generated from the biorefinery process for additional value-added products or incorporating them into other industrial processes. Efforts to minimize waste and maximize resource efficiency align with sustainability goals and contribute to the overall environmental and economic viability of bioethanol production from lignocellulosic biomass. Research in this direction may lead to the development of comprehensive and closed-loop biorefinery systems that optimize resource utilization and minimize environmental impact.

## References

- Adney, W. S., Himmel, Æ. M. E., Johnson, D. K., Davis, Æ. M. F., & Digestibility, Á. A. Á. (2009). *Can delignification decrease cellulose digestibility in acid pretreated corn stover?* 677–686. <https://doi.org/10.1007/s10570-009-9313-1>
- Agarwal, U. P., Ralph, S. A., Reiner, R. S., Hunt, C. G., Baez, C., Ibach, R., & Hirth, K. C. (2018). Production of high lignin-containing and lignin-free cellulose nanocrystals from wood. *Cellulose*, 25(10), 5791–5805. <https://doi.org/10.1007/s10570-018-1984-z>
- Agarwal, U. P., Reiner, R. R., & Ralph, S. A. (2013). Estimation of cellulose crystallinity of lignocelluloses using near-IR FT-Raman spectroscopy and comparison of the Raman and Segal-WAXS methods. *Journal of Agricultural and Food Chemistry*, 61(1), 103–113. <https://doi.org/10.1021/jf304465k>
- Agarwal, U. P., Zhu, J. Y., & Ralph, S. A. (2013). Enzymatic hydrolysis of loblolly pine: Effects of cellulose crystallinity and delignification. *Holzforschung*, 67(4), 371–377. <https://doi.org/10.1515/hf-2012-0116>
- Andrade, M. S., Ishikawa, O. H., Costa, R. S., Seixas, M. V. S., Rodrigues, R. C. L. B., & Moura, E. A. B. (2022). Development of sustainable food packaging material based on biodegradable polymer reinforced with cellulose nanocrystals. *Food Packaging and Shelf Life*, 31(January). <https://doi.org/10.1016/j.fpsl.2021.100807>
- Anwar, B., Bundjali, B., & Arcana, I. M. (2015). Isolation of Cellulose Nanocrystals from Bacterial Cellulose Produced from Pineapple Peel Waste Juice as Culture Medium. *Procedia Chemistry*, 16, 279–284. <https://doi.org/10.1016/j.proche.2015.12.051>
- Araki, J., Wada, M., Kuga, S., & Okano, T. (1998). Flow properties of microcrystalline cellulose suspension prepared by acid treatment of native cellulose. *Colloids and Surfaces A: Physicochemical and Engineering Aspects*, 142(1), 75–82. [https://doi.org/https://doi.org/10.1016/S0927-7757\(98\)00404-X](https://doi.org/https://doi.org/10.1016/S0927-7757(98)00404-X)
- Asim, N., Badiei, M., & Mohammad, M. (2022). Recent advances in cellulose-based hydrophobic food packaging. In *Emergent Materials* (Vol. 5, Issue 3, pp. 703–718). Springer Nature. <https://doi.org/10.1007/s42247-021-00314-2>
- Atalla, R. H., & VanderHart, D. L. (1984). Native Cellulose: A Composite of Two Distinct Crystalline Forms. *Science*, 223(4633), 283–285. <https://doi.org/10.1126/science.223.4633.283>
- Bano, S., & Negi, Y. S. (2017). Studies on cellulose nanocrystals isolated from groundnut shells. *Carbohydrate Polymers*, 157, 1041–1049. <https://doi.org/10.1016/j.carbpol.2016.10.069>
- Behr, M., El Jaziri, M., & Baucher, M. (2021). Lignin-Based Materials for Biomedical Applications. In *Lignin-Based Materials for Biomedical Applications*. Elsevier. <https://doi.org/10.1016/c2019-0-01345-3>

- Beltramino, F., Roncero, M. B., Torres, A. L., Vidal, T., & Valls, C. (2016). Optimization of sulfuric acid hydrolysis conditions for preparation of nanocrystalline cellulose from enzymatically pretreated fibers. *Cellulose*, 23(3), 1777–1789. <https://doi.org/10.1007/s10570-016-0897-y>
- Beltramino, F., Roncero, M. B., Vidal, T., Torres, A. L., & Valls, C. (2015). Increasing yield of nanocrystalline cellulose preparation process by a cellulase pretreatment. *Bioresource Technology*, 192, 574–581. <https://doi.org/https://doi.org/10.1016/j.biortech.2015.06.007>
- Beyene, D., Chae, M., Dai, J., Danumah, C., Tosto, F., Demesa, A. G., & Bressler, D. C. (2017). Enzymatically-mediated co-production of cellulose nanocrystals and fermentable sugars. *Catalysts*, 7(11), 1–13. <https://doi.org/10.3390/catal7110322>
- Beyene, D., Chae, M., Dai, J., Danumah, C., Tosto, F., Demesa, A. G., & Bressler, D. C. (2018). Characterization of cellulase-treated fibers and resulting cellulose nanocrystals generated through acid hydrolysis. *Materials*, 11(8). <https://doi.org/10.3390/ma11081272>
- Beyene, D., Chae, M., Vasanthan, T., & Bressler, D. C. (2020). A Biorefinery Strategy That Introduces Hydrothermal Treatment Prior to Acid Hydrolysis for Co-generation of Furfural and Cellulose Nanocrystals. *Frontiers in Chemistry*, 8(April), 1–11. <https://doi.org/10.3389/fchem.2020.00323>
- Björquist, S., Aronsson, J., Henriksson, G., & Persson, A. (2018). Textile qualities of regenerated cellulose fibers from cotton waste pulp. *Textile Research Journal*, 88(21), 2485–2492. <https://doi.org/10.1177/0040517517723021>
- Bondeson, D., Mathew, A., & Oksman, K. (2006). *Optimization of the isolation of nanocrystals from microcrystalline cellulose by acid hydrolysis*. 171–180. <https://doi.org/10.1007/s10570-006-9061-4>
- Börjesson, M., & Westman, G. (2015). Crystalline Nanocellulose — Preparation, Modification, and Properties. *Cellulose - Fundamental Aspects and Current Trends, January 2015*. <https://doi.org/10.5772/61899>
- Brinchi, L., Cotana, F., Fortunati, E., & Kenny, J. M. (2013). Production of nanocrystalline cellulose from lignocellulosic biomass : Technology and applications. *Carbohydrate Polymers*, 94(1), 154–169. <https://doi.org/10.1016/j.carbpol.2013.01.033>
- Bura, R., Chandra, R., & Saddler, J. (2009). Influence of xylan on the enzymatic hydrolysis of steam-pretreated corn Stover and hybrid poplar. *Biotechnology Progress*, 25(2), 315–322. <https://doi.org/10.1002/btpr.98>
- Calvino, C., Macke, N., Kato, R., & Rowan, S. J. (2020). Development, processing and applications of bio-sourced cellulose nanocrystal composites. *Progress in Polymer Science*, 103. <https://doi.org/10.1016/j.progpolymsci.2020.101221>

- Camarero Espinosa, S., Kuhnt, T., Foster, E. J., & Weder, C. (2013). Isolation of thermally stable cellulose nanocrystals by phosphoric acid hydrolysis. *Biomacromolecules*, *14*(4), 1223–1230. <https://doi.org/10.1021/bm400219u>
- Camargo, L. A., Pereira, S. C., Correa, A. C., Farinas, C. S., Marconcini, J. M., & Mattoso, L. H. C. (2016). Feasibility of Manufacturing Cellulose Nanocrystals from the Solid Residues of Second-Generation Ethanol Production from Sugarcane Bagasse. *Bioenergy Research*, *9*(3), 894–906. <https://doi.org/10.1007/s12155-016-9744-0>
- Chen, L., Wang, Q., Hirth, K., Baez, C., Agarwal, U. P., & Zhu, J. Y. (2015). Tailoring the yield and characteristics of wood cellulose nanocrystals (CNC) using concentrated acid hydrolysis. *Cellulose*, *22*(3), 1753–1762. <https://doi.org/10.1007/s10570-015-0615-1>
- Chen, M., Parot, J., Hackley, V. A., Zou, S., & Johnston, L. J. (2021). AFM characterization of cellulose nanocrystal height and width using internal calibration standards. *Cellulose*, *28*(4), 1933–1946. <https://doi.org/10.1007/s10570-021-03678-0>
- Dai, J., Chae, M., Beyene, D., Danumah, C., Tosto, F., & Bressler, D. C. (2018). Co-production of cellulose nanocrystals and fermentable sugars assisted by endoglucanase treatment of wood pulp. *Materials*, *11*(9). <https://doi.org/10.3390/ma11091645>
- Druzhinina, A. S., Parshina, A. E., Shul, E. V., Semushina, M. P., & Aleshina, L. A. (2017). *Isolation and structural characterization of cellulose from arctic brown algae*. *53*(3), 452–456. <https://doi.org/10.1007/s10600-017-2039-7>
- Du, L., Wang, J., Zhang, Y., Qi, C., Wolcott, M. P., & Yu, Z. (2017). A co-production of sugars, lignosulfonates, cellulose, and cellulose nanocrystals from ball-milled woods. *Bioresource Technology*, *238*, 254–262. <https://doi.org/10.1016/j.biortech.2017.03.097>
- El-Sakhawy, M., Kamel, S., Salama, A., & Sarhan, H.-A. (2014). Carboxymethyl Cellulose Acetate Butyrate: A Review of the Preparations, Properties, and Applications. *Journal of Drug Delivery*, *2014*, 1–6. <https://doi.org/10.1155/2014/575969>
- Eyley, S., & Thielemans, W. (2014). Surface modification of cellulose nanocrystals. *Nanoscale*, *6*(14), 7764–7779. <https://doi.org/10.1039/c4nr01756k>
- Felix Santana, M., Maria De Sousa, M., Yamashita, F. M., Castro Moreira, B., Mauro De Almeida, J., Vianna, A., De Carvalho Teixeira, N., De, D., & Silva, J. (2019). *Cellulose nanocrystal production focusing on cellulosic material pre-treatment and acid hydrolysis time* (Vol. 80).
- Ferreira, F. V., Mariano, M., Rabelo, S. C., Gouveia, R. F., & Lona, L. M. F. (2018). Applied Surface Science Isolation and surface modification of cellulose nanocrystals from sugarcane bagasse waste : From a micro- to a nano-scale view. *Applied Surface Science*, *436*, 1113–1122. <https://doi.org/10.1016/j.apsusc.2017.12.137>

- Festucci-Buselli, A., R., Otoni, W. C., & Joshi, C. P. (2007). Structure, organization, and functions of cellulose synthase complexes in higher plants. *Brazilian Journal of Plant Physiology*, *19*(1), 1–13. <https://doi.org/10.1590/s1677-04202007000100001>
- Filson, P. B., Dawson-andoh, B. E., & Schwegler-berry, D. (2009). *Enzymatic-mediated production of cellulose nanocrystals from recycled pulp*. 1808–1814. <https://doi.org/10.1039/b915746h>
- Fu, X., Ji, H., Wang, B., Zhu, W., & Pang, Z. (2020). Preparation of thermally stable and surface-functionalized cellulose nanocrystals by a fully recyclable organic acid and ionic liquid mediated technique under mild conditions. *Cellulose*, *27*(3), 1289–1299. <https://doi.org/10.1007/s10570-019-02875-2>
- Geddes, C. C., Nieves, I. U., & Ingram, L. O. (2011). Advances in ethanol production. In *Current Opinion in Biotechnology* (Vol. 22, Issue 3, pp. 312–319). <https://doi.org/10.1016/j.copbio.2011.04.012>
- George, J., & Sabapathi, S. N. (2015). Cellulose nanocrystals: Synthesis, functional properties, and applications. *Nanotechnology, Science and Applications*, *8*, 45–54. <https://doi.org/10.2147/NSA.S64386>
- Grishkewich, N., Mohammed, N., Tang, J., & Tam, K. C. (2017). Recent advances in the application of cellulose nanocrystals. *Current Opinion in Colloid and Interface Science*, *29*, 32–45. <https://doi.org/10.1016/j.cocis.2017.01.005>
- Gupta, P. K., Raghunath, S. S., Prasanna, D. V., Venkat, P., Shree, V., Chithananthan, C., Choudhary, S., Surender, K., & Geetha, K. S. (2019). An Update on Overview of Cellulose, Its Structure and Applications. *Cellulose*. <https://api.semanticscholar.org/CorpusID:182667018>
- Habibi, Y., Lucia, L. A., & Rojas, O. J. (2010). Cellulose nanocrystals: Chemistry, self-assembly, and applications. *Chemical Reviews*, *110*(6), 3479–3500. <https://doi.org/10.1021/cr900339w>
- Hall, M., Bansal, P., Lee, J. H., Realff, M. J., & Bommarius, A. S. (2010). Cellulose crystallinity - A key predictor of the enzymatic hydrolysis rate. *FEBS Journal*, *277*(6), 1571–1582. <https://doi.org/10.1111/j.1742-4658.2010.07585.x>
- Hon, D. N.-S. (1994). Cellulose: a random walk along its historical path. *Cellulose*, *1*(1), 1–25. <https://doi.org/10.1007/BF00818796>
- Hon-meng, Tin, L., Tee, T., Bee, S., Hui, D., Low, C., & Rahmat, A. R. (2015). Extraction of cellulose nanocrystals from plant sources for application as reinforcing agent in polymers. *Composites Part B*, *75*, 176–200. <https://doi.org/10.1016/j.compositesb.2015.01.008>
- Houfani, A. A., Anders, N., Spiess, A. C., Baldrian, P., & Benallaoua, S. (2020). Insights from enzymatic degradation of cellulose and hemicellulose to fermentable sugars— a review. In *Biomass and Bioenergy* (Vol. 134). Elsevier Ltd. <https://doi.org/10.1016/j.biombioe.2020.105481>

- Huang, L. Z., Ma, M. G., Ji, X. X., Choi, S. E., & Si, C. (2021). Recent Developments and Applications of Hemicellulose From Wheat Straw: A Review. In *Frontiers in Bioengineering and Biotechnology* (Vol. 9). Frontiers Media S.A. <https://doi.org/10.3389/fbioe.2021.690773>
- Hubbell, C. A., & Ragauskas, A. J. (2010). Bioresource Technology Effect of acid-chlorite delignification on cellulose degree of polymerization. *Bioresource Technology*, *101*(19), 7410–7415. <https://doi.org/10.1016/j.biortech.2010.04.029>
- Isikgor, F. H., & Becer, C. R. (2015). Lignocellulosic biomass: a sustainable platform for the production of bio-based chemicals and polymers. *Polymer Chemistry*, *6*(25), 4497–4559. <https://doi.org/10.1039/c5py00263j>
- Jiang, F., & Hsieh, Y. Lo. (2015). Cellulose nanocrystal isolation from tomato peels and assembled nanofibers. *Carbohydrate Polymers*, *122*, 60–68. <https://doi.org/10.1016/j.carbpol.2014.12.064>
- Kalita, E., Nath, B. K., Agan, F., More, V., & Deb, P. (2015). Isolation and characterization of crystalline, autofluorescent, cellulose nanocrystals from saw dust wastes. *Industrial Crops and Products*, *65*, 550–555. <https://doi.org/10.1016/j.indcrop.2014.10.004>
- Kapoor, M., Raj, T., Vijayaraj, M., Chopra, A., Gupta, R. P., Tuli, D. K., & Kumar, R. (2015). Structural features of dilute acid, steam exploded, and alkali pretreated mustard stalk and their impact on enzymatic hydrolysis. *Carbohydrate Polymers*, *124*, 265–273. <https://doi.org/10.1016/j.carbpol.2015.02.044>
- Kathahira, R., Elder, T. J., & Beckham, G. T. (2018). *A Brief Introduction to Lignin Structure*. <https://api.semanticscholar.org/CorpusID:139367151>
- Kim, H., Jeon, H., Shin, G., Lee, M., Jegal, J., Hwang, S. Y., Oh, D. X., Koo, J. M., Eom, Y., & Park, J. (2021). Biodegradable nanocomposite of poly(ester-co-carbonate) and cellulose nanocrystals for tough tear-resistant disposable bags. *Green Chemistry*, *23*(6), 2293–2299. <https://doi.org/10.1039/d0gc04072j>
- Klemm, D., Heublein, B., Fink, H. P., & Bohn, A. (2005). Cellulose: Fascinating biopolymer and sustainable raw material. *Angewandte Chemie - International Edition*, *44*(22), 3358–3393. <https://doi.org/10.1002/anie.200460587>
- Kovalenko, V. I. (2010). Crystalline cellulose: structure and hydrogen bonds. *Russian Chemical Reviews*, *79*(3), 231–241. <https://doi.org/10.1070/rc2010v079n03abeh004065>
- Kusmono, Listyanda, R. F., Wildan, M. W., & Ilman, M. N. (2020). Preparation and characterization of cellulose nanocrystal extracted from ramie fibers by sulfuric acid hydrolysis. *Heliyon*, *6*(11), e05486. <https://doi.org/10.1016/j.heliyon.2020.e05486>

- Lam, N. T., Chollakup, R., Smitthipong, W., Nimchua, T., & Sukyai, P. (2017). Characterization of Cellulose Nanocrystals Extracted from Sugarcane Bagasse for Potential Biomedical Materials. *Sugar Tech*, 19(5), 539–552. <https://doi.org/10.1007/s12355-016-0507-1>
- Lavoine, N., Desloges, I., Dufresne, A., & Bras, J. (2012). Microfibrillated cellulose – Its barrier properties and applications in cellulosic materials : A review. *Carbohydrate Polymers*, 90(2), 735–764. <https://doi.org/10.1016/j.carbpol.2012.05.026>
- Laxmeshwar, S. S., Madhu Kumar, D. J., Viveka, S., & Nagaraja, G. K. (2012). Preparation and Properties of Biodegradable Film Composites Using Modified Cellulose Fibre-Reinforced with PVA. *ISRN Polymer Science*, 2012, 1–8. <https://doi.org/10.5402/2012/154314>
- Li, B., Xu, W., Kronlund, D., Määttä, A., Liu, J., Smätt, J., Peltonen, J., Willför, S., Mu, X., & Xu, C. (2015). Cellulose nanocrystals prepared via formic acid hydrolysis followed by TEMPO-mediated oxidation. *Carbohydrate Polymers*, 133, 605–612. <https://doi.org/10.1016/j.carbpol.2015.07.033>
- Li, R., Fei, J., Cai, Y., Li, Y., Feng, J., & Yao, J. (2009). Cellulose whiskers extracted from mulberry : A novel biomass production. *Carbohydrate Polymers*, 76(1), 94–99. <https://doi.org/10.1016/j.carbpol.2008.09.034>
- Lin, N. (2014). *Cellulose nanocrystals : surface modification and advanced materials*. <https://api.semanticscholar.org/CorpusID:138710936>
- Liu, C. G., Xiao, Y., Xia, X. X., Zhao, X. Q., Peng, L., Srinophakun, P., & Bai, F. W. (2019). Cellulosic ethanol production: Progress, challenges and strategies for solutions. In *Biotechnology Advances* (Vol. 37, Issue 3, pp. 491–504). Elsevier Inc. <https://doi.org/10.1016/j.biotechadv.2019.03.002>
- Longaresi, R. H., de Menezes, A. J., Pereira-da-Silva, M. A., Baron, D., & Mathias, S. L. (2019). The maize stem as a potential source of cellulose nanocrystal: Cellulose characterization from its phenological growth stage dependence. *Industrial Crops and Products*, 133(July 2018), 232–240. <https://doi.org/10.1016/j.indcrop.2019.02.046>
- Lu, P., & Hsieh, Y. (2010). Preparation and properties of cellulose nanocrystals : Rods , spheres , and network. *Carbohydrate Polymers*, 82(2), 329–336. <https://doi.org/10.1016/j.carbpol.2010.04.073>
- Lu, S., Ma, T., Hu, X., Zhao, J., Liao, X., Song, Y., & Hu, X. (2022). Facile extraction and characterization of cellulose nanocrystals from agricultural waste sugarcane straw. *Journal of the Science of Food and Agriculture*, 102(1), 312–321. <https://doi.org/10.1002/jsfa.11360>
- Mahfoudhi, N., & Boufi, S. (2017). Nanocellulose: A challenging nanomaterial towards environment remediation. In *Cellulose-Reinforced Nanofibre Composites: Production, Properties and Applications* (pp. 277–304). Elsevier Inc. <https://doi.org/10.1016/B978-0-08-100957-4.00012-7>

- Mahmud, M. M., Perveen, A., Jahan, R. A., Matin, M. A., Wong, S. Y., Li, X., & Arafat, M. T. (2019). Preparation of different polymorphs of cellulose from different acid hydrolysis medium. *International Journal of Biological Macromolecules*, 130, 969–976. <https://doi.org/https://doi.org/10.1016/j.ijbiomac.2019.03.027>
- Malik, K., Sharma, P., Yang, Y., Zhang, P., Zhang, L., Xing, X., Yue, J., Song, Z., Nan, L., Yujun, S., El-Dalatony, M. M., Salama, E. S., & Li, X. (2022). Lignocellulosic biomass for bioethanol: Insight into the advanced pretreatment and fermentation approaches. In *Industrial Crops and Products* (Vol. 188). Elsevier B.V. <https://doi.org/10.1016/j.indcrop.2022.115569>
- Marchessault, R. H., & Sundararajan, P. R. (1983). 2 - Cellulose. In G. O. ASPINALL (Ed.), *The Polysaccharides* (pp. 11–95). Academic Press. <https://doi.org/https://doi.org/10.1016/B978-0-12-065602-8.50007-8>
- Mariano, M., El Kissi, N., & Dufresne, A. (2014). Cellulose nanocrystals and related nanocomposites: Review of some properties and challenges. *Journal of Polymer Science, Part B: Polymer Physics*, 52(12), 791–806. <https://doi.org/10.1002/polb.23490>
- Mishra, S. P., Manent, A. S., Chabot, B., & Daneault, C. (2012). Production of nanocellulose from native cellulose - Various options utilizing ultrasound. *BioResources*, 7(1), 422–435. <https://doi.org/10.15376/biores.7.1.0422-0436>
- Mohaiyiddin, M. S., Lin, O. H., Owi, W. T., Chan, C. H., Chia, C. H., Zakaria, S., Villagrancia, A. R., & Akil, H. M. (2016). Characterization of nanocellulose recovery from *Elaeis guineensis* frond for sustainable development. *Clean Technologies and Environmental Policy*, 18(8), 2503–2512. <https://doi.org/10.1007/s10098-016-1191-2>
- Mohd Amin, K. N., Annamalai, P. K., Morrow, I. C., & Martin, D. (2015). Production of cellulose nanocrystals via a scalable mechanical method. *RSC Advances*, 5(70), 57133–57140. <https://doi.org/10.1039/c5ra06862b>
- Moradbak, A., Tahir, P., & Mohamed, A. Z. (2018). Isolation of cellulose nanocrystals from *Gigantochloa scortechinii* ASAM pulp. *European Journal of Wood and Wood Products*, 76(3), 1021–1027. <https://doi.org/10.1007/s00107-017-1244-1>
- Mu, R., Hong, X., Ni, Y., Li, Y., Pang, J., Wang, Q., Xiao, J., & Zheng, Y. (2019). Recent trends and applications of cellulose nanocrystals in food industry. *Trends in Food Science and Technology*, 93(December 2018), 136–144. <https://doi.org/10.1016/j.tifs.2019.09.013>
- Naduparambath, S., T.V., J., Shaniba, V., M.P., S., Balan, A. K., & Purushothaman, E. (2018). Isolation and characterisation of cellulose nanocrystals from sago seed shells. *Carbohydrate Polymers*, 180(April 2017), 13–20. <https://doi.org/10.1016/j.carbpol.2017.09.088>
- Nagarajan, K. J., Ramanujam, N. R., Sanjay, M. R., Siengchin, S., Surya Rajan, B., Sathick Basha, K., Madhu, P., & Raghav, G. R. (2021). A comprehensive review on cellulose nanocrystals

- and cellulose nanofibers: Pretreatment, preparation, and characterization. In *Polymer Composites* (Vol. 42, Issue 4). <https://doi.org/10.1002/pc.25929>
- Oun, A. A., & Rhim, J. W. (2016). Isolation of cellulose nanocrystals from grain straws and their use for the preparation of carboxymethyl cellulose-based nanocomposite films. *Carbohydrate Polymers*, *150*, 187–200. <https://doi.org/10.1016/j.carbpol.2016.05.020>
- Paukszta, D., & Borysiak, S. (2013). The influence of processing and the polymorphism of lignocellulosic fillers on the structure and properties of composite materials-A review. *Materials*, *6*(7), 2747–2767. <https://doi.org/10.3390/ma6072747>
- Pereira, B., & Arantes, V. (2020). Production of cellulose nanocrystals integrated into a biochemical sugar platform process via enzymatic hydrolysis at high solid loading. *Industrial Crops and Products*, *152*(December 2019), 112377. <https://doi.org/10.1016/j.indcrop.2020.112377>
- Prado, K. S., & Spinacé, M. A. S. (2019). Isolation and characterization of cellulose nanocrystals from pineapple crown waste and their potential uses. *International Journal of Biological Macromolecules*, *122*, 410–416. <https://doi.org/10.1016/j.ijbiomac.2018.10.187>
- Prasanna, N. S., & Mitra, J. (2020). Isolation and characterization of cellulose nanocrystals from Cucumis sativus peels. *Carbohydrate Polymers*, *247*(March), 116706. <https://doi.org/10.1016/j.carbpol.2020.116706>
- Rambabu, N., Panthapulakkal, S., Sain, M., & Dalai, A. K. (2016). Production of nanocellulose fibers from pinecone biomass: Evaluation and optimization of chemical and mechanical treatment conditions on mechanical properties of nanocellulose films. *Industrial Crops and Products*, *83*, 746–754. <https://doi.org/10.1016/j.indcrop.2015.11.083>
- Rana, A. K., Frollini, E., & Thakur, V. K. (2021). Cellulose nanocrystals: Pretreatments, preparation strategies, and surface functionalization. *International Journal of Biological Macromolecules*, *182*, 1554–1581. <https://doi.org/10.1016/j.ijbiomac.2021.05.119>
- Rånby, B. G. (1951). Fibrous macromolecular systems. Cellulose and muscle. The colloidal properties of cellulose micelles. *Discussions of the Faraday Society*, *11*(0), 158–164. <https://doi.org/10.1039/DF9511100158>
- Rao, J., Lv, Z., Chen, G., & Peng, F. (2023). Hemicellulose: Structure, chemical modification, and application. In *Progress in Polymer Science* (Vol. 140). Elsevier Ltd. <https://doi.org/10.1016/j.progpolymsci.2023.101675>
- Raza, M., & Abu-Jdayil, B. (2022a). Cellulose nanocrystals from lignocellulosic feedstock: a review of production technology and surface chemistry modification. In *Cellulose* (Vol. 29, Issue 2). Springer Netherlands. <https://doi.org/10.1007/s10570-021-04371-y>

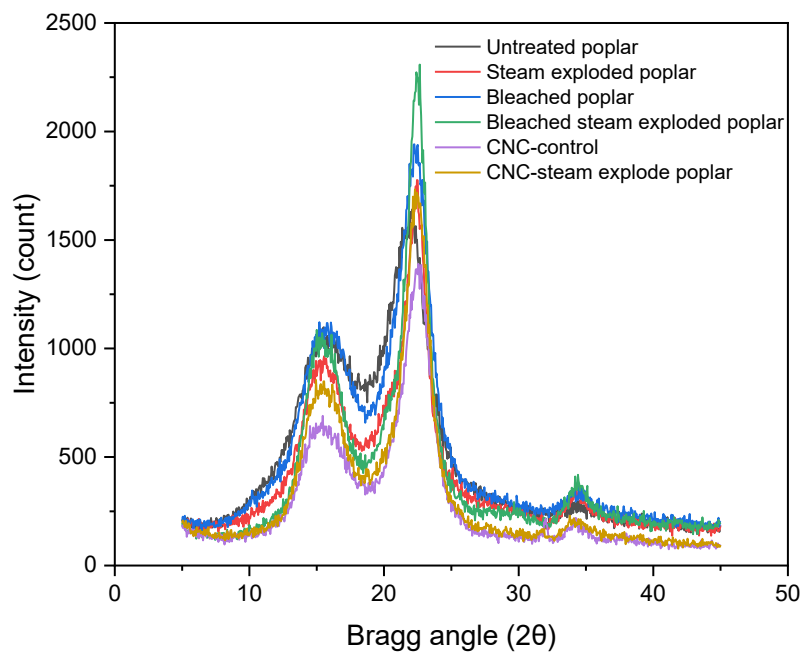
- Raza, M., & Abu-Jdayil, B. (2022b). Cellulose nanocrystals from lignocellulosic feedstock: a review of production technology and surface chemistry modification. In *Cellulose* (Vol. 29, Issue 2, pp. 685–722). Springer Science and Business Media B.V.  
<https://doi.org/10.1007/s10570-021-04371-y>
- Rowell, R. M., Pettersen, R., & Tshabalala, M. A. (2012). Chapter 3 Cell Wall Chemistry. *In: Handbook of Wood Chemistry and Wood Composites, 2nd Edition; Chapter 3. Pp. 33-72. 2013., 3, 33–72.*
- Sai Prasanna, N., & Mitra, J. (2020a). Isolation and characterization of cellulose nanocrystals from Cucumis sativus peels. *Carbohydrate Polymers*, 247(March), 116706.  
<https://doi.org/10.1016/j.carbpol.2020.116706>
- Sai Prasanna, N., & Mitra, J. (2020b). Isolation and characterization of cellulose nanocrystals from Cucumis sativus peels. *Carbohydrate Polymers*, 247(July), 116706.  
<https://doi.org/10.1016/j.carbpol.2020.116706>
- Sarker, T. R., Pattnaik, F., Nanda, S., Dalai, A. K., Meda, V., & Naik, S. (2021). Hydrothermal pretreatment technologies for lignocellulosic biomass: A review of steam explosion and subcritical water hydrolysis. *Chemosphere*, 284, 131372.  
<https://doi.org/https://doi.org/10.1016/j.chemosphere.2021.131372>
- Seddiqi, H., Oliaei, E., Honarkar, H., Jin, J., Geonzon, L. C., Bacabac, R. G., & Klein-Nulend, J. (2021). Cellulose and its derivatives: towards biomedical applications. In *Cellulose* (Vol. 28, Issue 4, pp. 1893–1931). Springer Science and Business Media B.V.  
<https://doi.org/10.1007/s10570-020-03674-w>
- Segal, L., Creely, J. J., Martin, A. E., & Conrad, C. M. (1959). An empirical method for estimating the degree of crystallinity of native cellulose using the x-ray diffractometer. *Textile Research Journal*, 29(10), 786–794. <https://doi.org/10.1177/004051755902901003>
- Seymour, R. B. , Mark, H. F., Pauling, L., Fisher, C. H., Stahl, G. A., Sperling, L. H., Marvel, C., & Carraher, C. E. , Jr. (1989). Pioneers in polymer science. In *Kluwer Academic Publishers* (Vol. 53, Issue 9). <https://doi.org/10.1017/CBO9781107415324.004>
- Shin, H. K., Jeun, J. P., Kim, H. Bin, & Hyun, P. (2012). Isolation of cellulose fibers from kenaf using electron beam. *Radiation Physics and Chemistry*, 81(8), 936–940.  
<https://doi.org/10.1016/j.radphyschem.2011.10.010>
- Siqueira, G., Kokkinis, D., Libanori, R., Hausmann, M. K., Gladman, A. S., Neels, A., Tingaut, P., Zimmermann, T., Lewis, J. A., & Studart, A. R. (2017). Cellulose Nanocrystal Inks for 3D Printing of Textured Cellular Architectures. *Advanced Functional Materials*, 27(12).  
<https://doi.org/10.1002/adfm.201604619>

- Sousa, M. M. De, Vianna, A., Carvalho, N. De, & Silva, D. D. J. (2019). *Cellulose nanocrystal production focusing on cellulosic material pre-treatment and acid hydrolysis time*. 80(March), 59–66.
- Spagnuolo, L., D’Orsi, R., & Operamolla, A. (2022). Nanocellulose for paper and textile coating: the importance of surface chemistry. *ChemPlusChem*, 87(8).  
<https://doi.org/10.1002/cplu.202200204>
- Srivastava, D., Kuklin, M. S., Ahopelto, J., & Karttunen, A. J. (2020). Electronic band structures of pristine and chemically modified cellulose allomorphs. *Carbohydrate Polymers*, 243(May), 116440. <https://doi.org/10.1016/j.carbpol.2020.116440>
- Sukyai, P., Anongjanya, P., Bunyahwuthakul, N., Kongsin, K., Harnkarnsujarit, N., Sukatta, U., Sothornvit, R., & Chollakup, R. (2018). Effect of cellulose nanocrystals from sugarcane bagasse on whey protein isolate-based films. *Food Research International*, 107(December 2017), 528–535. <https://doi.org/10.1016/j.foodres.2018.02.052>
- Sun, Y., & Cheng, J. (n.d.). *Hydrolysis of lignocellulosic materials for ethanol production: a review q*.
- Sundari, M. T., & Ramesh, A. (2012). Isolation and characterization of cellulose nanofibers from the aquatic weed water hyacinth — *Eichhornia crassipes*. *Carbohydrate Polymers*, 87(2), 1701–1705. <https://doi.org/10.1016/j.carbpol.2011.09.076>
- Tang, Y., Shen, X., Zhang, J., & Guo, D. (2015). Extraction of cellulose nano-crystals from old corrugated container fiber using phosphoric acid and enzymatic hydrolysis followed by sonication. *Carbohydrate Polymers*, 125, 360–366.  
<https://doi.org/10.1016/j.carbpol.2015.02.063>
- Thakur, M., Sharma, A., Ahlawat, V., Bhattacharya, M., & Goswami, S. (2020). Process optimization for the production of cellulose nanocrystals from rice straw derived  $\alpha$ -cellulose. *Materials Science for Energy Technologies*, 3, 328–334.  
<https://doi.org/10.1016/j.mset.2019.12.005>
- Trilokesh, C., & Uppuluri, K. B. (2019). Isolation and characterization of cellulose nanocrystals from jackfruit peel. *Scientific Reports*, 1–8. <https://doi.org/10.1038/s41598-019-53412-x>
- Tsukamoto, J., Durán, N., & Tasic, L. (2013). Nanocellulose and bioethanol production from orange waste using isolated microorganisms. *Journal of the Brazilian Chemical Society*, 24(9), 1537–1543. <https://doi.org/10.5935/0103-5053.20130195>
- Vanderfleet, O. M., & Cranston, E. D. (2021). Production routes to tailor the performance of cellulose nanocrystals. *Nature Reviews Materials*, 6(2), 124–144.  
<https://doi.org/10.1038/s41578-020-00239-y>

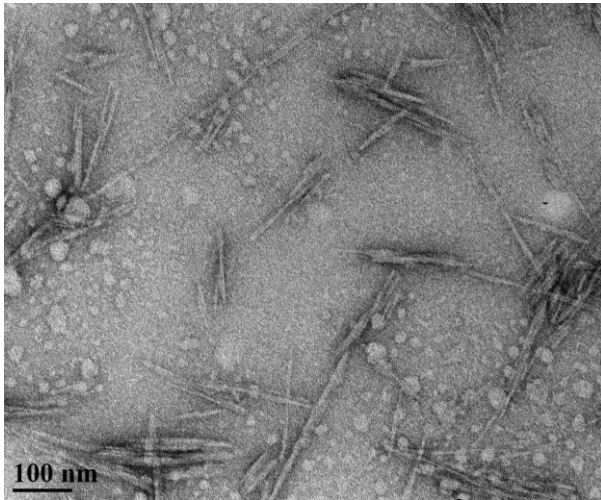
- Wan, J. Q., Wang, Y., & Xiao, Q. (2010). Effects of hemicellulose removal on cellulose fiber structure and recycling characteristics of eucalyptus pulp. *Bioresource Technology*, *101*(12), 4577–4583. <https://doi.org/10.1016/j.biortech.2010.01.026>
- Wang, H., Liu, Z., Hui, L., Ma, L., Zheng, X., Li, J., & Zhang, Y. (2020). Understanding the structural changes of lignin in poplar following steam explosion pretreatment. *Holzforschung*, *74*(3), 275–285. <https://doi.org/10.1515/hf-2019-0087>
- Wang, J., Chae, M., Beyene, D., Sauvageau, D., & Bressler, D. C. (2021). Co-production of ethanol and cellulose nanocrystals through self-cycling fermentation of wood pulp hydrolysate. *Bioresource Technology*, *330*. <https://doi.org/10.1016/j.biortech.2021.124969>
- Xiang, H., Wang, B., Zhong, M., Liu, W., Yu, D., Wang, Y., Tam, K. C., Zhou, G., & Zhang, Z. (2022). Sustainable and Versatile Superhydrophobic Cellulose Nanocrystals. *ACS Sustainable Chemistry and Engineering*. <https://doi.org/10.1021/acssuschemeng.2c00311>
- Xiao, L.-P., Song, G.-Y., & Sun, R.-C. (2017). Effect of Hydrothermal Processing on Hemicellulose Structure. In H. A. Ruiz, M. Hedegaard Thomsen, & H. L. Trajano (Eds.), *Hydrothermal Processing in Biorefineries: Production of Bioethanol and High Added-Value Compounds of Second and Third Generation Biomass* (pp. 45–94). Springer International Publishing. [https://doi.org/10.1007/978-3-319-56457-9\\_3](https://doi.org/10.1007/978-3-319-56457-9_3)
- Xie, H., Du, H., Yang, X., & Si, C. (2018). Recent Strategies in Preparation of Cellulose Nanocrystals and Cellulose Nanofibrils Derived from Raw Cellulose Materials. *International Journal of Polymer Science*, *2018*, 7923068. <https://doi.org/10.1155/2018/7923068>
- Xu, W., Gr, Ø., Liu, J., Kronlund, D., Li, B., Backman, P., Peltonen, J., Willfçr, S., Sundberg, A., & Xu, C. (2017). *Mild oxalic-acid-catalyzed hydrolysis as a novel approach to prepare cellulose nanocrystals*. <https://doi.org/10.1002/cnma.201600347>
- Yang, Z., Peng, H., Wang, W., & Liu, T. (2010). Crystallization behavior of poly( $\epsilon$ -caprolactone)/layered double hydroxide nanocomposites. *Journal of Applied Polymer Science*, *116*(5), 2658–2667. <https://doi.org/10.1002/app>
- Yu, H., Qin, Z., Liang, B., Liu, N., Zhou, Z., & Chen, L. (2013). Facile extraction of thermally stable cellulose nanocrystals with a high yield of 93% through hydrochloric acid hydrolysis under hydrothermal conditions. *Journal of Materials Chemistry A*, *1*(12), 3938–3944. <https://doi.org/10.1039/c3ta01150j>
- Yupanqui-Mendoza, S. L., Prado, C. A., Santos, J. C. dos, & Arantes, V. (2023). Hydrodynamic cavitation as a promising pretreatment technology to enhance the efficiency of cellulose nanocrystal production via enzymatic hydrolysis. *Chemical Engineering Journal*, *472*. <https://doi.org/10.1016/j.cej.2023.144821>

- Zhang, F., Shen, R., Li, N., Yang, X., & Lin, D. (2023). Nanocellulose: An amazing nanomaterial with diverse applications in food science. *Carbohydrate Polymers*, 304(September 2022), 120497. <https://doi.org/10.1016/j.carbpol.2022.120497>
- Zhao, G., Du, J., Chen, W., Pan, M., & Chen, D. (2019). Preparation and thermostability of cellulose nanocrystals and nanofibrils from two sources of biomass: rice straw and poplar wood. *Cellulose*, 26(16), 8625–8643. <https://doi.org/10.1007/s10570-019-02683-8>
- Zhao, X., & Liu, D. (2019). Multi-products co-production improves the economic feasibility of cellulosic ethanol: A case of Formiline pretreatment-based biorefining. *Applied Energy*, 250, 229–244. <https://doi.org/10.1016/j.apenergy.2019.05.045>
- Zhu, J. Y., Sabo, R., & Luo, X. (2011). Integrated production of nano-fibrillated cellulose and cellulosic biofuel (ethanol) by enzymatic fractionation of wood fibers. *Green Chemistry*, 13(5), 1339–1344. <https://doi.org/10.1039/c1gc15103g>
- Zimmermann, T., Bordeanu, N., & Strub, E. (2010). Properties of nanofibrillated cellulose from different raw materials and its reinforcement potential. *Carbohydrate Polymers*, 79(4), 1086–1093. <https://doi.org/10.1016/j.carbpol.2009.10.045>

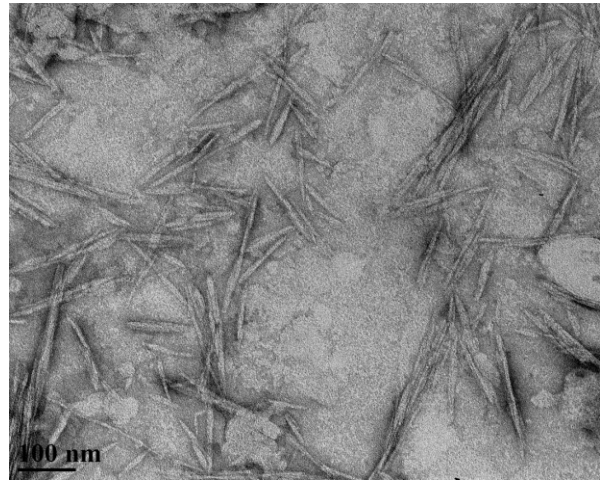
## Appendix A: supplementary material on result discussion



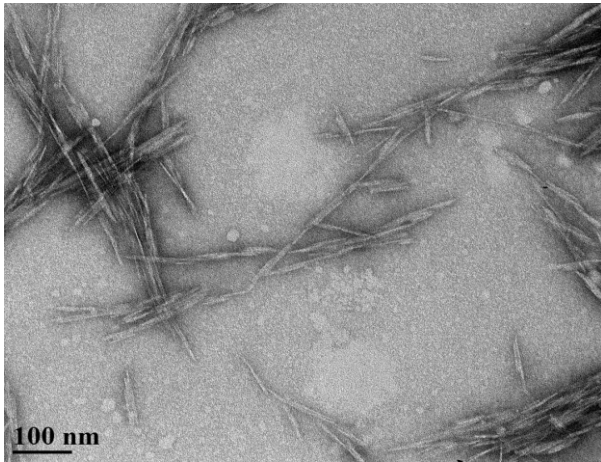
**Additional Figure 1.** X-ray diffraction pattern of untreated poplar, steam exploded poplar, Bleached poplar, bleached steam exploded poplar, cellulose nanocrystal from poplar and cellulose nanocrystal from steam exploded poplar.



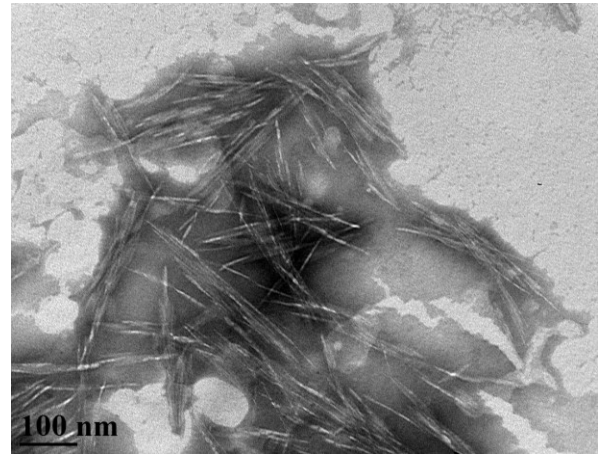
CNC- control (0 h)



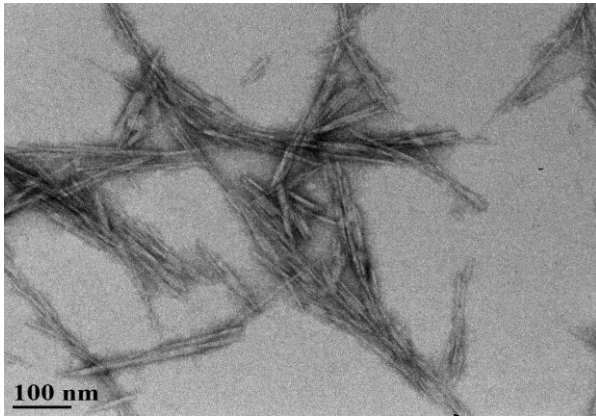
CNC-steam exploded poplar (0 h)



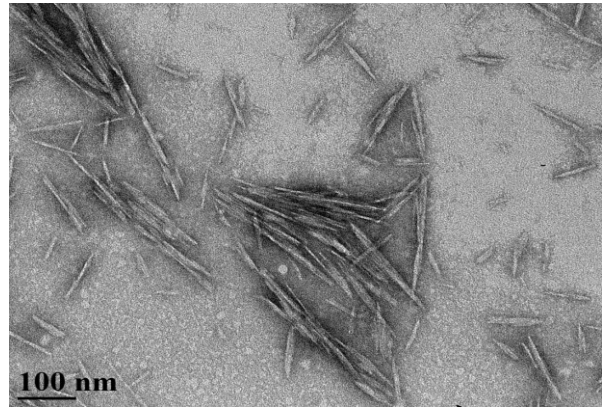
CNC-control (6 h)



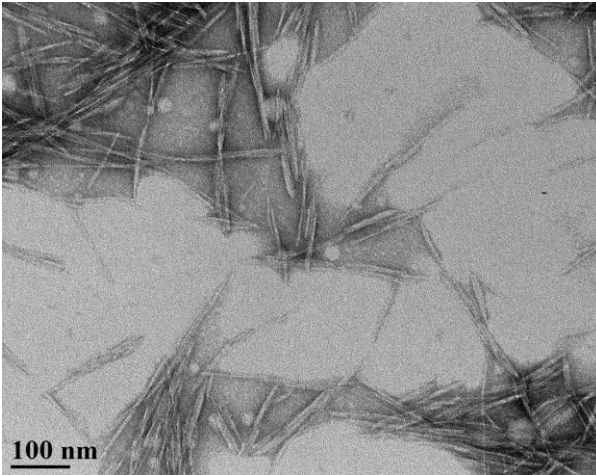
CNC-steam exploded poplar (6 h)



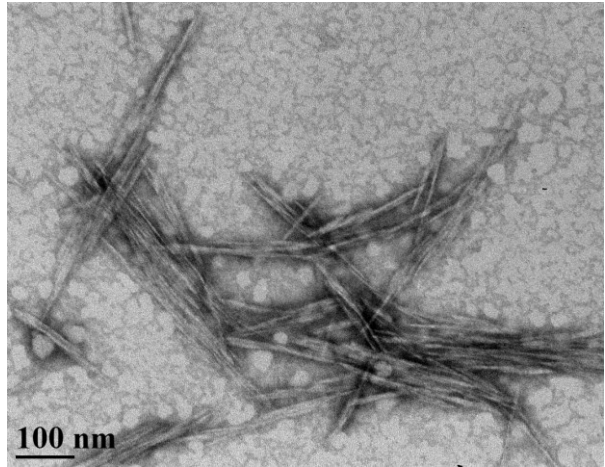
CNC-control (6 h)



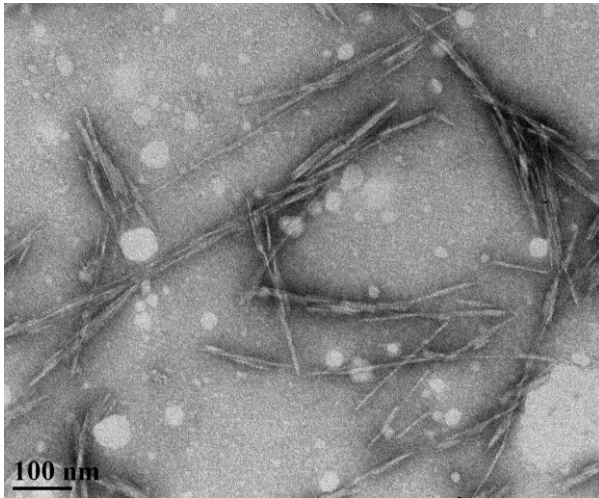
CNC-steam exploded poplar (12 h)



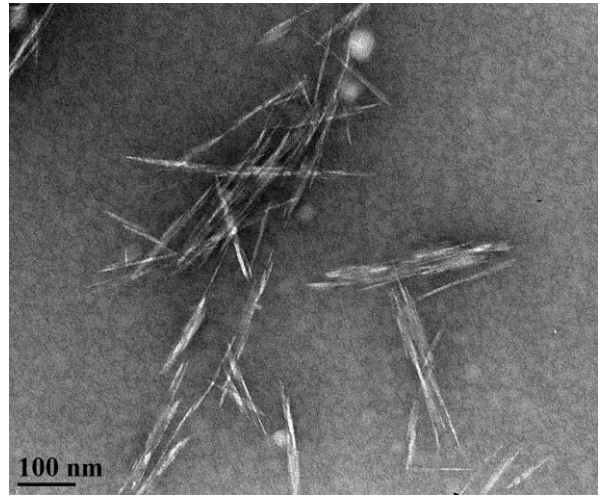
CNC-control (6 h)



CNC-steam exploded poplar (18 h)



CNC-control (6 h)



CNC-steam exploded poplar (24 h)

**Additional Figure 2.** Transmission electron microscopy of CNC isolated from steam explosion and enzymatic treated poplar wood